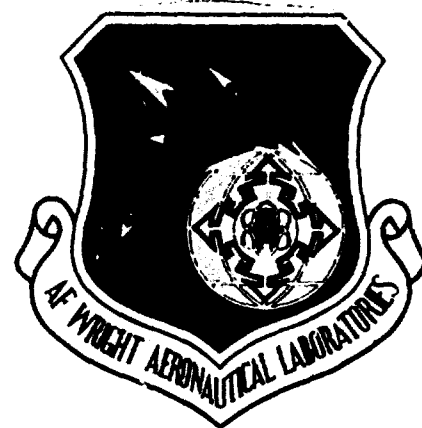


AD-A161 876

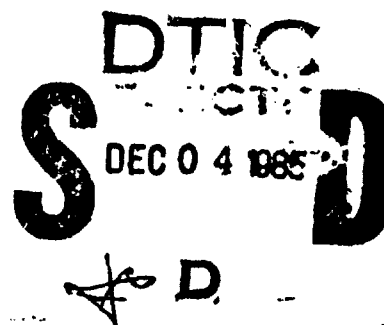


**VALIDATION OF USAF. STABILITY AND CONTROL DATCOM METHODOLOGIES
FOR STRAIGHT-TAPERED SWEPTFORWARD WINGS**

Daniel G. Sharpes

Design Prediction Group
Control Dynamics Branch

July 1985



Final Report - November 1980 to April 1984

FILE COPY

Approved for public release; distribution unlimited

FLIGHT DYNAMICS LABORATORY
AIR FORCE WRIGHT AERONAUTICAL LABORATORIES
AIR FORCE SYSTEMS COMMAND
WRIGHT-PATTERSON AIR FORCE BASE, OHIO

NOTICE

When Government drawings, specifications, or other data are used for any purpose other than in connection with a definitely related Government procurement operation, the United States Government thereby incurs no responsibility nor any obligation whatsoever; and the fact that the government may have formulated, furnished, or in any way supplied the said drawings, specifications, or other data, is not to be regarded by implication or otherwise as in any manner licensing the holder or any other person or corporation, or conveying any rights or permission to manufacture use, or sell any patented invention that may in any way be related thereto.

This report has been reviewed by the Office of Public Affairs (ASD/PA) and is releasable to the National Technical Information Service (NTIS). At NTIS, it will be available to the general public, including foreign nations.

This technical report has been reviewed and is approved for publication.



DANIEL G. SHARPES
Project Engineer
Control Dynamics Branch



RONALD O. ANDERSON, Chief
Control Dynamics Branch
Flight Control Division

FOR THE COMMANDER



JAMES D. LANG, Colonel, USAF
Chief, Flight Control Division
Flight Dynamics Laboratory

"If your address has changed, if you wish to be removed from our mailing list, or if the addressee is no longer employed by your organization please notify AFWAL/FIGC, W-PAFB, OH 45433 to help us maintain a current mailing list".

Copies of this report should not be returned unless return is required by security considerations, contractual obligations, or notice on a specific document.

REPORT DOCUMENTATION PAGE

1a. REPORT SECURITY CLASSIFICATION Unclassified			1b. RESTRICTIVE MARKINGS None	
2a. SECURITY CLASSIFICATION AUTHORITY			3. DISTRIBUTION/AVAILABILITY OF REPORT Approved for Public Release Distribution Unlimited	
2b. DECLASSIFICATION/DOWNGRADING SCHEDULE				
4. PERFORMING ORGANIZATION REPORT NUMBER(S) AFWAL-TR-84-3084			5. MONITORING ORGANIZATION REPORT NUMBER(S)	
6a. NAME OF PERFORMING ORGANIZATION AFWAL/FIGC		6b. OFFICE SYMBOL (If applicable) AFWAL/FIGC		7a. NAME OF MONITORING ORGANIZATION
6c. ADDRESS (City, State and ZIP Code) Wright-Patterson AFB, OH 45433			7b. ADDRESS (City, State and ZIP Code) Wright-Patterson AFB, OH 45433	
8a. NAME OF FUNDING/SPONSORING ORGANIZATION		8b. OFFICE SYMBOL (If applicable) AFWAL/FIGC		9. PROCUREMENT INSTRUMENT IDENTIFICATION NUMBER
8c. ADDRESS (City, State and ZIP Code) Wright-Patterson AFB, OH 45433			10. SOURCE OF FUNDING NOS.	
			PROGRAM ELEMENT NO. 62201F	PROJECT NO. 2403
			TASK NO. 05	WORK UNIT NO. 52
11. TITLE (Include Security Classification) Validation of USAF Stability and Control DATCOM (over)				
12. PERSONAL AUTHOR(S) Sharpes, Daniel Gregory				
13a. TYPE OF REPORT Final		13b. TIME COVERED FROM 1 Nov 80 to 30 Apr 84		14. DATE OF REPORT (Yr., Mo., Day) July 1985
15. PAGE COUNT 213				
16. SUPPLEMENTARY NOTATION				
17. COSATI CODES			18. SUBJECT TERMS (Continue on reverse if necessary and identify by block number)	
FIELD	GROUP	SUB. GR.		
			Datcom, Stability and Control, Aerodynamics, Stability	
			Derivative Estimation, Design Methodologies, Sweptforward	
			(over)	
19. ABSTRACT (Continue on reverse if necessary and identify by block number)				
<p>A detailed review of USAF Stability and Control Datcom methodologies was conducted to determine their validity for application to straight tapered, sweptforward wing configurations. To the extent possible the format found in the Datcom is repeated in this report.</p> <p>Several methods were modified to enable more accurate coefficient prediction (e.g., Wing Zero-Lift Angle of Attack, Downwash and Yawing Moment due to Yaw Rate) irrespective of sweep sign. At supersonic speeds, the reversibility theorem enabled most methodologies to be used without any modifications to account for sweptforward leading-edge designs. For the methodologies validated, sweptforward-wing estimation results were generally as accurate as the sweptback-wing results presented in the Datcom. Unfortunately, lack of test data prevented validation of several empirical methodologies (e.g., Subsonic High Angle-of-Attack Pitching Moment and Transonic Pitching Moment). No estimation (over)</p>				
20. DISTRIBUTION/AVAILABILITY OF ABSTRACT UNCLASSIFIED/UNLIMITED <input type="checkbox"/> SAME AS RPT. <input checked="" type="checkbox"/> DTIC USERS <input type="checkbox"/>			21. ABSTRACT SECURITY CLASSIFICATION Unclassified	
22a. NAME OF RESPONSIBLE INDIVIDUAL Daniel G. Sharpes			22b. TELEPHONE NUMBER (Include Area Code) (513) 476-2087	22c. OFFICE SYMBOL AFWAL/FIGC

UNCLASSIFIED

SECURITY CLASSIFICATION OF THIS PAGE

11. Methodologies for Straight-Tapered Sweptforward Wings

18. Wings, Forward Swept Wings

19. methodologies are proposed in these cases.

T

UNCLASSIFIED

FOREWORD

This report describes an in-house effort of the Control Dynamics Branch, Flight Control Division, Flight Dynamics Laboratory, Air Force Wright Aeronautical Laboratories, Wright-Patterson Air Force Base, Ohio under Work Unit 24030552, "Stability and Control Design Methods".

The work reported herein was performed during the period 1 November 1980 to 30 April 1984 by the author Lt Daniel Sharpes (AFWAL/FIGC), Project Engineer. The report was released by the author in August 1984.

This report is a complement to the USAF Stability and Control Datcom (AFWAL-TR-83-3048) and was written to expedite use of the Datcom in estimating straight-tapered sweptforward wing stability and control characteristics.

Special thanks are in order for Dana Bauer for her patient endurance at the word processor.

Accession For	
NTIS CRA&I	<input checked="" type="checkbox"/>
DTIC TAB	<input type="checkbox"/>
Unannounced	<input type="checkbox"/>
Justification	
By	
Distribution/	
Availability Codes	
Dist	Avail and/or Special
A-1	



TABLE OF CONTENTS

<u>Section</u>	<u>Page</u>
INTRODUCTION	1
VALIDATION OF DATCOM METHODOLOGIES	
4.1 Wings at Angle of Attack	2
4.3 Wing-Body, Tail-Body Combinations at Angle of Attack	40
4.4 Wing-Wing Combinations at Angle of Attack	53
4.5 Wing-Body-Tail Combinations at Angle of Attack	57
4.6 Power Effects at Angle of Attack	61
4.7 Ground Effects at Angle of Attack	61
4.8 Low-Aspect-Ratio Wings and Wing-Body Combinations at Angle of Attack	61
5.1 Wings in Sideslip	62
5.2 Wing-Body Combinations in Sideslip	70
5.3 Tail-Body Combinations in Sideslip	73
5.4 Flow Fields in Sideslip	78
5.5 Low-Aspect-Ratio Wings and Wing-Body Combinations at Angle of Attack	78
5.6 Wing-Body-Tail Combinations in Sideslip	79
6.1 Symmetrically Deflected Flaps and Control Devices on Wing-Body and Tail-Body Combinations	84
6.2 Asymmetrically Deflected Controls on on Wing-Body and Tail-Body Combinations	98
6.3 Special Control Methods	101

TABLE OF CONTENTS (concl'd)

<u>Section</u>	<u>Page</u>
7.1 Wing Dynamic Derivatives	108
7.3 Wing-Body Dynamic Derivatives	126
7.4 Wing-Body-Tail Dynamic Derivatives	134
APPENDIX - Summary of Datcom Modifications Necessary to Estimate Forward Swept Wing Stability and Control Characteristics	145
REFERENCES	160

LIST OF ILLUSTRATIONS

<u>FIGURE</u>		<u>PAGE</u>
1	Zero-Lift Angle of Attack Correlation	
	a) Current Datcom Method	2
	b) Using Equation 2	3
2	Effect of Linear Twist on Wing Zero-Lift Angle of Attack	
	a) Taper Ratio = 0.0	4
	b) Taper Ratio = 0.5	5
	c) Taper Ratio = 1.0	6
3	Transonic Wing-Body Lift-Curve Slope Correlation	
	a) $\Lambda c/4 = -28^\circ$, $A = 4.0$	8
	b) $\Lambda c/4 = -48^\circ$, $A = 2.8$	8
4	Effect of Reynolds Number on Maximum Lift Method Accuracy	
	a) $C_{L_{max}}$	13
	b) $\alpha_{C_{L_{max}}}$	14
5	Effect of Linear Twist on Wing Zero-Lift Pitching Moment	
	a) Taper Ratio = 0.0	16
	b) Taper Ratio = 0.5	17
	c) Taper Ratio = 1.0	18
6	Wing Aerodynamic-Center Position	
	a) Taper Ratio = 0.0	21
	b) Taper Ratio = 0.2	21
	c) Taper Ratio = 0.25	22
	d) Taper Ratio = 0.33	22
	e) Taper Ratio = 0.5	23
	f) Taper Ratio = 1.0	24
7	Datcom Figure 4.1.4.3-25, "Empirical Pitch-Up Boundary"	26
8	Lift-Dependent Drag Factor Due to Linear Twist	
	a) Taper Ratio = 0.1	30
	b) Taper Ratio = 0.2	31
	c) Taper Ratio = 0.25	32
	d) Taper Ratio = 0.3	33
	e) Taper Ratio = 0.4	34
	f) Taper Ratio = 0.5	35
	g) Taper Ratio = 0.6	36
	h) Taper Ratio = 0.75	37
	i) Taper Ratio = 1.0	38

LIST OF ILLUSTRATIONS (Cont'd)

-0

<u>FIGURE</u>		<u>PAGE</u>
9	Forward Swept Wing Wing-Body Maximum Lift Correction Factor	
	a) $C_{L_{max}}$	43
	b) $\alpha_{C_{L_{max}}}$	44
10	Effective Wing Aspect Ratio and Span For Sweptforward Planforms	52
11	Wing-Vortex Lateral Positions at Subsonic Speeds	54
12	Wing-Vortex Lateral Positions at Supersonic Speeds	56
13	Comparison of Calculated and Experimental Values of C_{Y_B}	62
14	Datcom Figure 5.1.2.1-27, "Wing Sweep Contribution to C_{ℓ_B} "; (b) $\lambda = .5$	64
15	Comparison of Calculated and Experimental Values of C_{ℓ_B}	65
16	Comparison of Calculated and Experimental Values of C_{n_B}	68
17	Planform Correction Factor - Trailing-Edge Flaps (Replaces Datcom Figure 6.1.4.3-10)	86
18	Spanwise Load Distribution Due to Symmetric Flap Deflection	
	a) $\frac{\beta \Delta}{\kappa_{av}} = 2$	89
	b) $\frac{\beta \Delta}{\kappa_{av}} = 6$	89
	c) $\frac{\beta \Delta}{\kappa_{av}} = 10$	89
19	Pitching-Moment Derivative for <u>Untapered</u> Trailing-Edge Control Surfaces <u>located at the Wing Tip</u>	90

FIGUREPAGE

20

Pitching-Moment Derivative for Tapered Trailing-Edge Control Surfaces Having Outboard Edge Coincident with Wing Tip

$$a) \frac{\text{TAN } \Lambda_{HL}}{\beta} = -.20 \quad 91$$

$$b) \frac{\text{TAN } \Lambda_{HL}}{\beta} = -.40 \quad 91$$

$$c) \frac{\text{TAN } \Lambda_{HL}}{\beta} = -.60 \quad 91$$

$$d) \frac{\text{TAN } \Lambda_{HL}}{\beta} = -.80 \quad 91$$

21

Supersonic Theoretical Hinge-Moment Derivative $C_{h\delta}$

$$a) \frac{\text{TAN } \Lambda_{HL}}{\beta} = -.20 \quad 96$$

$$b) \frac{\text{TAN } \Lambda_{HL}}{\beta} = -.40 \quad 96$$

$$c) \frac{\text{TAN } \Lambda_{HL}}{\beta} = -.60 \quad 96$$

$$d) \frac{\text{TAN } \Lambda_{HL}}{\beta} = -.80 \quad 96$$

22

Rolling-Moment Derivative for Tapered Control Surfaces Having Outboard Edge Coincident with Wing Tip

$$a) \frac{\text{TAN } \Lambda_{HL}}{\beta} = -.20 \quad 99$$

$$b) \frac{\text{TAN } \Lambda_{HL}}{\beta} = -.40 \quad 99$$

$$c) \frac{\text{TAN } \Lambda_{HL}}{\beta} = -.60 \quad 100$$

$$d) \frac{\text{TAN } \Lambda_{HL}}{\beta} = -.80 \quad 100$$

LIST OF ILLUSTRATIONS (Concluded)

<u>FIGURE</u>		<u>PAGE</u>
23	Rolling-Moment Derivative for Tapered Control Surfaces Having Outboard Edge Not Coincident with Wing Tip	
	a) $\frac{\text{TAN } \Lambda}{\beta} \text{HL} = -.20$	101
	b) $\frac{\text{TAN } \Lambda}{\beta} \text{HL} = -.40$	101
	c) $\frac{\text{TAN } \Lambda}{\beta} \text{HL} = -.60$	102
	d) $\frac{\text{TAN } \Lambda}{\beta} \text{HL} = -.80$	102
24	Rolling-Moment Derivative for Untapered Control Surfaces Having Outboard Edge Coincident with Wing Tip	103
25	Rolling Moment Derivative for Untapered Control Surfaces Having Outboard Edge Not Coincident with Wing Tip	103
26	Roll-Damping Parameter at Zero Lift	
	a) Taper Ratio = 0.0	113
	b) Taper Ratio = 0.25	114
	c) Taper Ratio = 0.5	115
	d) Taper Ratio = 1.0	116
27	Low-Speed Drag-Due-To-Lift Yaw-Damping Parameter	121
28	Low-Speed Profile-Drag Yaw-Damping Parameter	122

LIST OF TABLES

<u>TABLE</u>		<u>PAGE</u>
1	Subsonic Wing-Alone Lift-Curve Slope Data Summary and Substantiation	161
2	Supersonic Wing-Body Normal-Force-Curve Slope Data Summary and Substantiation	161
3	Subsonic Wing-Alone Lift Variation with Angle of Attack Data Summary and Substantiation	162
4	Maximum Lift and Angle of Attack for Maximum Lift for Wing-Alone Configurations at Subsonic Speeds	165
5	Wing-Alone Zero-Lift Pitching Moment Data Summary and Substantiation	165
6	Subsonic Wing-Alone Aerodynamics-Center Location Data Summary and Substantiation	166
7	Supersonic Wing-Body Aerodynamic Center Location Data Summary and Substantiation	167
8	Zero-Lift Drag Data Summary and Substantiation	168
9	Subsonic Wing-Alone Drag Due to Lift Data Summary and Substantiation	169
10	Transonic Wing-Body Drag Due to Lift and Data Summary and Substantiation	171
11	Supersonic Wing-Body Drag Due to lift Data Summary and Substantiation	173
12	Subsonic Wing-Body Lift-Curve Slope Data Summary and Substantiation	174
13	Subsonic Wing-Body Lift Variation with Angle of Attack Data Summary and Substantiation	175
14	Subsonic Wing-Body Maximum Lift Data Summary and Substantiation	176
15	Subsonic Wing-Body Aerodynamic-Center Location	176
16	Subsonic Wing-Body Zero-Lift Drag Data Summary and Substantiation	176

<u>TABLE</u>		<u>PAGE</u>
17	Supersonic Wing-Body Zero-Lift Drag Data Summary and Substantiation	177
18	Subsonic Wing-Body Drag Due to Lift Data Summary and Substantiation	177
19	Subsonic Downwash - Method 1 Data Summary and Substantiation	178
20	Subsonic Downwash Gradient - Method 2 Data Summary and Substantiation	179
21	Downwash Due to Flap Deflection Data Summary and Substantiation	179
22	Subsonic Dynamic Pressure Ratio Data Summary and Substantiation	179
23	Transonic Wing-Body Rolling Moment Due to Sideslip Data Summary and Substantiation	180
24	Supersonic Wing-Body Rolling Moment Due to Sideslip Data Summary and Substantiation	181
25	Subsonic Wing-Body Rolling Moment Due to Sideslip Data Summary and Substantiation	181
26	Subsonic Wing-Body-Tail Rolling Moment Due to Sideslip Data Summary and Substantiation	182
27	Effect of Control Surface Deflection on Lift Data Summary and Substantiation	183
28	Effect of Control Surface Deflection on Lift-Curve Slope Data Summary and Substantiation	184
29	Effect of Control Surface Deflection on Maximum Lift Coefficient Data Summary and Substantiation	185
30	Effect of Control Surface Deflection on Pitching Moment Data Summary and Substantiation	186
31	Effect of Angle of Attack on Control Surface Hinge Moment Data Summary and Substantiation	187
32	Effect of Control Surface Deflection on Rolling Moment Data Summary and Substantiation	187

<u>TABLE</u>		<u>PAGE</u>
33	Effect of Control Surface Deflection on Yawing Moment Data Summary and Substantiation	188
34	Subsonic Wing-Alone C_{L_q} Data Summary and Substantiation	188
35	Subsonic Wing-Alone C_{m_q} Data Summary and Substantiation	189
36	Subsonic Wing-Alone C_{Y_p} Data Summary and Substantiation	190
37	Subsonic Wing-Alone C_{ℓ_p} Data Summary and Substantiation	190

LIST OF SYMBOLS

ENGLISH SYMBOLS

A, AR	Wing aspect ratio
A_{eff}	Effective wing aspect ratio
b	Wing span
b_{eff}	Effective wing span
b_f	Total span of flaps, measured normal to the plane of symmetry
C_2	Empirical taper ratio constant
c_{fr}	Root chord of flap measured parallel to the plane of symmetry
c_{ft}	Tip chord of flap measured parallel to the plane of symmetry
c_r	Root chord
c_t	Tip chord
\bar{c}	Wing mean aerodynamic chord
d	Maximum fuselage diameter
e	Oswald efficiency factor for induced drag
$\frac{G}{\delta}$	Subsonic spanwise loading coefficient
h_H	Height of aft-surface MAC quarter-chord point above or below the forward surface root chord, measured in plane of symmetry normal to forward surface root chord, positive for aft-surface MAC above root chord plane
$K_{B(W)}$	Ratio of the lift of the body in the presence of the wing to that of the wing alone
K_N	Ratio of the body-nose lift to that of wing alone
$K_{W(B)}$	Ratio of the lift of the wing in the presence of the body to that of the wing alone
K_A	Flap span factor

$K_{B(W)}$	Ratio of lift-curve slope of body in presence of wing to that of wing alone
$K_{W(B)}$	Ratio of lift-curve slope of wing in presence of body to that of wing alone
M	Mach number
NDM	No Datcom method
n	Chordwise distance from wing apex to the pitching-moment reference center measured in root chords, positive for reference center aft of apex
$\frac{q}{q_\infty}$	Average dynamic pressure ratio
Re	Reynolds number
S_e	Exposed wing area
S_w	Wing area
v	induced-drag factor
w	induced-drag factor
$X_{a.c.}$	Distance between aerodynamic center and wing apex, parallel to the MAC, positive for a.c. aft of wing apex
\bar{X}	Distance between a.c. and c.g., positive when c.g. is ahead of a.c.
y	Lateral coordinate measured positive to right of plane of symmetry

GREEK SYMBOLS

α	Angle of attack, degrees
$\alpha_{C_{L_{\max}}}$	Wing angle of attack at maximum lift coefficient
α_o	Angle of attack at zero lift
$\Delta\alpha_o$	Change in wing zero-lift angle of attack due to linear wing twist
β	Mach number parameter, $\sqrt{M^2-1}$ or $\sqrt{1-M^2}$
Γ	Dihedral angle, positive wing tips up
Δ	Increment, difference between test and calculated values
ϵ	Downwash angle in plane of symmetry
$\Delta\epsilon$	Downwash increment due to flaps
$\frac{\partial\epsilon}{\partial\alpha}$	Downwash gradient acting on the aft surface
η	Dimensionless span station, $\frac{y}{b/2}$
η_f	Dimensionless distance from plane of symmetry to edge of flap or control surface
η_{stall}	Spanwise location where stall will first occur on an untwisted, tapered wing
θ	Linear angle of twist of wing tip with respect to root, negative for washout
κ, κ_{av}	Ratio of two-dimensional lift-curve slope at appropriate Mach number to 2π
Λ	Surface sweep angle (positive for sweepback)
Λ_β	Compressible sweep parameter, $\tan^{-1}\left(\frac{\tan \Lambda_{C/4}}{\beta}\right)$
λ	Taper ratio, $\frac{C_t}{C_r}$

COEFFICIENTS AND DERIVATIVES

C_D	Drag coefficient
C_{D_L}	Drag coefficient due to lift
C_{D_q}	Drag pitching derivative
C_{D_0}	Zero-lift drag coefficient
$C_{D_{\dot{\alpha}}}$	Change in drag coefficient with variation in rate of change of angle of attack
$C_{h_{\alpha}}$	Rate of change of hinge moment with angle of attack at constant flap or control deflection
$C_{h_{\delta}}$	Rate of change of hinge moment with control surface deflection at constant angle of attack
$C'_{h_{\delta}}$	Value of derivative for zero-thickness control surface
$\Delta C_{h_{\alpha}}$	Increment in derivative accounting for induced camber effects
C_L	Lift coefficient
$C_{L_{\dot{\alpha}}}$	Rate of change of lift coefficient with wing incidence
$C_{L_{\max}}$	Maximum lift coefficient
C_{L_q}	Lift pitching derivative
$C_{L_{\alpha}}$	Lift-curve slope
$(C_{L_{\alpha}})_{\delta}$	Lift-curve slope of the flap-deflected wing
$C_{L_{\dot{\alpha}}}$	Change in lift coefficient with variation in rate of change of angle of attack

$C_{L\delta}$	Rate of change of lift coefficient with wing flap deflection at constant angle of attack
ΔC_L	Increment of wing lift coefficient due to flap or control surface deflection
$\Delta C_{L_{max}}$	Increment in wing maximum lift coefficient due to flap deflection
C_ℓ	Rolling moment coefficient
C_{ℓ_p}	Rotary derivative
C_{ℓ_r}	Rotary derivative
C_{ℓ_β}	Rate of change of rolling moment with sideslip angle
$C_{\ell_{\dot{\beta}}}$	Change in rolling moment coefficient with variation in the rate of change of sideslip angle
C_{ℓ_δ}	Rate of change of rolling moment with control deflection
C_m	Pitching moment coefficient
C_{m_q}	Pitching moment pitching derivative
C_{m_0}	Pitching moment coefficient at zero lift
C_{m_α}	Rate of change of pitching moment coefficient with angle of attack
$C_{m_{\dot{\alpha}}}$	Rate of change of pitching moment coefficient with rate of change of angle of attack
$C_{m_{\dot{\delta}}}$	Rate of change of pitching moment coefficient with rate of change of angle of attack

ΔC_{m_0}	Increment in pitching moment coefficient at zero lift due to linear twist
$\frac{dC_m}{dC_L}$	Wing pitching-moment-curve slope
C_N	Normal force coefficient
C_{N_α}	Rate of change of normal-force coefficient with angle of attack
C_n	Yawing-moment coefficient
C_{n_p}	Rotary derivative
C_{n_r}	Rotary derivative
C_{n_β}	Rate of change of yawing moment with sideslip angle
$C_{n_{\dot{\beta}}}$	Change in yawing moment coefficient with variation in the rate of change of sideslip angle
ΔC_n	Yawing moment due to aileron deflection
C_Y	Side-force coefficient
C_{Y_p}	Rotary derivative
C_{Y_r}	Rotary derivative
C_{Y_β}	Rate of change of side force with sideslip angle
$C_{Y_{\dot{\beta}}}$	Change in side-force coefficient with variation in the rate of change of sideslip angle

ABBREVIATIONS

ASW	Aft swept wing
CALC	Calculated value
$c/2$	Mid-chord
$c/4$	Quarter-chord
e	exposed
FSW	Forward swept wing
HL	Hinge line
i	Inboard
LE	Leading edge
o	outboard
TEST	Tested value
TE	Trailing edge
W	Wing
WB	Wing-body

INTRODUCTION

When the USAF Stability and Control Datcom (Reference 1) was first being written, forward swept wing designs were not seriously considered and so were generally ignored in that text's prediction methodologies. Since then, advances in material technology has made sweptforward wings a viable design option, thus mandating the validation of Datcom relations and charts for sweptforward wing configurations.

A broad data search was begun in August of 1980 which eventually netted numerous configurations tested at speeds from low subsonic to supersonic. Interestingly, the majority of the data came from NACA in the 1946-49 time period. Pre-World War II drag data were also located for several German planforms.

The method of validation was performed in the following manner. The foundation of each of the Datcom methods was reviewed to determine its applicability to negative sweep angles. If the methodology appeared to be applicable, comparisons were made between calculated and wind tunnel tested values for those coefficients where data existed. Good agreement indicated that no major modifications were necessary. Poor agreement dictated a review of the methodology and its source, continuing for as many iterations as necessary to improve method accuracy. The situations where no tunnel data were located are so noted and the methodologies should be used with care. In some instances the methodology was not substantiated with test data. This was because those relations were strongly dependent on other methodologies whose results had already been correlated with test data (The wing-body-tail methods are an example, being made up of wing, wing-body and wing-wing relations).

The results of those validation efforts are contained herein and are presented in a format that the Datcom user will find most useful. The appendix lists the modifications necessary to enable the prediction of forward swept wing stability and control characteristics with the Datcom. The tables located in back of the report are similar to the Datcom tables and give the designer an idea of overall method accuracy.

4.1 WINGS AT ANGLE OF ATTACK

4.1.3.1 Wing Zero-Lift Angle of Attack

A. Subsonic

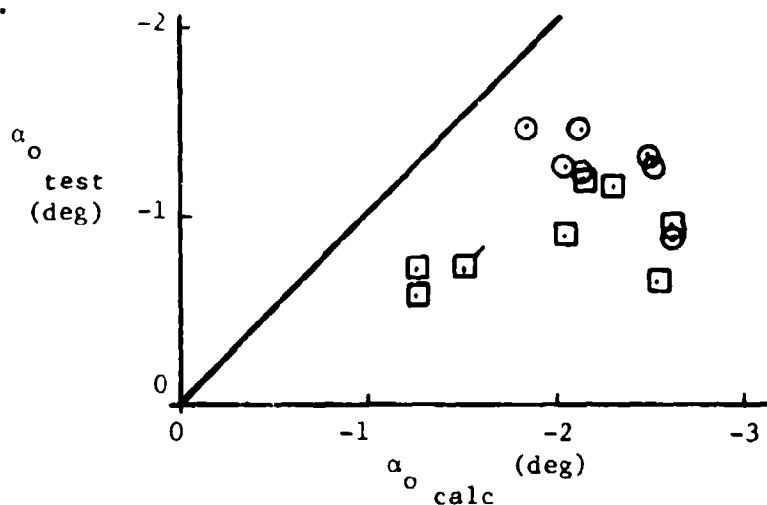
Datcom Equation 4.1.3.1-b,

$$(\alpha_0)_{\Lambda=0} = \tan^{-1} \left[\tan (\alpha_0)_{\Lambda=0} \frac{1}{\cos \Lambda} \right] \quad (1)$$

which is used to correct the airfoil zero-lift angle of attack for sweep, was found to consistently overestimate the true angle for both aft- and forwardswept wings (Figure 1a). A new sweep correction equation,

$$(\alpha_0)_{\Lambda=0} = (\alpha_0)_{\Lambda=0} \cos^2 \Lambda \quad (2)$$

was developed and gave better agreement with test data than Equation 1 did (Figure 1b). It is recommended that Equation 2 be used in place of Datcom Equation 4.1.3.1-b, (Equation 1).



(a) Current Datcom Method

- Sweptback
- Sweptforward

Note: Flagged values denote wing twist

Figure 1. Zero-Lift Angle of Attack Correlation

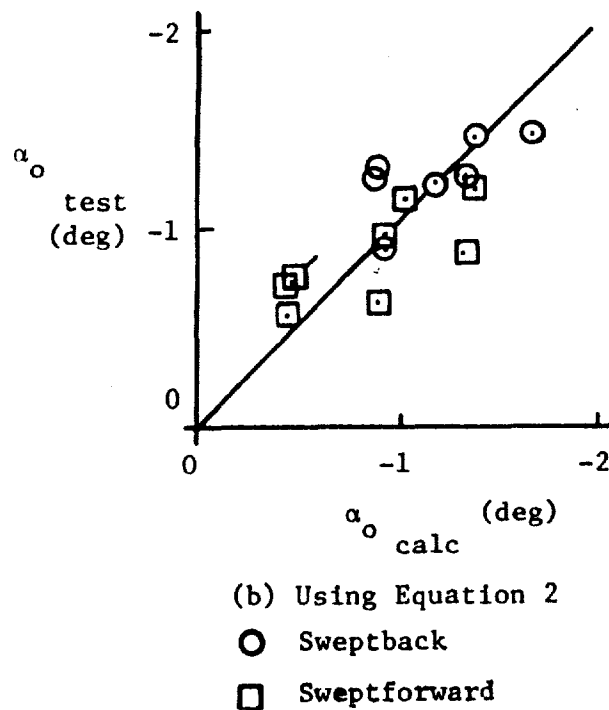


Figure 1. Zero-Lift Angle of Attack Correlation

The twist effect charts (Datcom Figure 4.1.3.1-4), developed by DeYoung and Harper (Reference 2), permitted estimation of twist effects for unswept and aft swept wings only. Following the procedure outlined in Reference 2, sweptforward wing twist effect factors were obtained. Expanded charts are presented in Figure 2 for taper ratios of 0.0 (Figure 2a), 0.5 (Figure 2b) and 1.0 (Figure 2c). As was the case for unswept and aft swept wings, insufficient data were found to substantiate the theoretical results.

B. Transonic

No Datcom method.

C. Supersonic

No Datcom method.

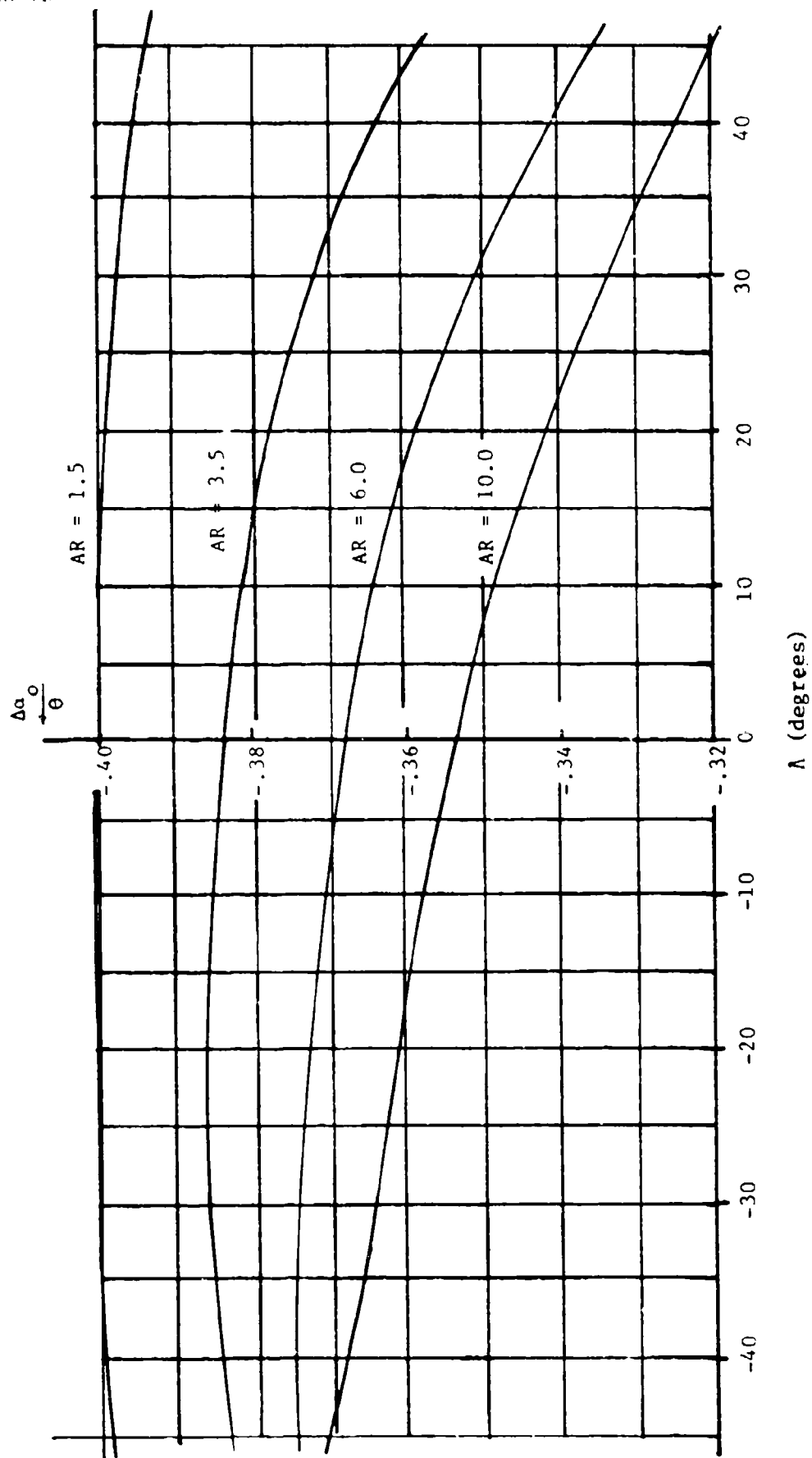
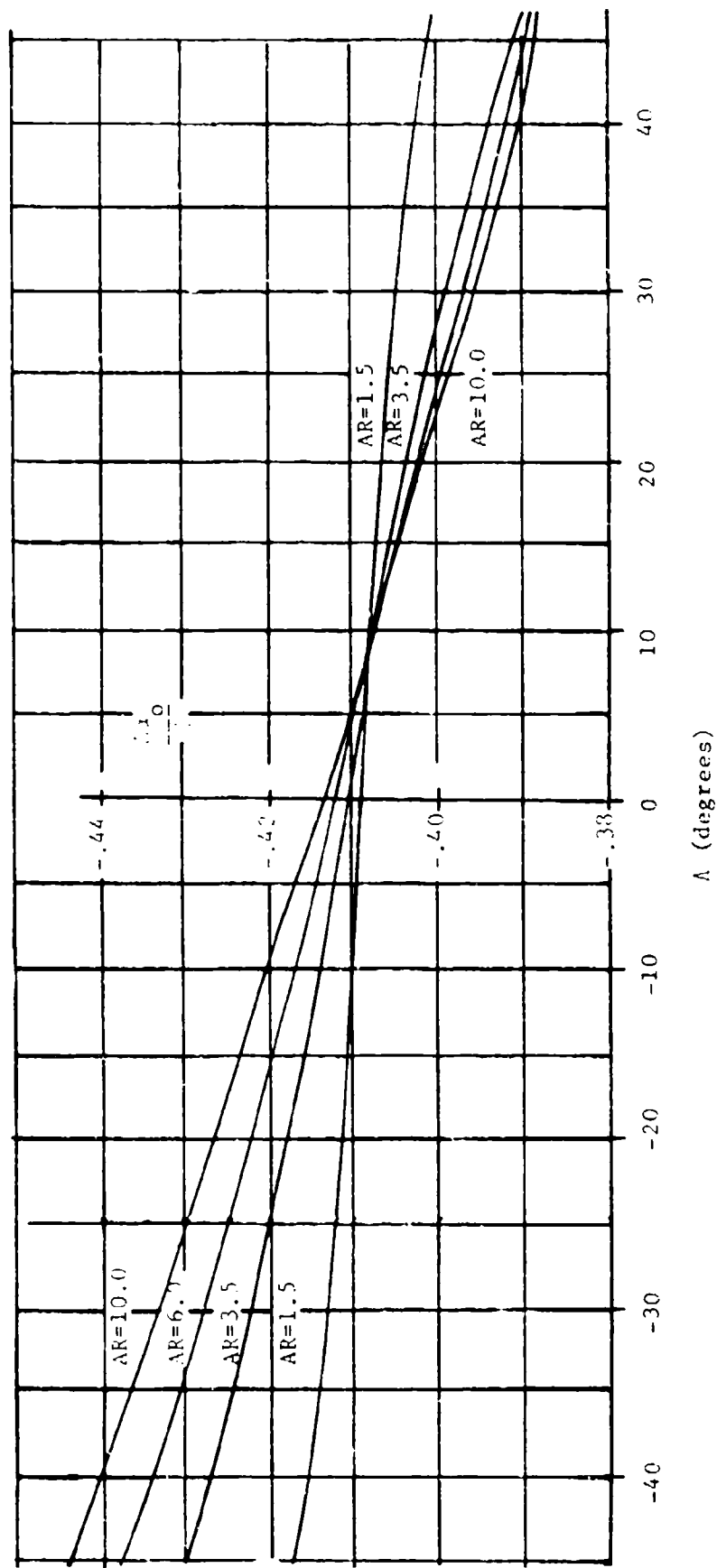
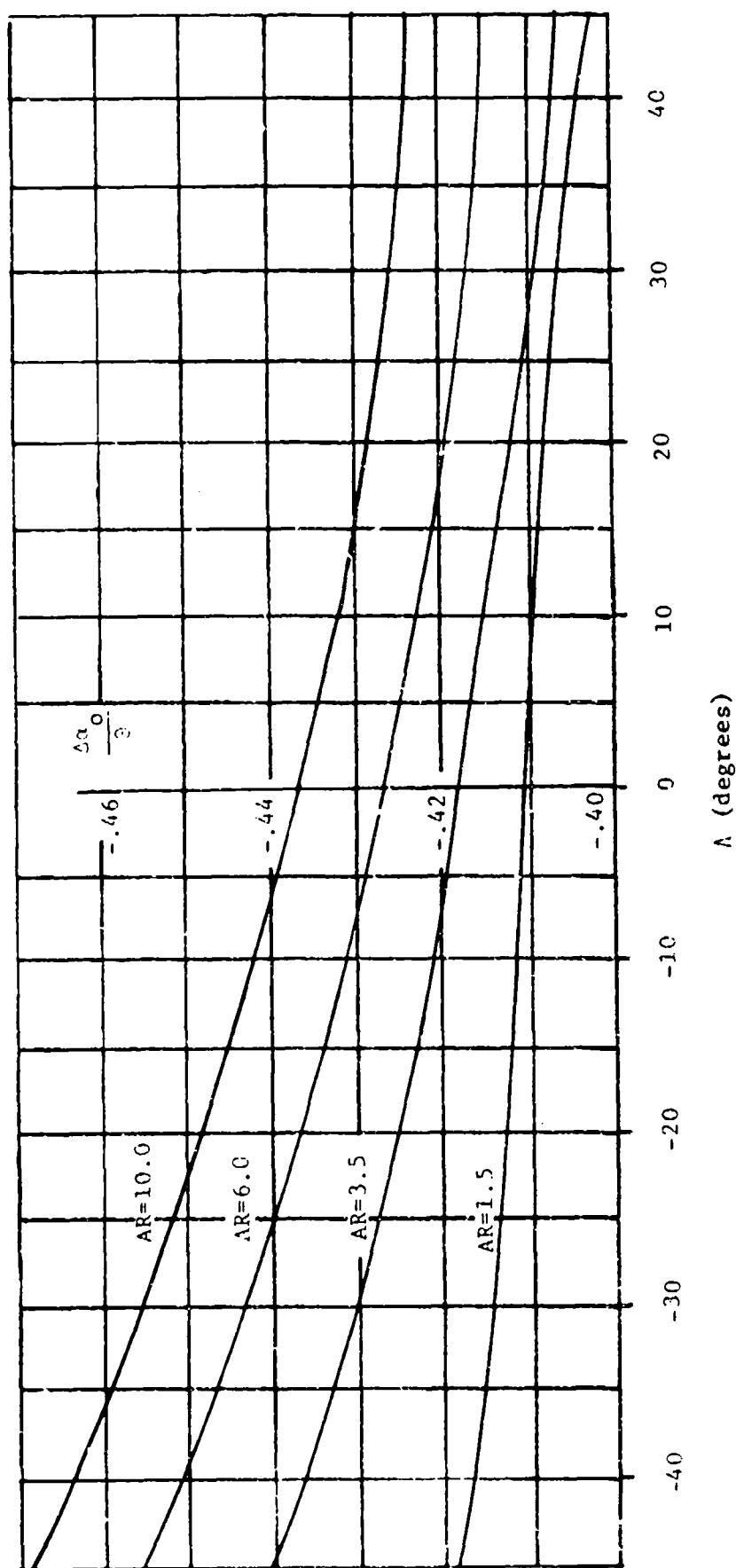


Figure 2. Effect of Linear Twist on Wing Zero-Lift Angle
 of Attack
 a) Taper Ratio = 0.0



(b) Taper Ratio = 0.5

Figure 2. Effect of Linear Twist on Wing Zero-Lift Angle of Attack



(c) Taper Ratio = 1.0

Figure 2. Effect of Linear Twist on Wing Zero-Lift Angle of Attack

4.1.3.2 WING LIFT-CURVE SLOPE

A. Subsonic

Method 1 required no modifications to predict the sweptforward wing lift-curve slope. Good agreement (5.85% average error) was noted between predicted and test values. Table 1 contains a description of the planforms evaluated and the test and predicted lift curve slopes.

Method 2 is unsuitable for sweptforward planforms and should not be used.

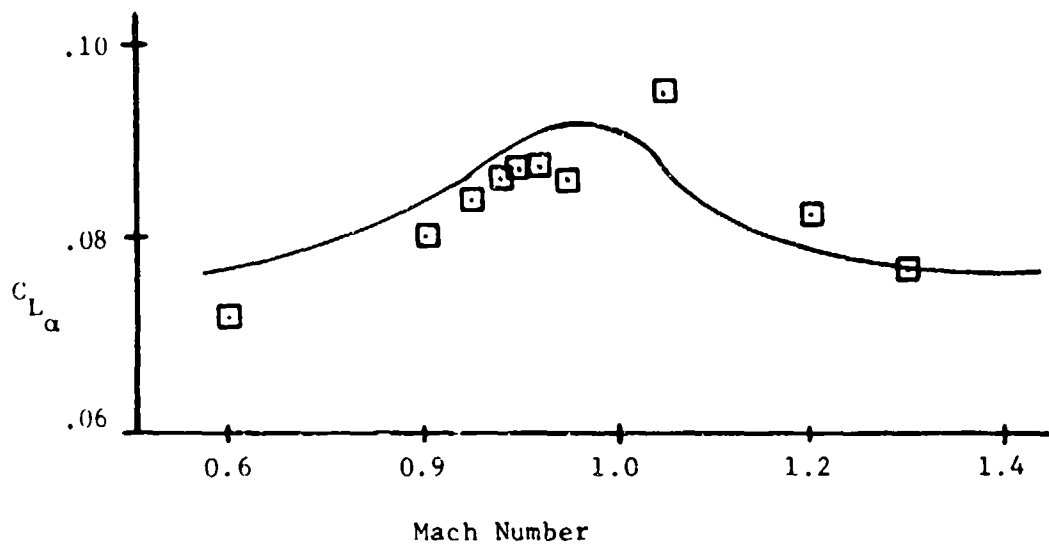
B. Transonic

No sweptforward-leading-edge wing-alone data were found but sufficient wing-body data were located to enable validation of the wing-alone prediction methodologies through wing-body analyses.

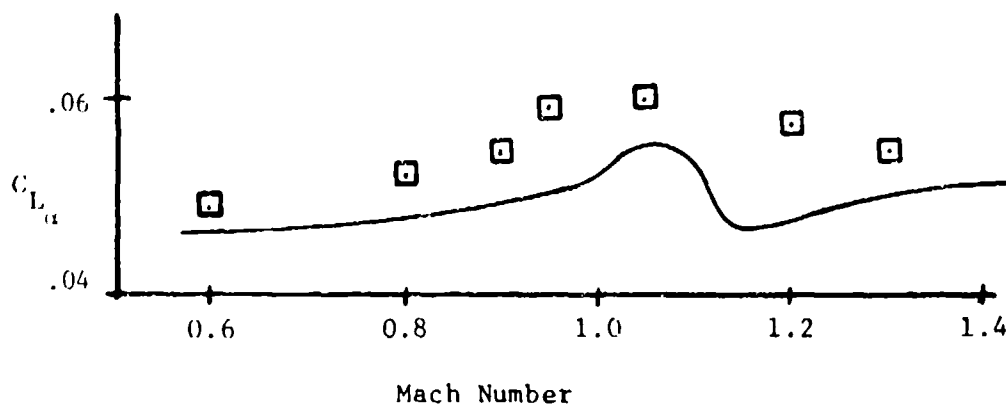
The absolute value of the mid-chord sweep angle should be used in Datcom Figure 4.1.3.2-53b, "Transonic Sweep Correction ...". No other modifications are necessary to predict transonic lift-curve slopes. Typical wing-body correlations between test and predicted lift-curve slopes are shown in Figure 3.

C. Supersonic

Through the use of the reversibility theorem, the normal-force-curve slope of sweptforward planforms can be obtained from Datcom Figures 4.1.3.2-56a through -56f, "Wing Supersonic Normal-Force-Curve Slope", by inserting the absolute value of the trailing-edge sweep angle wherever the leading-edge sweep angle is called for. For



a) $\Lambda_{c/4} = 28^\circ$, $A = 4.0$



b) $\Lambda_{c/4} = -48^\circ$, $A = 2.8$

Figure 3. Transonic Wing-Body Lift-Curve Slope Correlation

sweptforward wings approaching the sonic-leading-edge condition, the absolute value of the leading-edge sweep angle should be used in Datcom Figure 4.1.3.2-60, "Supersonic Wing Lift-Curve-Slope Correction Factor..."

As was the case at transonic speeds, no wing-alone data were found, but wing-alone methods were validated through wing-body analysis. Wing-body results gave very good correlation (4.79% average error) with data. Table 2 contains a description of the planforms evaluated and their test and predicted normal-force-curve slopes.

D. Hypersonic

No data were found in this speed regime.

As the hypersonic methodology uses Datcom Figures 4.1.3.2-56a through -56f, the comments of Paragraph C are relevant here.

4.1.3.3 WING LIFT IN THE NONLINEAR ANGLE-OF-ATTACK RANGE

A. Subsonic

The "General Method for Wings of Any Aspect Ratio" should be used to estimate forward swept wing lift in this angle of attack range. The absolute value of the leading-edge sweep angle should be used to obtain wing-shape parameter J. Table 3 shows good agreement (6.67% mean error) between estimated and test lift coefficients.

An occasional abnormality was noted for values of wing-shape parameter J greater than 1. This abnormality, the prediction of a false maximum lift peak, was explored by Williams and Vukelich (Reference 3). They suggest that when the false peak occurs, one replace the predicted lift values in the range between the angle of attack at which the lift curve slope ceases to be linear and the estimated angle of attack for maximum lift with a second-order polynomial such that the slope is zero at the maximum lift angle of attack. While this suggestion was not implemented, it would have reduced the 6.67% error noticeably. No other modifications are required other than those described in Paragraph A of Section 4.1.3.4, "Wing Maximum Lift".

No data were found for normal force at angles of attack beyond the stall. The modifications mentioned above should be sufficient to provide predictions of the normal force at post-stall angles of attack with accuracy comparable to afterswept wing results.

B. Transonic

While no data were found for this speed range, the absolute value of the leading-edge sweep angle should be used in all equations as well as in Datcom Figures 4.1.3.3-59a, "Thickness Correction Factor ..." and 4.1.3.3-59b, "Supersonic Lift Variation ...". The modifications described in Paragraph C of Section 4.1.3.2, "Wing Lift-Curve Slope" should be utilized when estimating the wing normal-force-curve slope.

C. Supersonic

While no data were found for this speed range, the absolute value of the leading edge sweep angle should be used in all equations and in Datcom Figures 4.1.3.3-59a, "Thickness Correction Factor ..." and 4.1.3.3-59b, "Supersonic Lift Variation ...". The modifications described in Paragraph C of Section 4.1.3.2, "Wing Lift-Curve Slope" should be utilized when estimating the wing normal-force-curve slope.

D. Hypersonic

No modifications are required to predict the normal-force curve for this speed range other than those described in Paragraph C of this section and Paragraph D of Section 4.1.3.2, "Wing Lift-Curve Slope".

4.1.3.4 WING MAXIMUM LIFT

A. Subsonic

Method 1 requires use of a wing spanwise-loading computer program. No modifications are required to the steps outlined in order to estimate maximum lift characteristics. However, the equation

$$\eta_{\text{stall}} = 1 - \lambda \quad (3)$$

(Datcom Equation 4.1.3.4-a), used to approximate the spanwise location where stall will first occur, should be applied cautiously, as stall tends to occur more inboard on forward swept wings than on aft swept wings.

Method 2 is an empirical relation for high-aspect-ratio wings. To estimate sweptforward maximum lift characteristics, the absolute value of the leading-edge sweep should be used in Datcom Figures 4.1.3.4-21a, "Subsonic Maximum Lift ..."; 4.1.3.4.-21b, "Angle-of-Attack Increment ..."; and 4.1.3.4-22, Mach Number Correction ...". Modifications described in Section 4.1.3.1, "Wing Zero-Lift Angle of Attack", should be applied when estimating the zero-lift angle of attack.

Good agreement with test data was noted for the configurations analyzed. The average maximum lift coefficient error was 4.80% and the average error of the angle of attack for maximum lift coefficient was 2.45%. Table 4 contains a summary of the planform parameters with the test and estimated maximum lift characteristics.

Method 3, also empirical, is for low-aspect-ratio wings. Sweptforward wing maximum lift characteristics estimates can be obtained by using the absolute value of the leading-edge sweep angle in Datcom Figures 4.1.3.4-24a, "Maximum-Lift Increment..." and 4.1.3.4-25b, "Angle-of-Attack Increment...". Only one sweptforward planform was found for this class of aspect ratio. Estimation error was 15.70% for the maximum lift coefficient and 8.20% for the angle of attack for maximum lift coefficient.

The remaining planforms analyzed had borderline-aspect-ratio wings. Maximum lift characteristics were obtained by averaging results obtained from Methods 2 and 3. Average error was 5.55% in predicting the maximum lift coefficient and 5.55% in estimating the angle of attack for maximum lift coefficient.

Table 4 shows planform parameters along with test and predicted maximum lift values for the three aspect-ratio classifications.

The effect of Reynolds number was very noticeable in terms of method accuracy (Figure 4). Above a value of 2 million (based on mean aerodynamic chord length) good agreement was noted with Datcom estimates. Below that Reynolds number, however, the Datcom predictions correlated poorly with test results. Due to the many variables in wind tunnel testing (i.e., application and location of grit, inherent tunnel turbulence, etc), users of the Datcom maximum lift methodologies can only be alerted to discrepancies that may exist between test and predicted maximum lift values at lower Reynolds numbers.

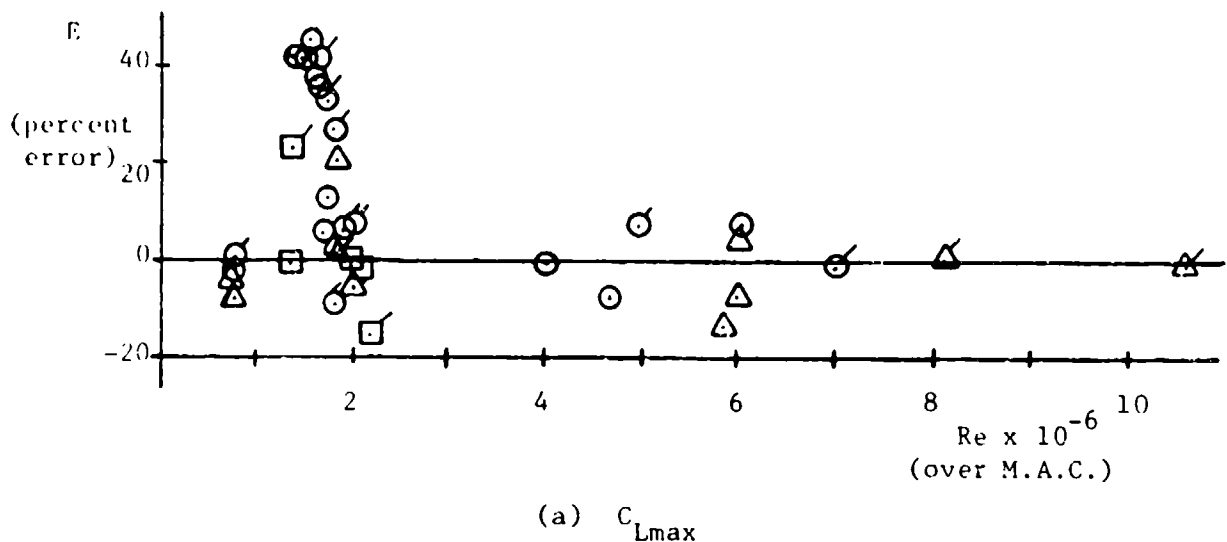


Figure 4. Effect of Reynolds Number on Maximum Lift Method

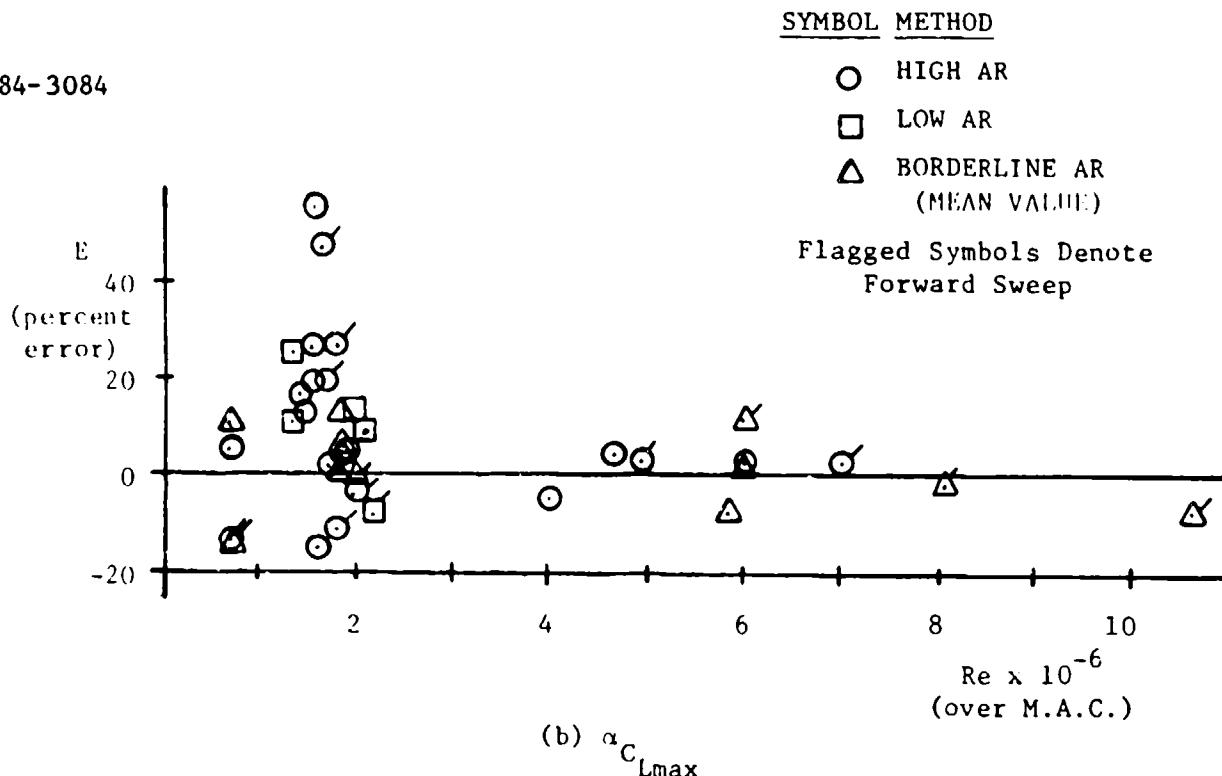


Figure 4. Effect of Reynolds Number on Maximum Lift Method

B. Transonic

The comments pertaining to Method 3 above are pertinent here. Also, the absolute value of the leading-edge sweep angle should be used in Datcom Figure 4.1.3.4-26b, "Maximum-Lift Correction Factor". No data were found in this speed range.

C. Supersonic

The comments in Paragraph C of Sections 4.1.3.2, "Wing Lift-Curve Slope" and 4.1.3.3, "Wing Lift in the Nonlinear Angle-of-Attack Range" are appropriate here. No other modifications are necessary.

No data were found in this speed range.

D. Hypersonic

The comments in Paragraph C of this section are appropriate here.

No data were found in this speed range.

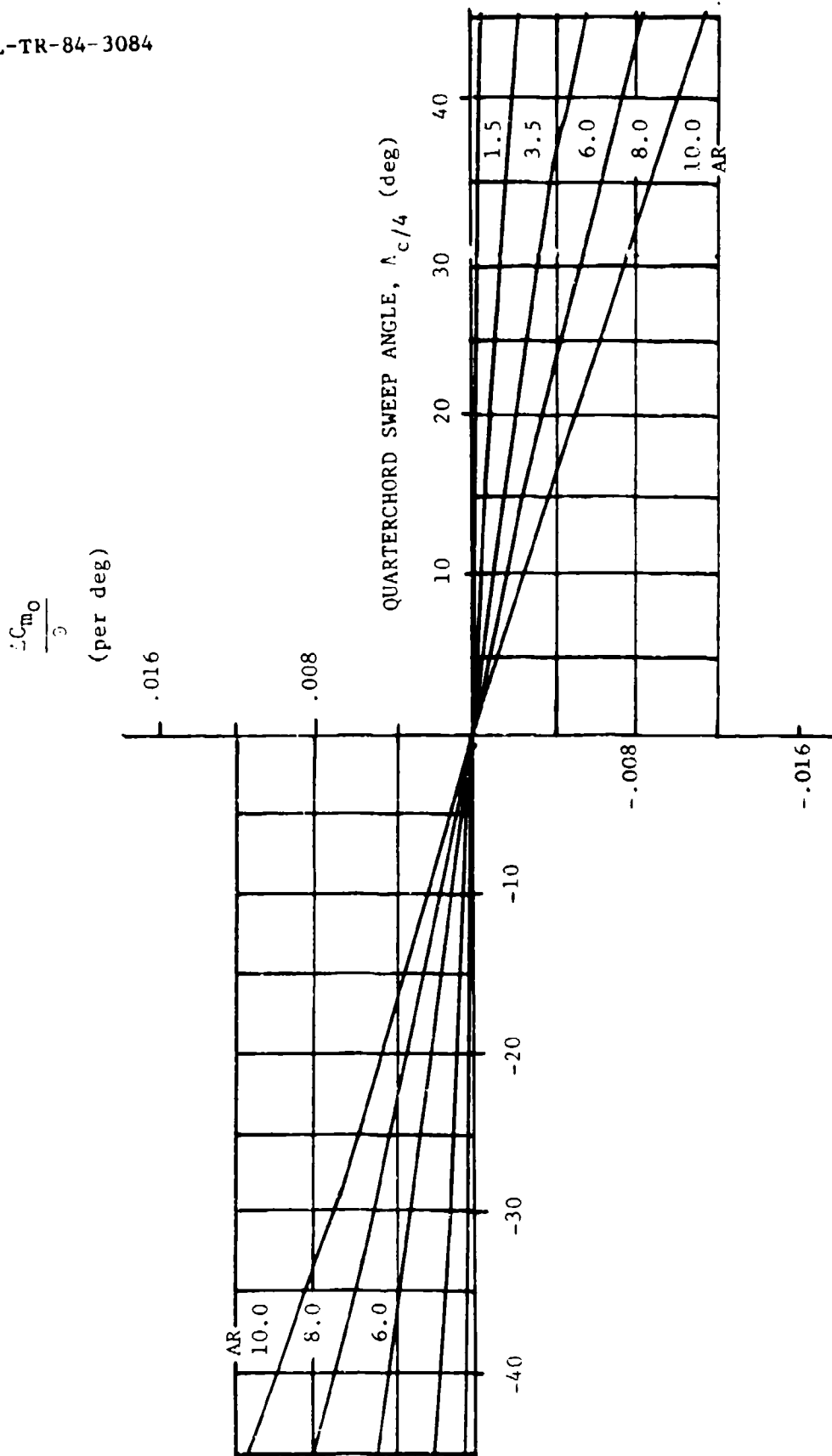
4.1.4.1 WING ZERO-LIFT PITCHING MOMENT

A. Subsonic

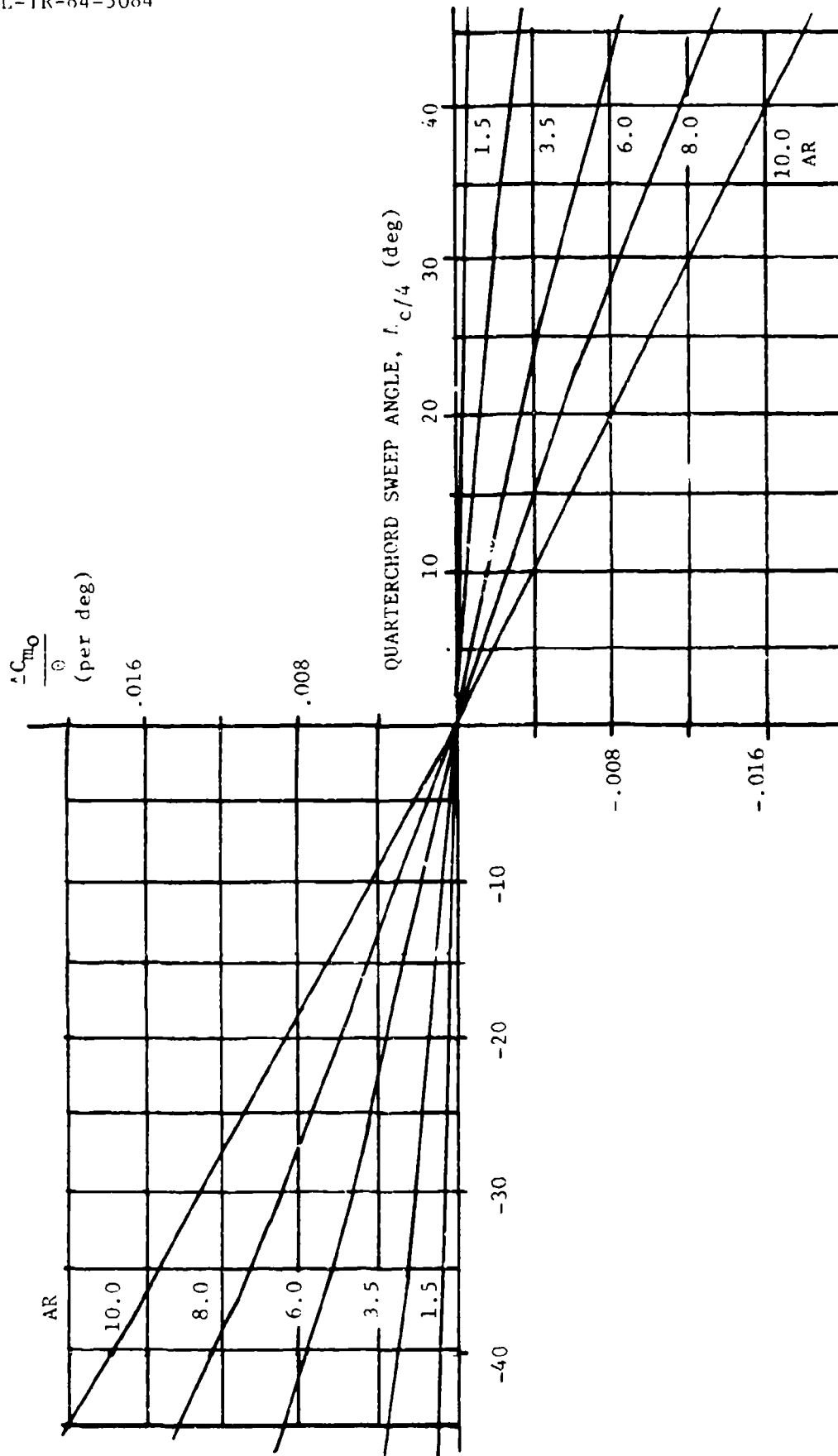
No modifications to the equations of Method 1 are required. The twist effect charts (Datcom Figure 4.1.4.1-5) were limited to unswept and aft swept wings. Charts based on DeYoung and Harper (Reference 2), expanded to include forward sweep, are presented in Figure 5 for taper ratios of 0.0 (Figure 5a), 0.5 (Figure 5b) and 1.0 (Figure 5c).

Insufficient data were found to substantiate the twist effect charts but eight planforms were available to validate the equations. The average difference between the test and predicted zero-lift pitching moment was 0.0030. Table 5 contains a summary of the planform parameters and the test and predicted pitching-moment values.

Method 2 is totally unsuited to forward-swept-wing planforms and should not be used.

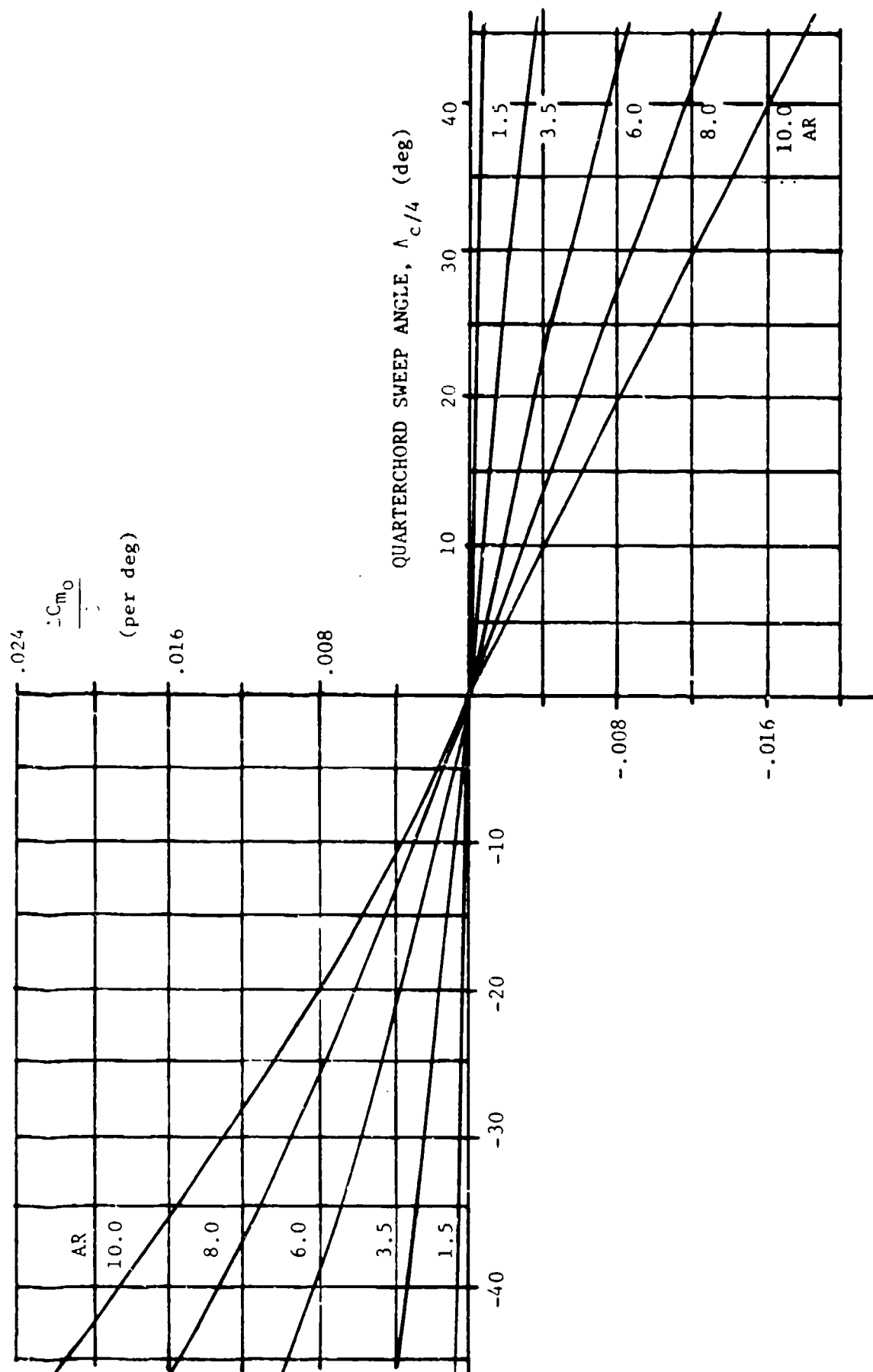


a) Taper Ratio = 0.0
Figure 5. Effect of Linear Twist on Wing Zero-lift Pitching Moment



b) Taper Ratio = 0.5

Figure 5. Effect of Linear Twist on Wing Zero-Lift Pitching Moment



c) Taper Ratio = 1.0

Figure 5. Effect of Linear Twist on Wing Zero-Lift Pitching Moment

B. Transonic

No Datcom method.

C. Supersonic

No Datcom method.

4.1.4.2 WING PITCHING-MOMENT-CURVE SLOPE

A. Subsonic

Estimation of the wing pitching-moment-curve slope is accomplished by using Datcom Equation 4.1.4.2-a

$$\frac{dC_m}{dC_L} = \left(n - \frac{x_{a.c.}}{c_r} \right) \frac{c_r}{\bar{c}} \quad (4)$$

While n , c_r , and \bar{c} are planform dependent, $\frac{x_{a.c.}}{c_r}$ is

obtained from Datcom Figures 4.1.4.2-26a through -26f, "Wing Aerodynamic-Center Position". The aerodynamic-center locations given by those charts are for aft swept wings only. Figure 6a through 6f should be used for sweptforward wing analysis. These charts were constructed by using a vortex-lattice computer code.

An average difference of 6.25% of the root chord was noted between test and predicted results using Method 1. Method 2 is totally unsuited for sweptforward wings and should not be used. Table 6 contains a summary of the planforms analyzed with their parameters, and predicted and test aerodynamic center locations.

B. Transonic

The methods of this section are based entirely on aft swept wing data and should not be used to estimate sweptforward wing characteristics. No method is presented to estimate transonic forward sweptwing aerodynamic-center characteristics.

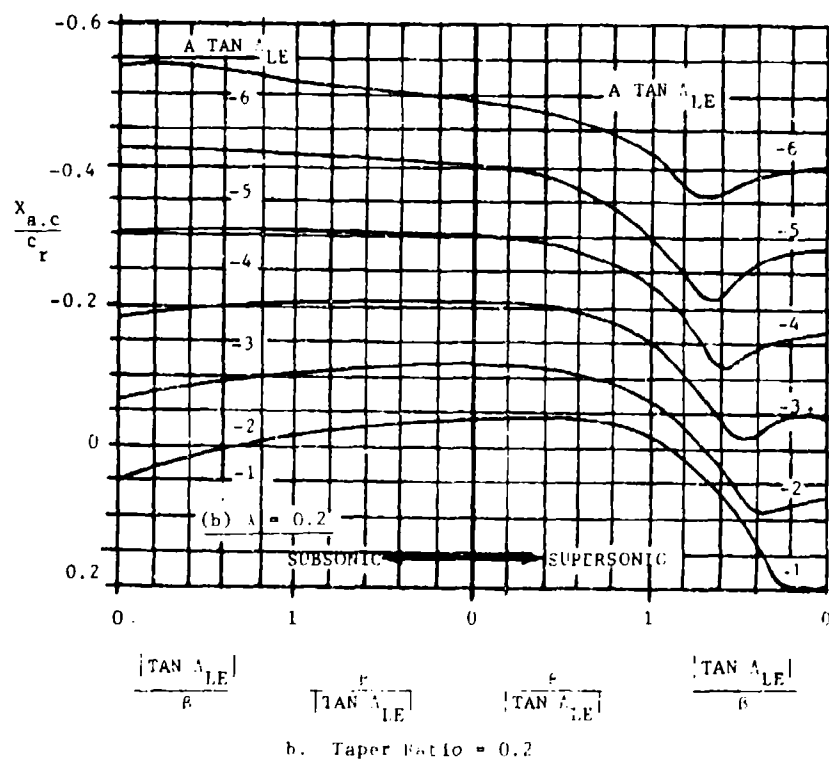
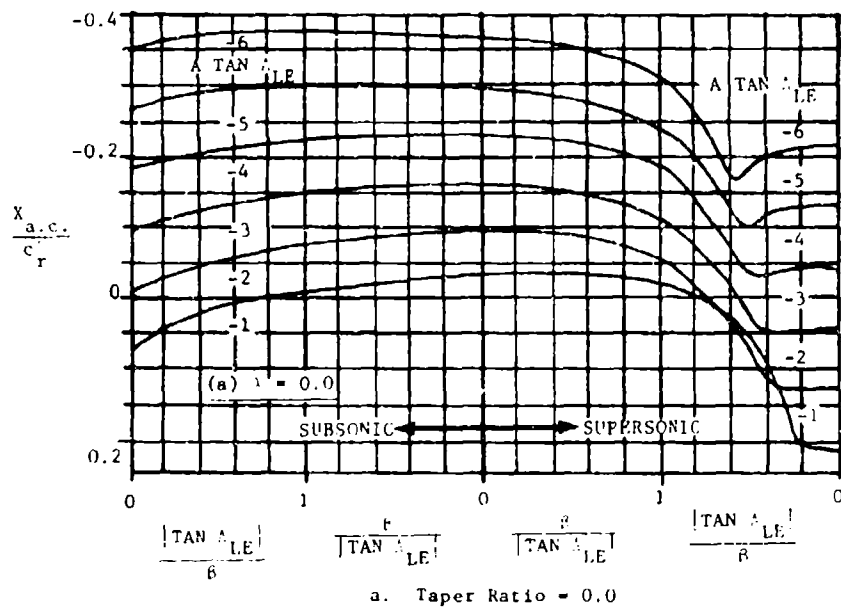


Figure 6. Wing Aerodynamic-Center Position

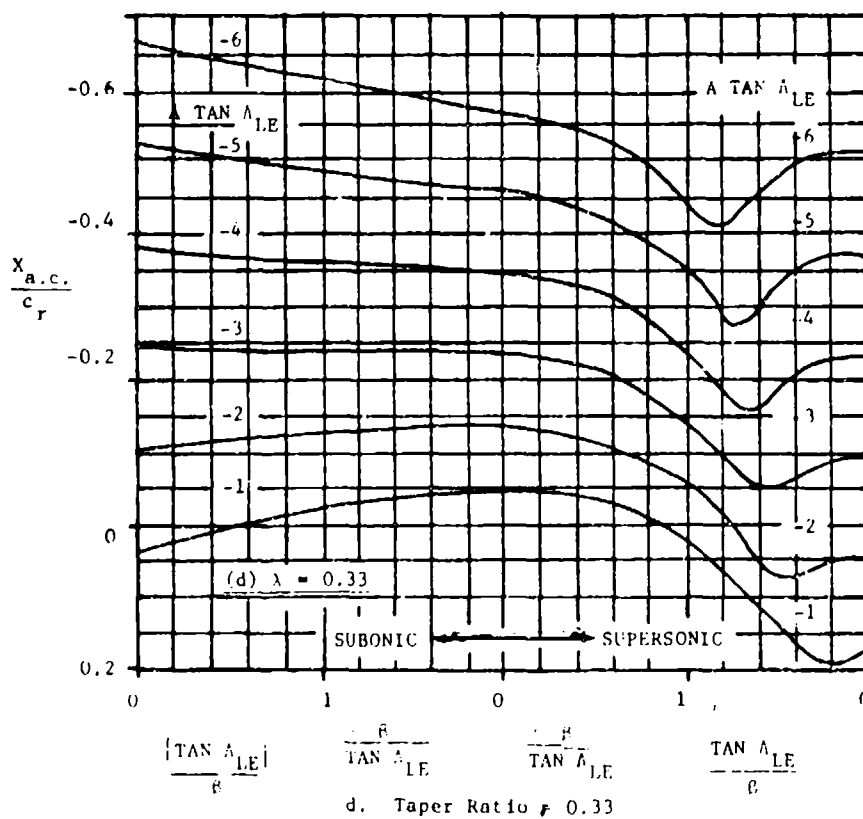
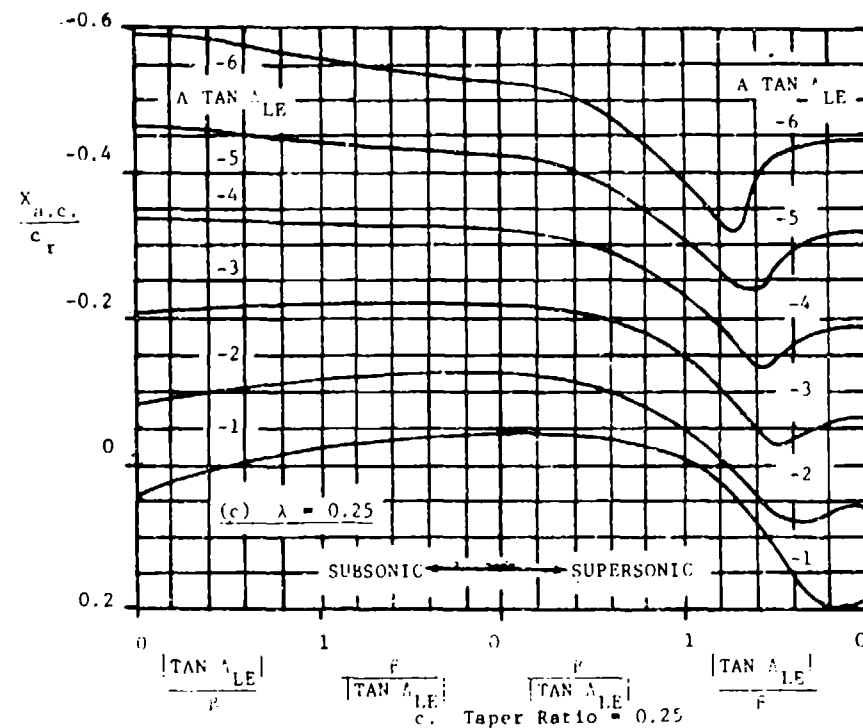
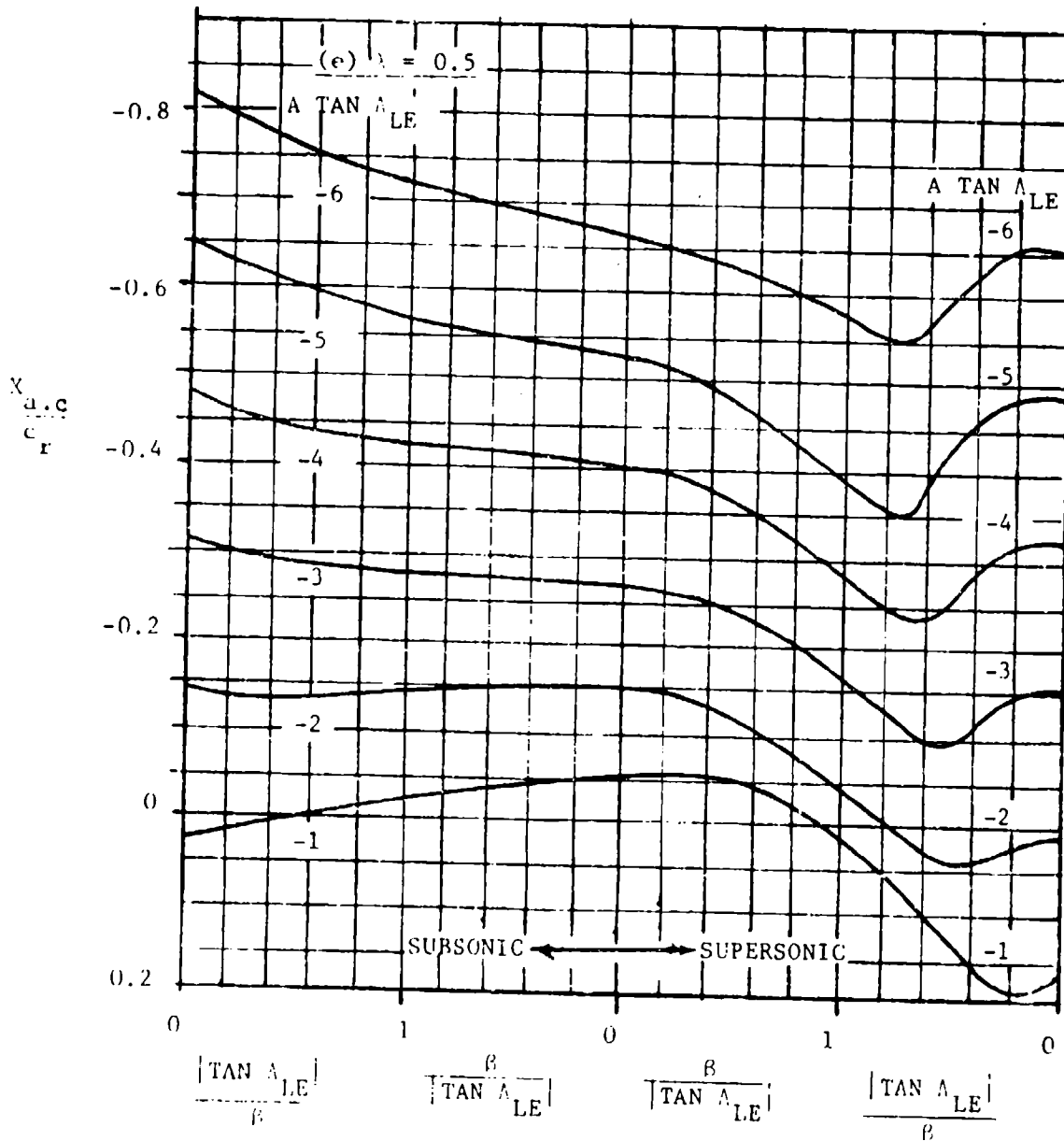
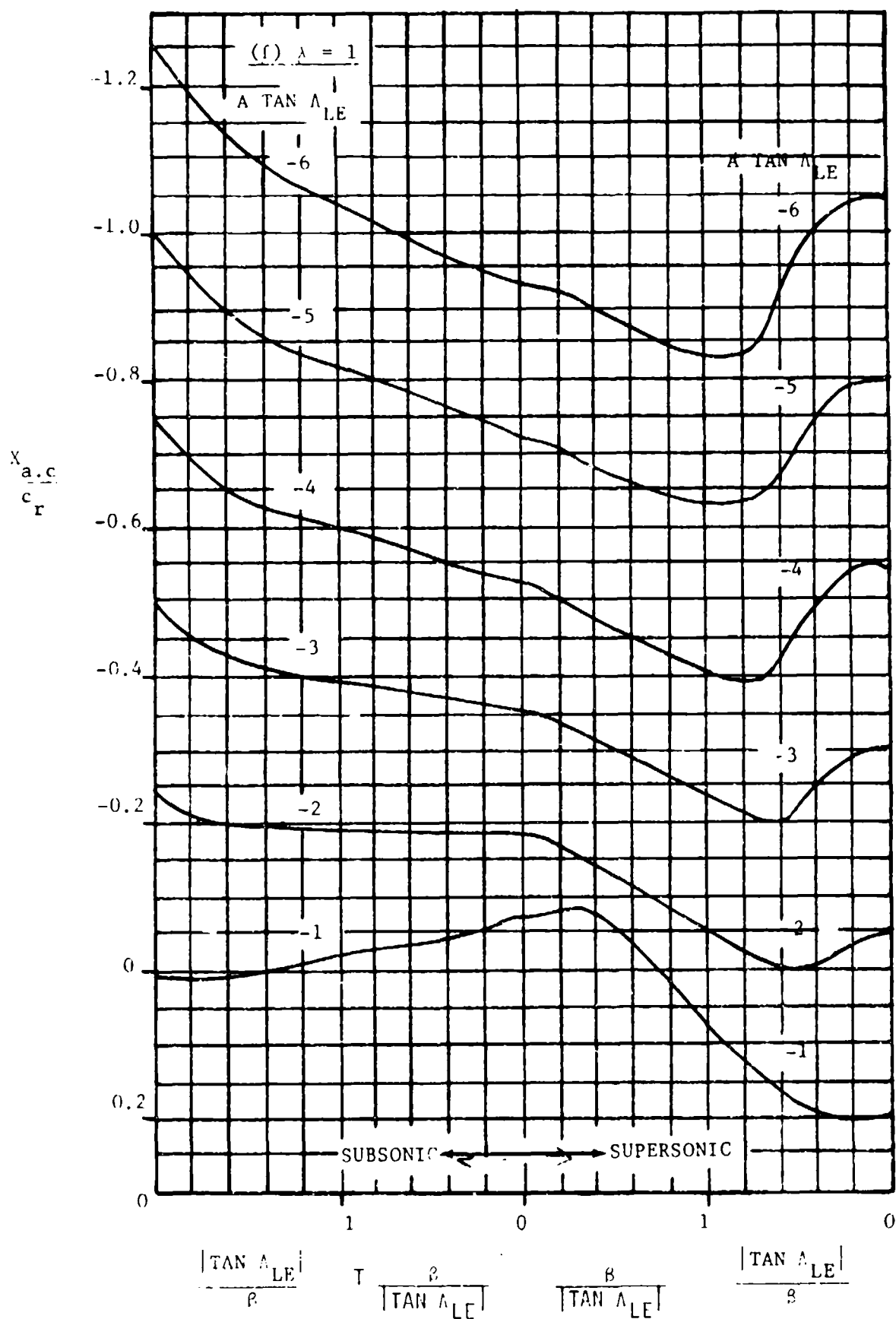


Figure 6. Wing Aerodynamic-Center Position



e. Taper Ratio = 0.5

Figure 6. Wing Aerodynamic-Center Position



f. Taper Ratio = 1.0

Figure 6. Wing Aerodynamic-Center Position

C. Supersonic

The method discussed in Paragraph A of this section is also applicable to the supersonic speed range.

While no wing-alone data were found at this speed, wing-body prediction results showed fair agreement with test data, the average difference being 10.29% of the root chord. Table 7 contains a summary of the planforms analyzed, their parameters, and the test and predicted aerodynamic-center location.

D. Hypersonic

No data were found at this speed.

The method discussed in Paragraph A of this section is applicable in the hypersonic speed range. Values for $\frac{x_{a.c.}}{c_r}$ would come from the extreme right-hand side of Figures 6a through 6f.

4.1.4.3 WING PITCHING MOMENT IN THE NONLINEAR ANGLE-OF-ATTACK RANGE

A. Subsonic

The methods presented in this section are empirical, based entirely on an afterswept wing data base. All attempts to predict sweptforward wing characteristics with any accuracy failed. However, as Figure 7 shows, overall trends can be obtained from Datcom Figure 4.1.4.3 -25, "Empirical Pitch-Up Boundary", by using the absolute value of the quarter-chord sweep angle.

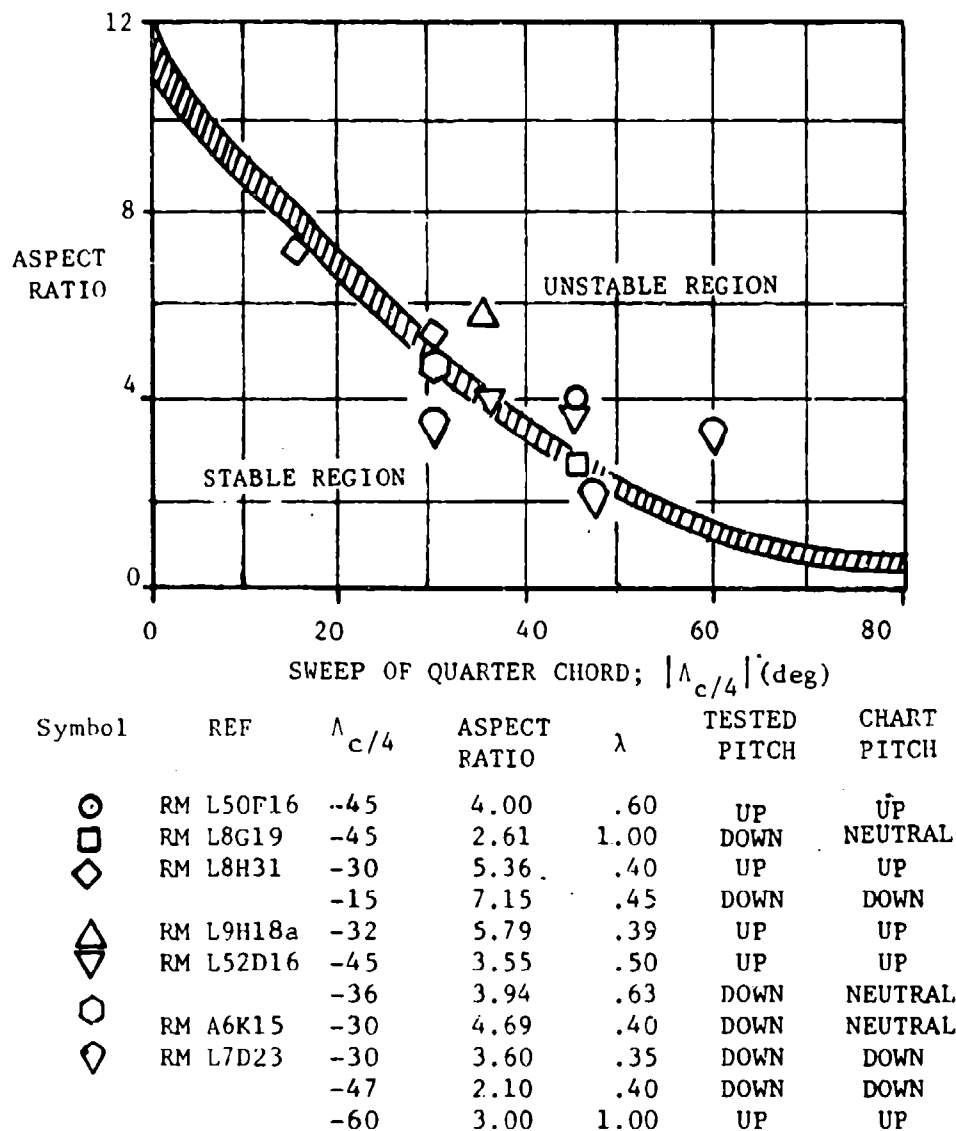


Figure 7. Datcom Figure 4.1.4.3-25, "Empirical Pitch-Up Boundary"

B. Transonic

No sweptforward wing method is presented. Do not use the existing Datcom method.

C. Supersonic

No sweptforward wing method is presented. Do not use the existing Datcom method.

4.1.5.1 WING ZERO-LIFT DRAG

A. All Speeds

No modifications to the Datcom methods are required in any speed range. Table 8 contains a description of the planforms analyzed and their test and predicted values. As no transonic wing-along data were found, wing-body data and results are presented.

At subsonic speeds, the average difference between predicted and test drag values was .00855 (or 85.5 counts). At transonic speeds the difference was .02298 (229.8 counts) and at supersonic speeds the average difference was .03938 (393.8 counts). While these results are adequate for stability and control purposes, they should not be used for performance estimations.

4.1.5.2 WING DRAG AT ANGLE OF ATTACK

A. Subsonic

Datcom Equation 4.1.5.2-h,

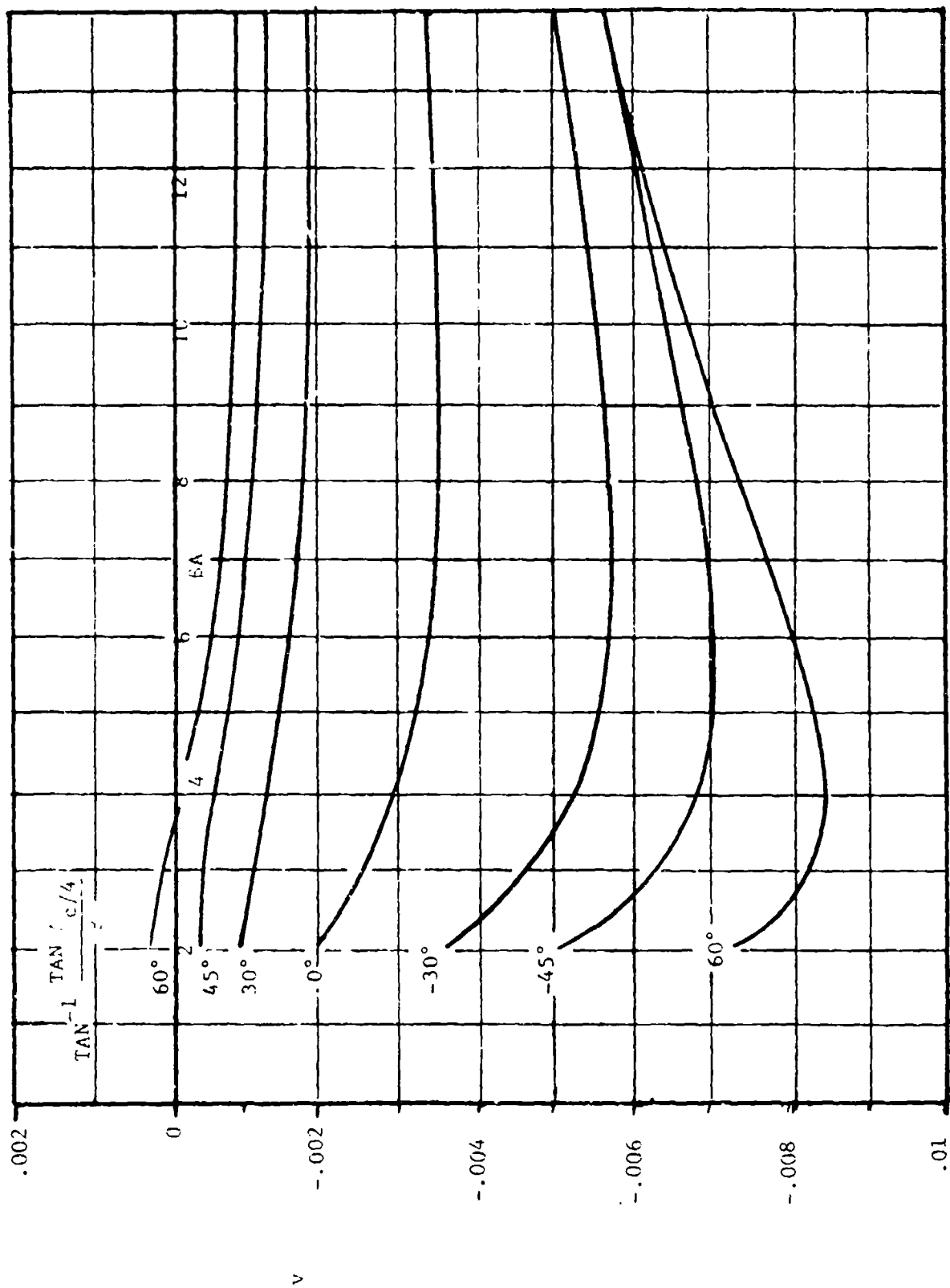
$$C_{D_L} = \frac{C_L^2}{\pi A e} + C_L \odot C_{\ell_\alpha} v + (\odot C_{\ell_\alpha})^2 w \quad (5)$$

is used to estimate wing drag at subsonic speeds. The absolute value of the designated sweep angle is used to obtain values of the span-efficiency factor e and zero-lift drag-due-to-twist factor, w . The induced-drag-due-to-twist factor v , should be obtained from Figure 8 for sweptforward wings. Figure 8 was developed from the methodologies outlined by Lundry in Reference 4. His work appears in the Datcom as Figures 4.1.5.2-42, "Lift-Dependent Drag Factor..." and 4.1.5.2-48, "Zero-Lift Drag Factor...".

An average difference between test and predicted values of 58.2 counts (.00582) was noted for the configurations studied. While this is adequate for stability and control purposes, performance estimates should not be based on Datcom predicted results. Table 9 contains a summary of the planforms examined, their parameters, and predicted and test drag values.

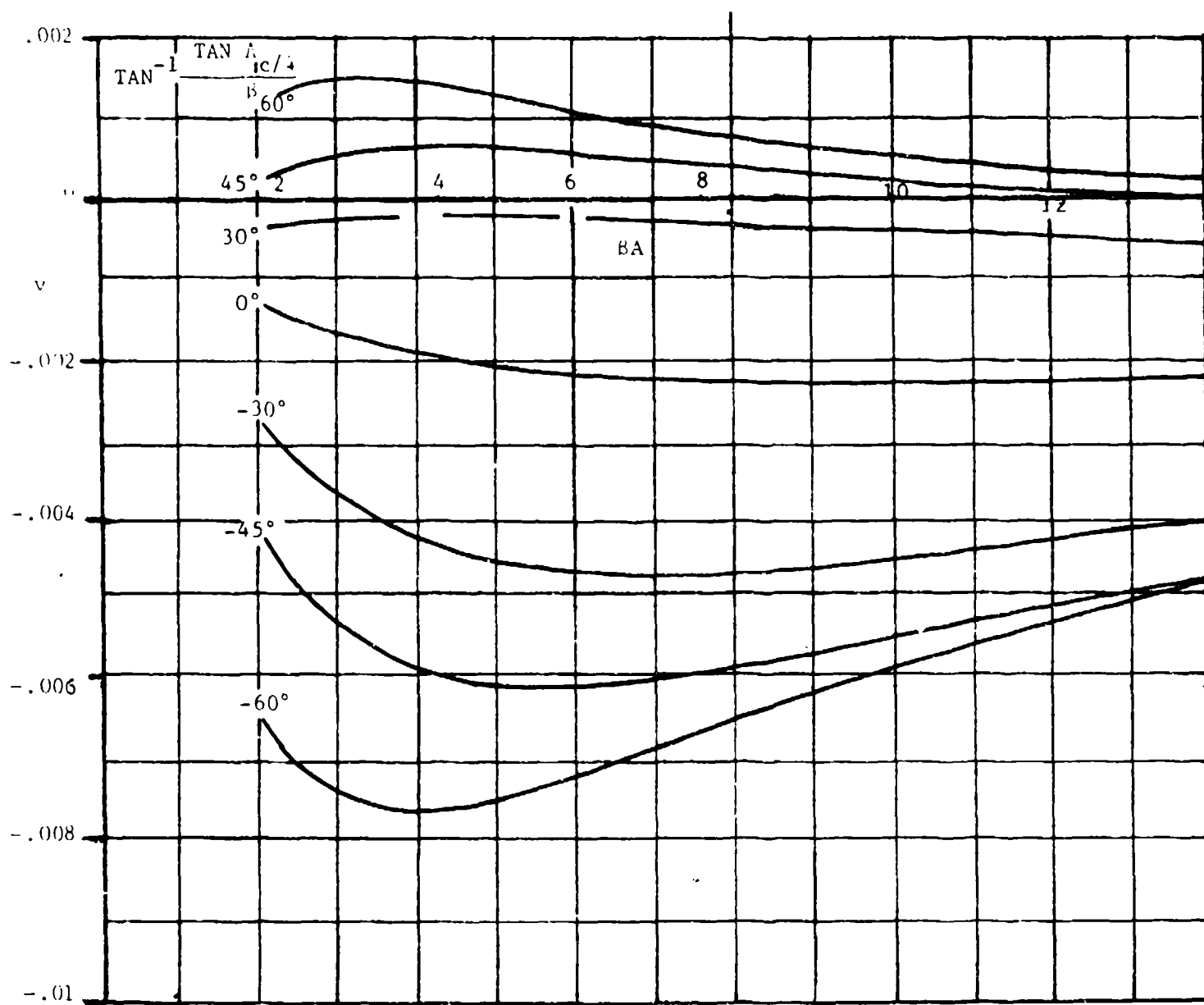
B. Transonic

The methodology in this speed range is entirely empirical, based on aft swept wing data. Accuracy sufficient for stability and control analyses (average difference of 188.8 counts) was obtained for several sweptforward wing configurations by using the absolute value of the leading-edge sweep angle in Datcom Figure 4.1.5.2-55, "Transonic Drag Due to Lift".



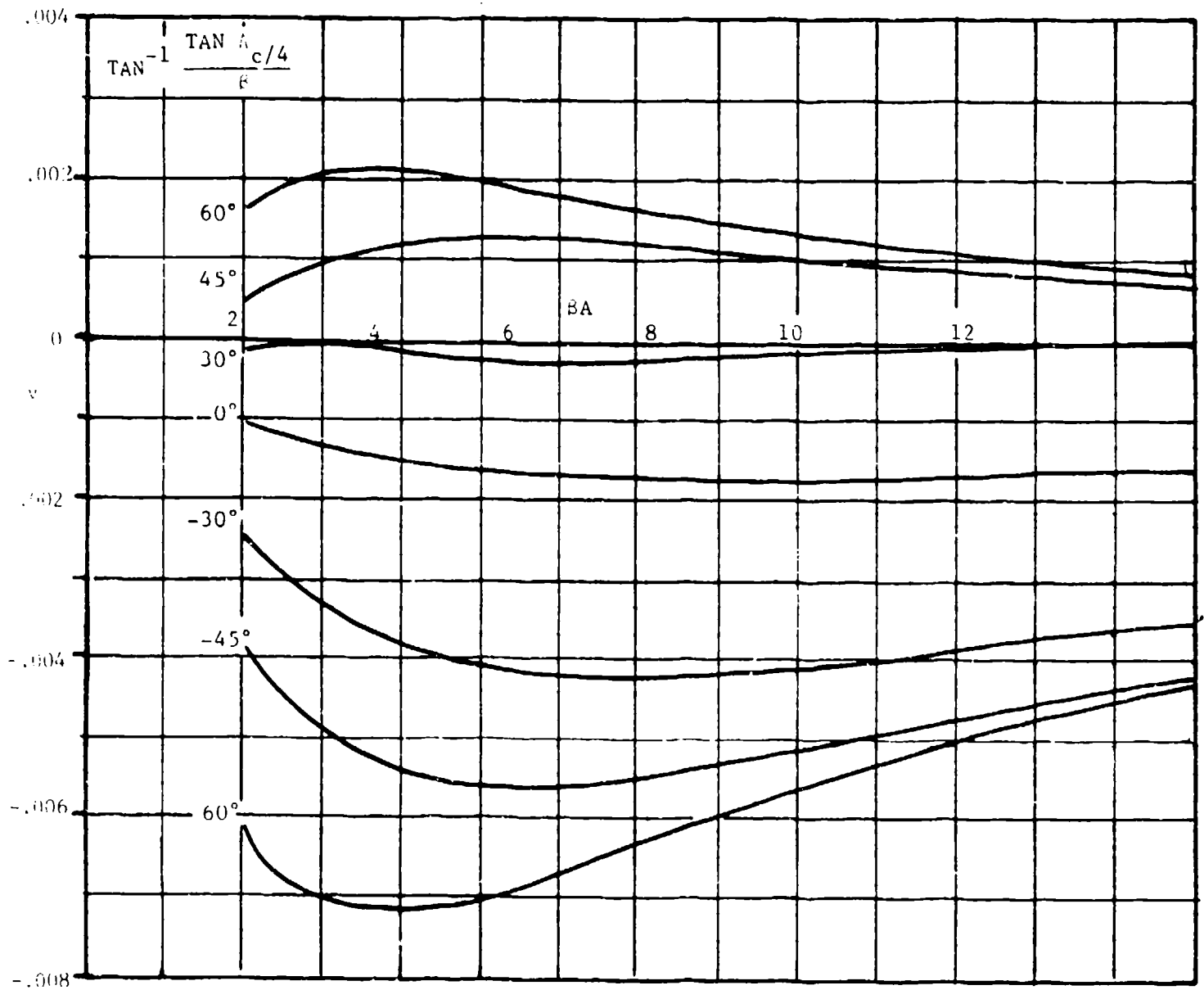
a. Taper Ratio = 0.1

Figure 8. Lift-Dependent Drag Factor Due to Linear Twist



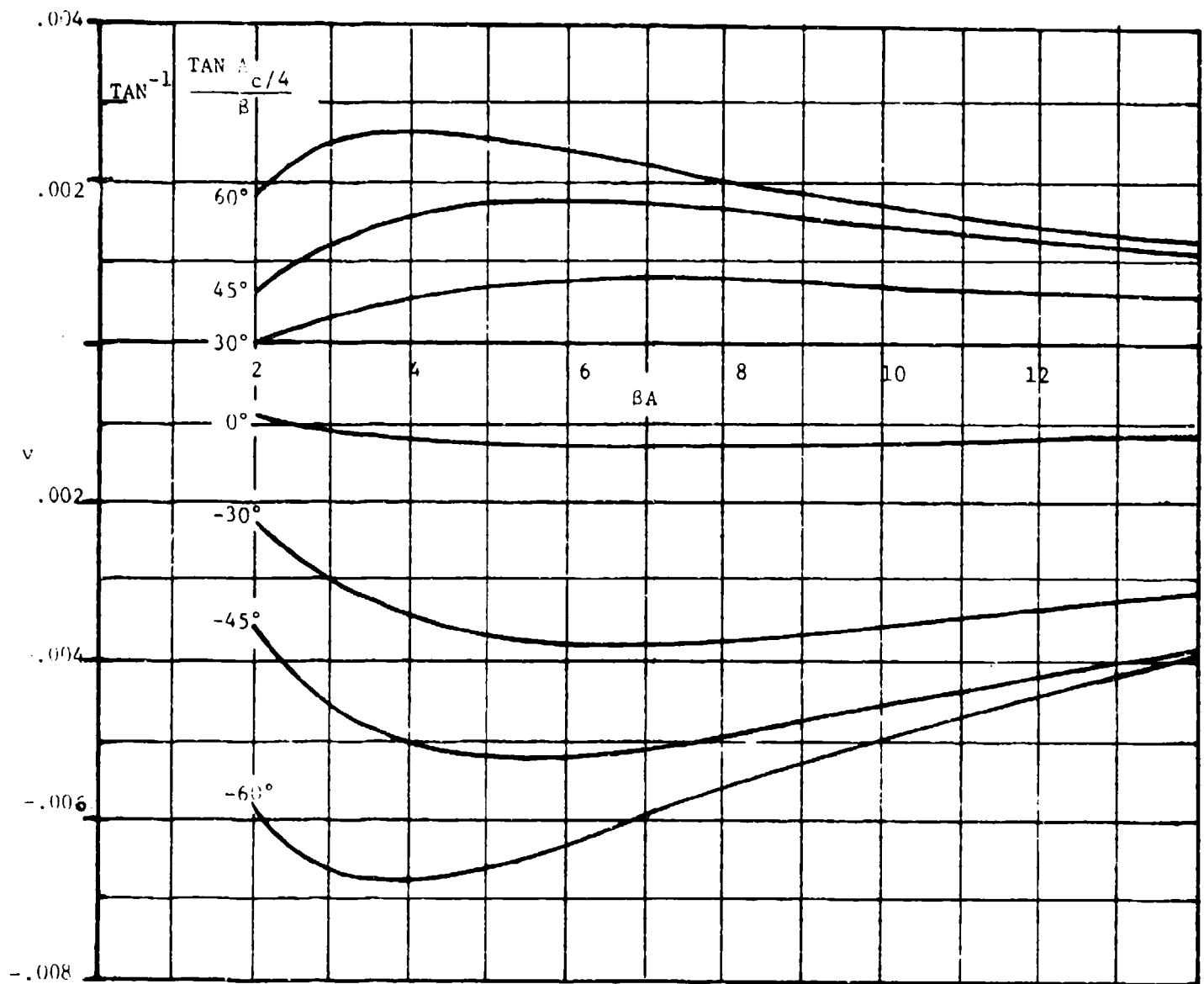
b. Taper Ratio = 0.2

Figure 8. Lift-Dependent Drag Factor Due to Linear Twist



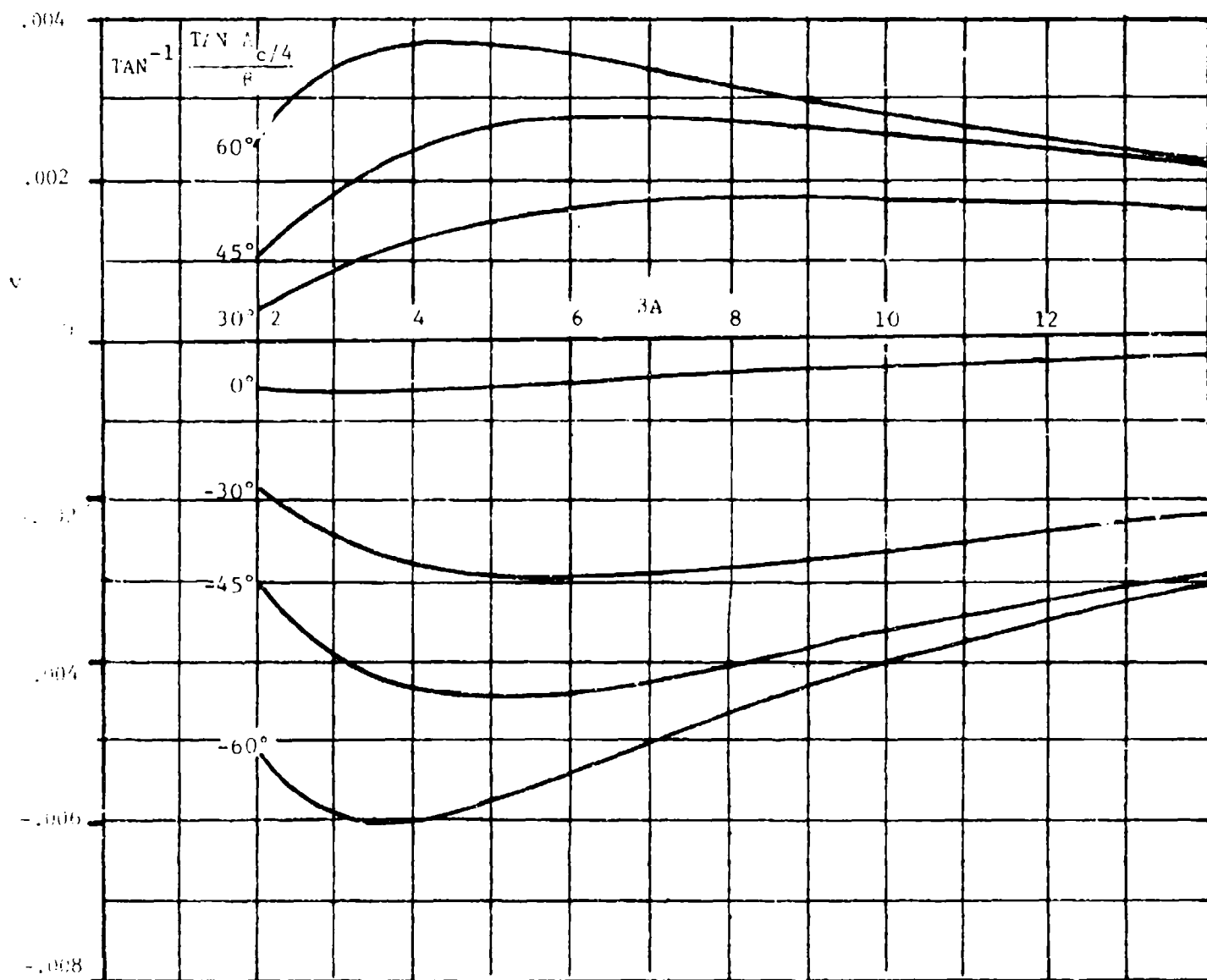
c. Taper Ratio = 0.25

Figure 8. Lift-Dependent Drag Factor Due to Linear Twist



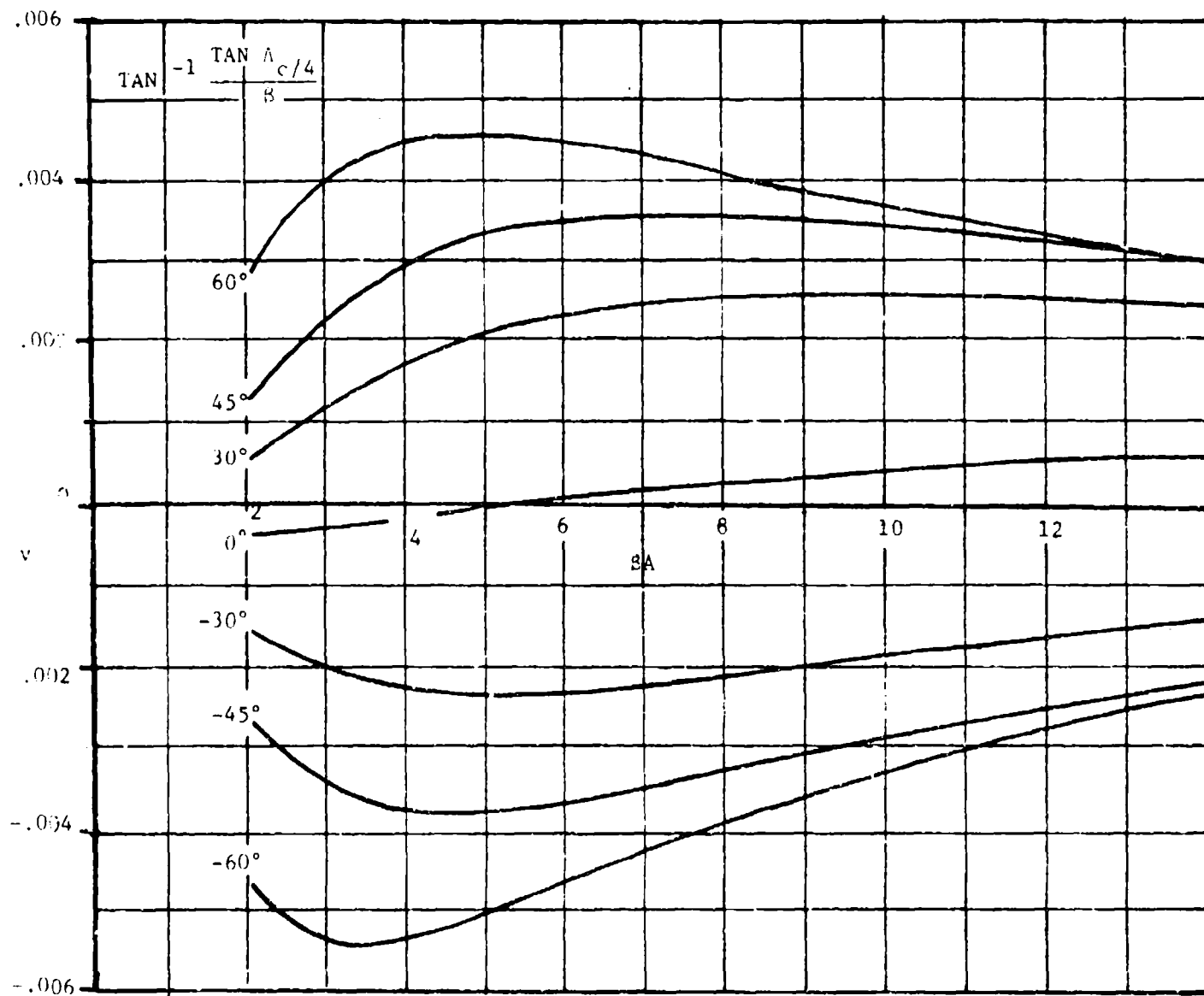
d. Taper Ratio = 0.3

Figure 8. Lift-Dependent Drag Factor Due to Linear Twist



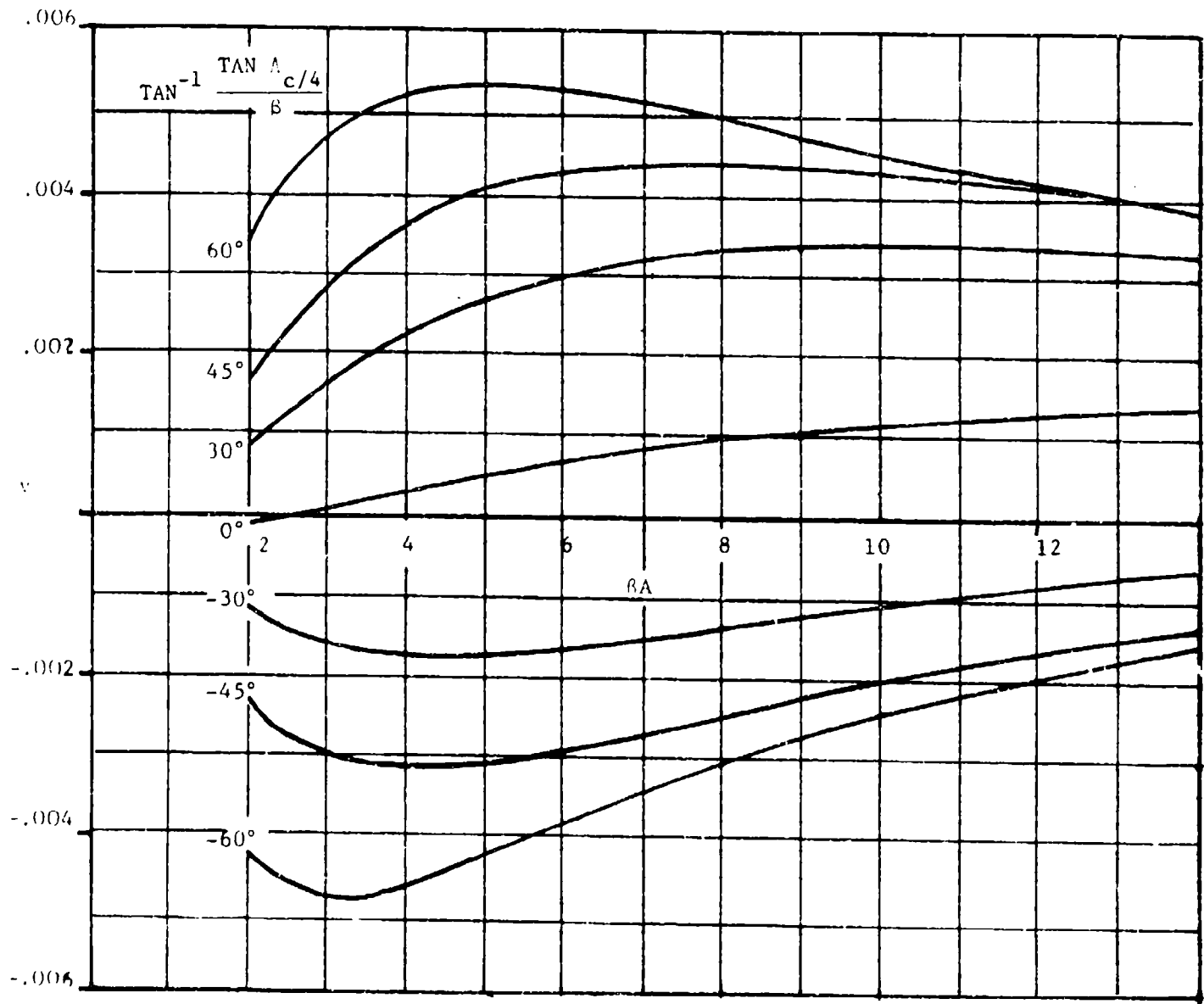
e. Taper Ratio = 0.4

Figure 8. Lift-Dependent Drag Factor Due to Linear Twist



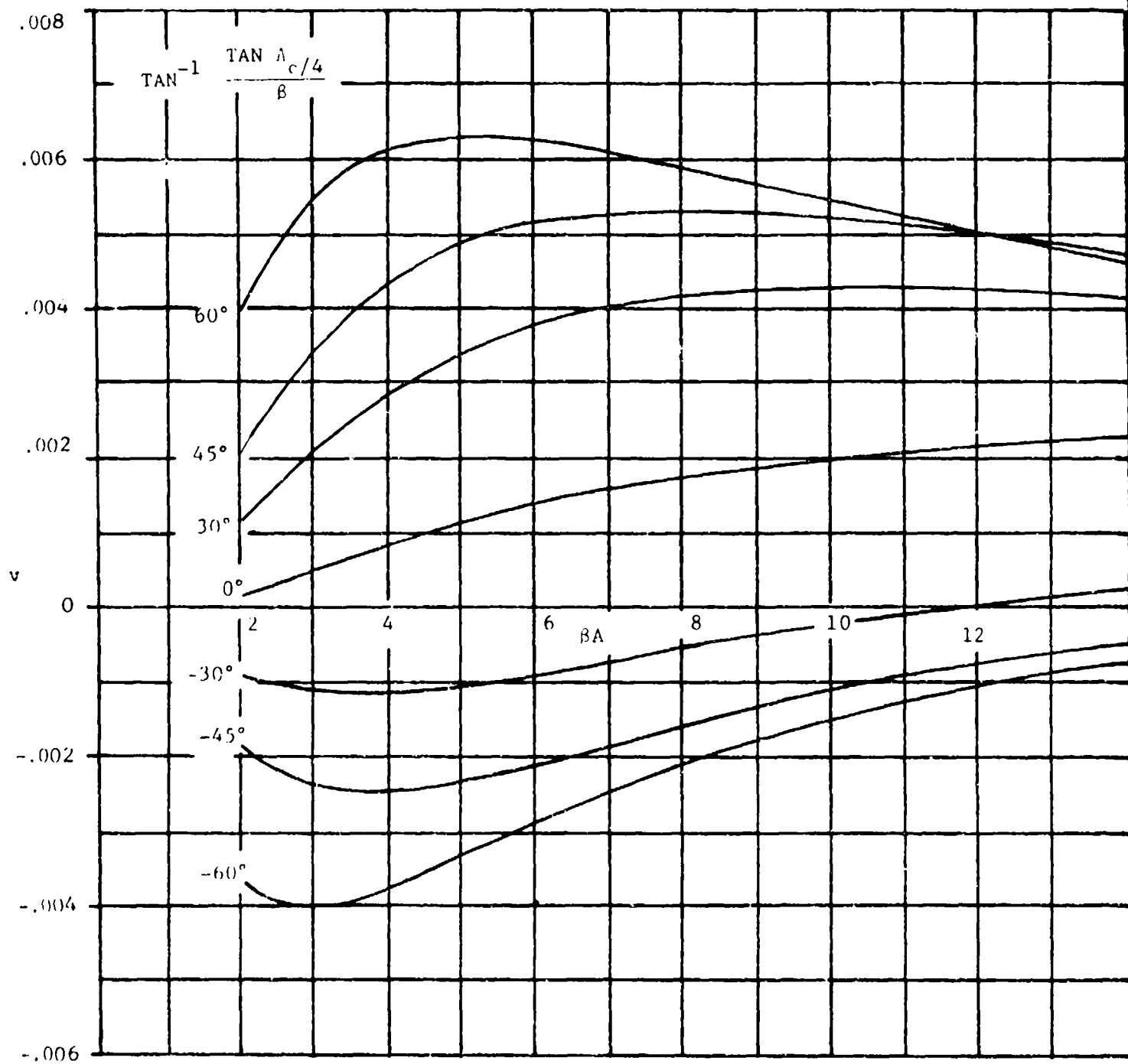
f. Taper Ratio = 0.5

Figure 8. Lift-Dependent Drag Factor Due to Linear Twist



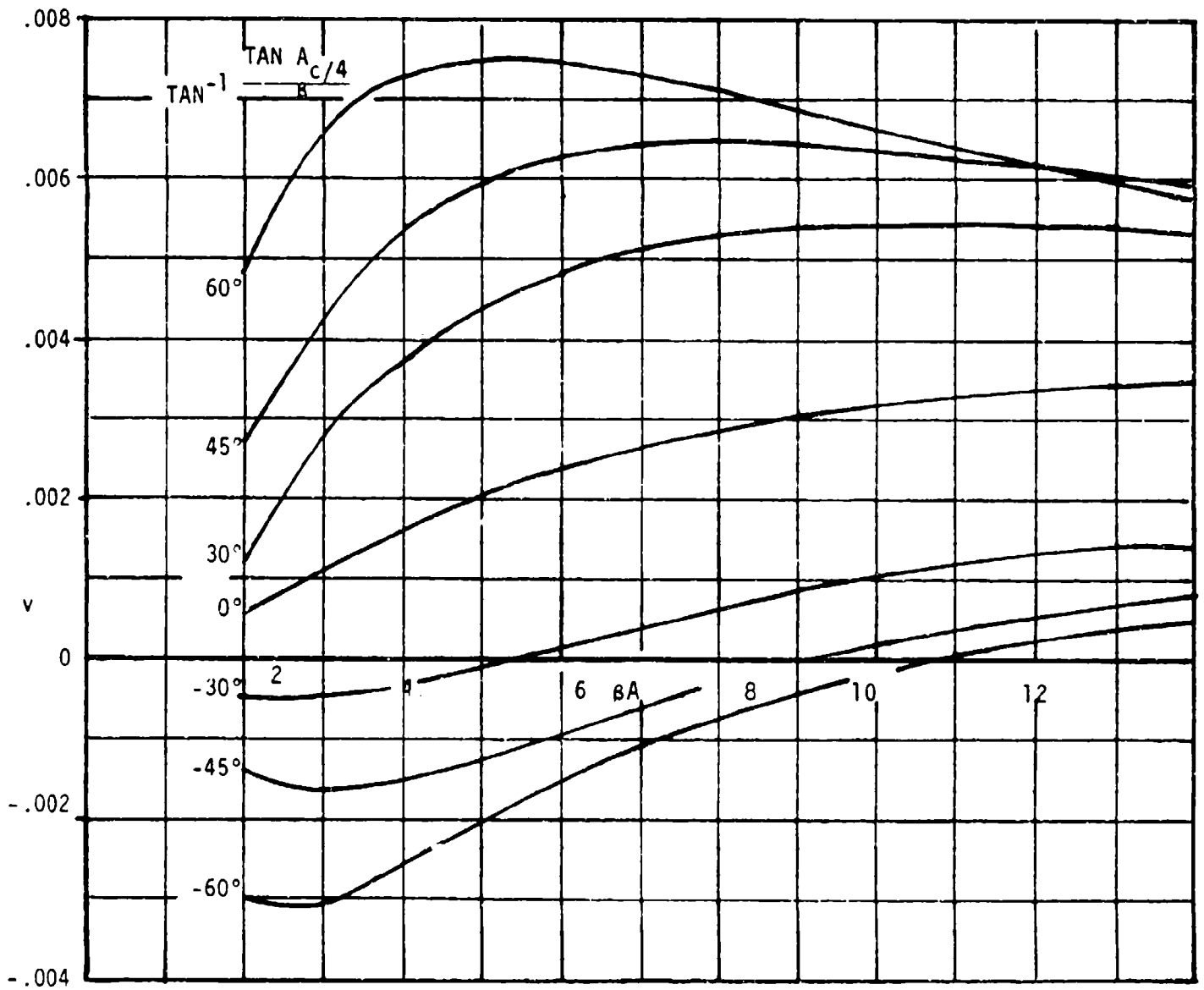
g. Taper Ratio = 0.6

Figure 8. Lift-Dependent Drag Factor Due to Linear Twist



h. Taper Ratio = 0.75

Figure 8. Lift-Dependent Drag Factor Due to Linear Twist



1) Taper Ratio = 1.0

Figure 8. Lift-Dependent Drag Factor Due to Linear Twist

The wing-body planforms analyzed (no wing-alone data were found) are described in Table 10 along with predicted and test drag values. As has been mentioned, the Datcom predicted drag values should not be used for performance estimates.

C. Supersonic

No modifications to the supersonic methodologies are required to estimate sweptforward-wing drag. Wing-body planforms were analyzed using wing-body relations, as no wing-alone data were available.

The difference between predicted and test drag values was an average of 215.6 counts. The individual predicted and test values, along with planform descriptions are listed in Table 11. As has been mentioned above, Datcom drag estimates should not be used for performance estimates.

4.3 WING-BODY, TAIL-BODY COMBINATIONS AT ANGLE OF ATTACK

4.3.1.2 WING-BODY LIFT-CURVE SLOPE

A. Subsonic

No modifications to either method are required. Good agreement between test and predicted lift-curve slopes (5.72% average error) was noted for the configurations analyzed. Table 12 contains a summary of the planforms, their parameters, and test and predicted lift-curve slopes.

B. Transonic

Two relations are used to predict transonic lift-curve slopes:

$$(C_{L_{\alpha}})_{WB} = [K_N + K_{w(B)} + K_{B(w)}] / C_{L_{\alpha}e} \frac{S_e}{S_w} \quad (6)$$

for panels fixed at zero incidence to the body and for panels capable of variable incidence relative to the body,

$$(C_{L_i})_{WB} = [k_{w(B)} + k_{B(w)}] (C_{L_{\alpha}e}) \frac{S_e}{S_w} \quad (7)$$

Modifications to the lift-curve slope of the exposed wing are discussed in Section 4.1.3.2 of this report. These modifications are also applicable when determining the factor K_N . If the factor $K_{B(w)}$ is obtained from Datcom Figure 4.3.1.2-11, "Lift on Body in Presence of Wing...", the absolute value of the trailing-edge sweep angle should be inserted wherever the leading-edge sweep angle is called for.

Figure 3 shows typical wing-body lift-curve slope agreement.

C. Supersonic

The comments of Paragraph B above are applicable here.

Good agreement between test and predicted normal-force-curve slopes (4.80% error) was noted for the configurations analyzed. The data summary and substantiation for this speed range can be found in Table 2.

4.3.1.3 WING-BODY LIFT IN THE NONLINEAR ANGLE-OF-ATTACK RANGE

A. Subsonic

No modifications to either method are required other than those described in Sections 4.1.3.3, "Wing Lift in the Nonlinear Angle-of-Attack Range" and 4.4.1, "Wing-Wing Combinations at Angle of Attack".

Table 13 contains a summary of the planforms, their parameters and test, and predicted lift coefficients in the nonlinear angle-of-attack range. An average error of 19.3% was noted from Method 1 and 14.5% from Method 2 for the planforms evaluated.

B. Transonic

Although no data are available at this speed, no modifications to either method should be needed other than those discussed in Sections 4.1.3.2, "Wing Lift-Curve Slope"; 4.1.3.3, "Wing Lift in the Nonlinear Angle-of-Attack Range"; 4.3.1.2 "Wing-Body Lift-Curve Slope"; and 4.4.1, "Wing-Wing Combinations at Angle of Attack".

C. Supersonic

The comments in Paragraph B of this section are appropriate here.

4.3.1.4 WING-BODY MAXIMUM LIFT

A. Subsonic

Method 1 requires use of a wing-body spanwise-loading computer program. The comments concerning Method 1 in Paragraph A of Section 4.1.3.4, "Wing Maximum Lift" are appropriate here.

Method 2 is based on empirical correlations and the wing-alone method of Datcom Section 4.1.3.4. To predict sweptforward wing maximum lift characteristics, Figure 9a should be used in place of Datcom Figure 4.3.1.4-12b, "Wing-Body Maximum Lift" and Figure 9b should be used in place of Datcom Figure 4.3.1.4-12c, "Angle of Attack for Maximum Lift". Figures 9a and 9b were developed from a vortex-lattice computer code.

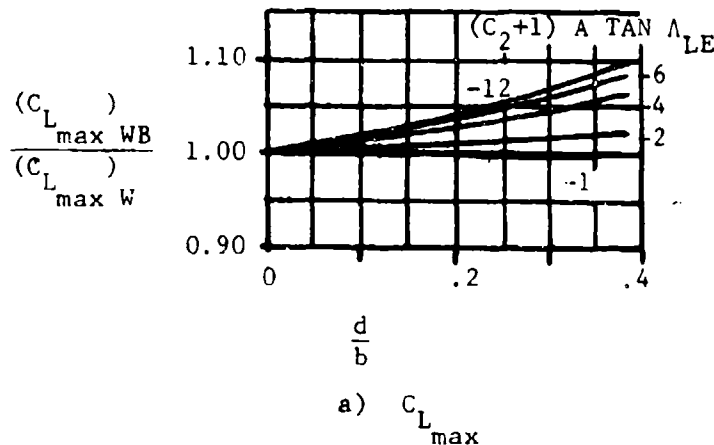


Figure 9. Forward Swept Wing Wing-Body Maximum Lift Correction Factor

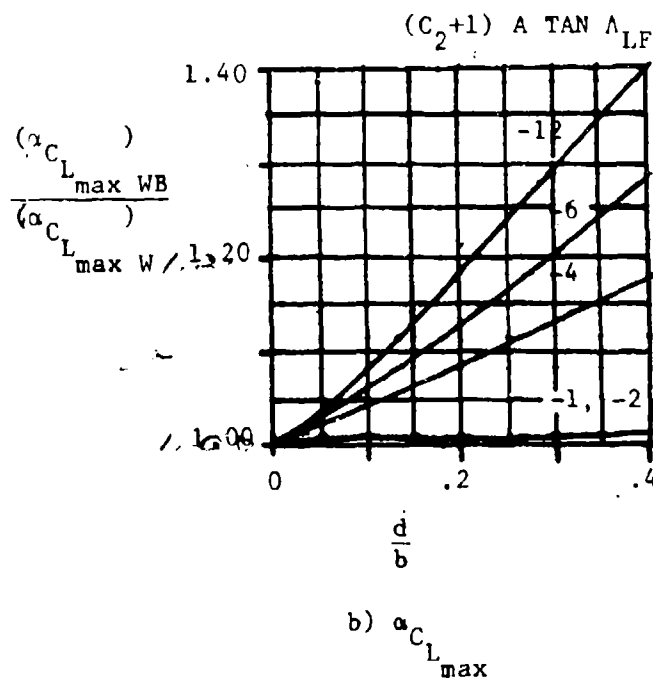


Figure 9. Forward Swept Wing Wing-Body
Maximum Lift Correction Factor

Average errors of 12.4% and 17.0% were noted between test and predicted maximum lift coefficients and angles of attack for maximum lift, respectively. Table 14 presents a summary of the planforms, their parameters, and the test and predicted maximum lift values.

B. Transonic

No Datcom method is presented.

C. Supersonic

While no data were found in this speed range, no modifications should be necessary for either method other than those described in Paragraph C of Sections 4.1.3.4, "Wing Maximum Lift" and 4.3.1.2, "Wing-Body Lift-Curve Slope" for Method 1 and Section 4.3.1.3, "Wing-Body Lift in the Nonlinear Angle-of-Attack Range" for Method 2.

4.3.2.1 WING-BODY ZERO-LIFT PITCHING MOMENT

A. Subsonic

No modifications to Method 1 are required other than those described in Paragraph A of Section 4.1.4.1, "Wing Zero-Lift Pitching Moment". Substantiation of this method was not performed. Several sweptforward configurations were analyzed using Method 2 with poor correlation noted between test and predicted values. Method 2, a linear regression method for fighter-type aircraft, should not be used to estimate forward-swept-wing characteristics.

B. Transonic

The comments in Paragraph A of this section are appropriate here.

C. Supersonic

There is no Datcom method appropriate for sweptforward configurations in this speed range.

4.3.2.2 WING-BODY PITCHING-MOMENT-CURVE SLOPE

A. Subsonic

No modifications are necessary other than those described in Paragraph A of Section 4.1.4.2, "Wing Pitching-Moment-Curve Slope".

Good agreement was noted between test and predicted values (3.67% mean error). Table 15 contains a summary of the planforms studied, their parameters, and test and predicted values.

B. Transonic

The methods in this speed range are based solely on empirical sweptback wing results and should not be used to predict sweptforward wing characteristics. No forward-swept-wing estimation method is presented.

C. Supersonic

The absolute value of the leading-edge sweep angle should be used in Datcom Figures 4.3.2.2-36b, "Theoretical Aerodynamic-Center..." and 4.3.2.2-37, "Aerodynamic-Center Locations...". Also, the modifications described in Paragraph C of Sections 4.1.3.2, "Wing Lift-Curve Slope"; 4.1.4.2, "Wing Pitching-Moment-Curve Slope"; and 4.3.1.2, "Wing-Body Lift-Curve Slope" are appropriate here.

Fair agreement (10.29% mean error) was noted between test and predicted values. Table 7 contains a summary of the planforms, their parameters, and test and predicted values.

4.3.3.1 WING-BODY ZERO-LIFT DRAG

A. Subsonic

No modifications to the Datcom methods are required at this speed. Agreement adequate for stability and control purposes (a mean difference of .00586, or 58.6 counts) was noted between test and predicted drag coefficients. Table 16 contains a summary of the wing-body planforms analyzed, their parameters, and predicted and test results. Datcom drag values should not be used for performance estimation.

B. Transonic

No modifications to the Datcom methods are required at this speed.

Agreement adequate for stability and control purposes (a mean difference of 229.8 counts) was noted between test and predicted drag coefficients. Table 8 contains a summary of the wing-body planforms analyzed, their parameters, and predicted and test results.

Datcom drag values should not be used for performance estimation.

C. Supersonic

The absolute value of the leading-edge sweep angle should be used in all the methodologies and figures at this speed. No other modifications are required.

Agreement adequate for stability and control purposes (a mean difference of 44.8 counts) was noted between test and predicted drag coefficients. Table 17 contains a summary of the wing-body planforms analyzed, their parameters, and predicted and test results.

Datcom drag values should not be used for performance estimation.

4.3.3.2 WING-BODY DRAG AT ANGLE OF ATTACK

A. Subsonic

Method 1 is a linear regression analysis for fighter-type aircraft. This method should not be used to estimate forward swept wing planform characteristics.

Method 2 can be used without any modifications other than those described in Paragraph A of Section 4.1.5.2, "Wing Drag at Angle of Attack". Agreement adequate for stability and control purposes (a mean difference of 169.0 counts) between test and predicted drag coefficients was noted. Table 18 contains a summary of the wing-body planforms analyzed, their parameters, and predicted and test results.

Datcom drag values should not be used for performance estimation.

B. Transonic

The comments concerning methodology use and modifications in Paragraph A of this section are applicable here.

Agreement adequate for stability and control purposes (an average difference of 188.8 counts) was noted between test and predicted drag coefficients. Table 10 contains a summary of the wing-body planforms analyzed, their parameters, and predicted and test results.

Datcom drag values should not be used for performance estimation.

C. Supersonic

The comments concerning methodology use and modification in Paragraph A of this section are applicable here.

Agreement adequate for stability and control purposes (an average difference of 215.6 counts) was noted between test and predicted drag coefficients. Table 11

contains a summary of the wing-body planforms analyzed, their parameters, and predicted and test results.

Datcom drag values should not be used for performance estimation.

4.4 WING-WING COMBINATIONS AT ANGLE OF ATTACK

4.4.1 WING-WING COMBINATIONS AT ANGLE OF ATTACK

A. Subsonic

DOWNWASH

For Method 1, Figure 10 (from Reference 3) should be used in place of Datcom Figure 4.4.1-66, "Effective Wing Aspect Ratio and Span..." when evaluating sweptforward wing planforms. (Increased accuracy can be obtained from Figure 10 and Datcom Figure 4.4.1-66 by multiplying the angle-of-attack parameter, $\frac{\alpha - \alpha_0}{iC_{L_{max}} - \alpha_0}$, by the Oswald efficiency factor, e , obtained from Datcom equation 4.1.5.2-i. The product of this operation, $e \left(\frac{\alpha - \alpha_0}{iC_{L_{max}} - \alpha_0} \right)$, should then be used in place of the angle-of-attack parameter called for in these figures.) The absolute value of the quarter-chord sweep angle should be used in Datcom Figure 4.4.1-67, "Downwash at the Plane of Symmetry...". There are no modifications to Method 1 other than those described in Paragraph A of Section 4.1.3.1, "Wing Zero-Lift Angle of Attack" and 4.1.3.4, "Wing Maximum Lift".

Very good agreement was noted between test and predicted downwash angles (average difference of 1.37°). Table 19 contains a summary of the planforms analyzed, their parameters, and test and predicted results.

Method 2 is an empirical method for estimating the downwash gradient. No modifications are required.

Fair agreement was noted between test and predicted downwash gradients (average difference of $= .0422$). Table 20 contains a summary of the planforms analyzed, their parameters, and test and predicted results.

Method 3 estimates the effect of canards on aft lifting surfaces. Datcom Figure 4.4.1-71, "Wing-Vortex Lateral Position..." should be replaced with Figure 11 for both aft and forward swept wings. No other modifications are necessary other than

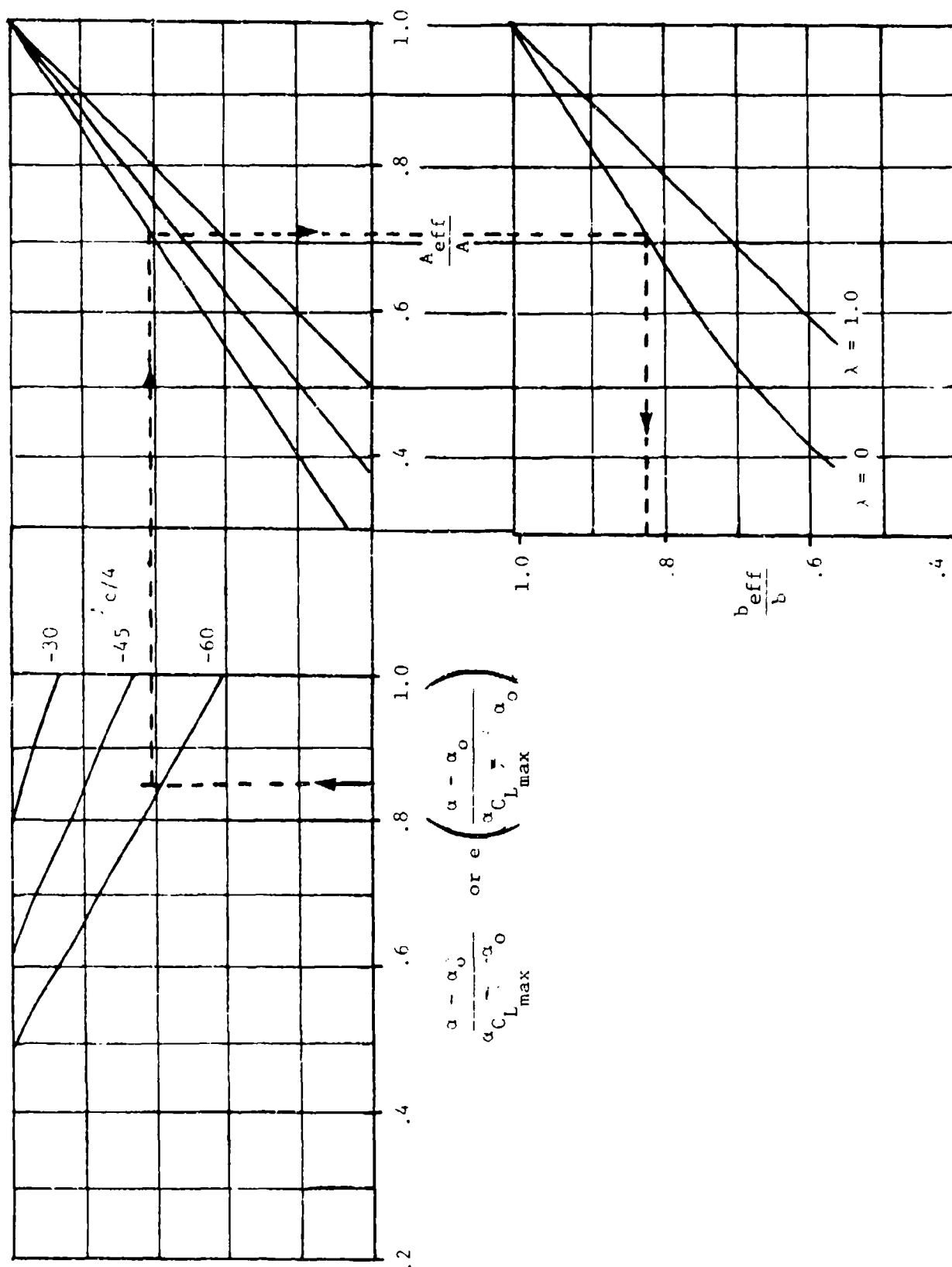


Figure 10. Effective Wing Aspect Ratio and Span for Sweptforward Planforms

those described in Paragraph A of Section 4.3.1.3, "Wing-Body Lift in the Nonlinear Angle-of-Attack Range."

No forward swept wing data were found. Correlation of Figure 11 (based on vortex-lattice code results) and Datcom Figure 4.4.1-71 with aft swept wing test data showed Figure 11 to be more accurate than Datcom Figure 4.4.1-71.

DOWNWASH DUE TO FLAP DEFLECTION

No modifications to this method are necessary. Good agreement was noted between test and predicted downwash angles (mean difference = 1.9887°). Table 21 contains a summary of the planforms analyzed, their parameters, and test and predicted results.

UPWASH

The Datcom method applies to unswept wings only.

DYNAMIC PRESSURE RATIO

No modifications for this method are necessary.

Good agreement between test and predicted values was noted (average difference = .053). Table 22 contains a summary of the planforms analyzed, their parameters, and test and predicted ratios.

B. Transonic

DOWNWASH

No modifications seem required other than those discussed in Paragraph B of Sections 4.1.3.2, "Wing Lift-Curve Slope" and 4.1.3.3, "Wing Lift in the Nonlinear Angle-of-Attack Range."

No data were found to substantiate this section.

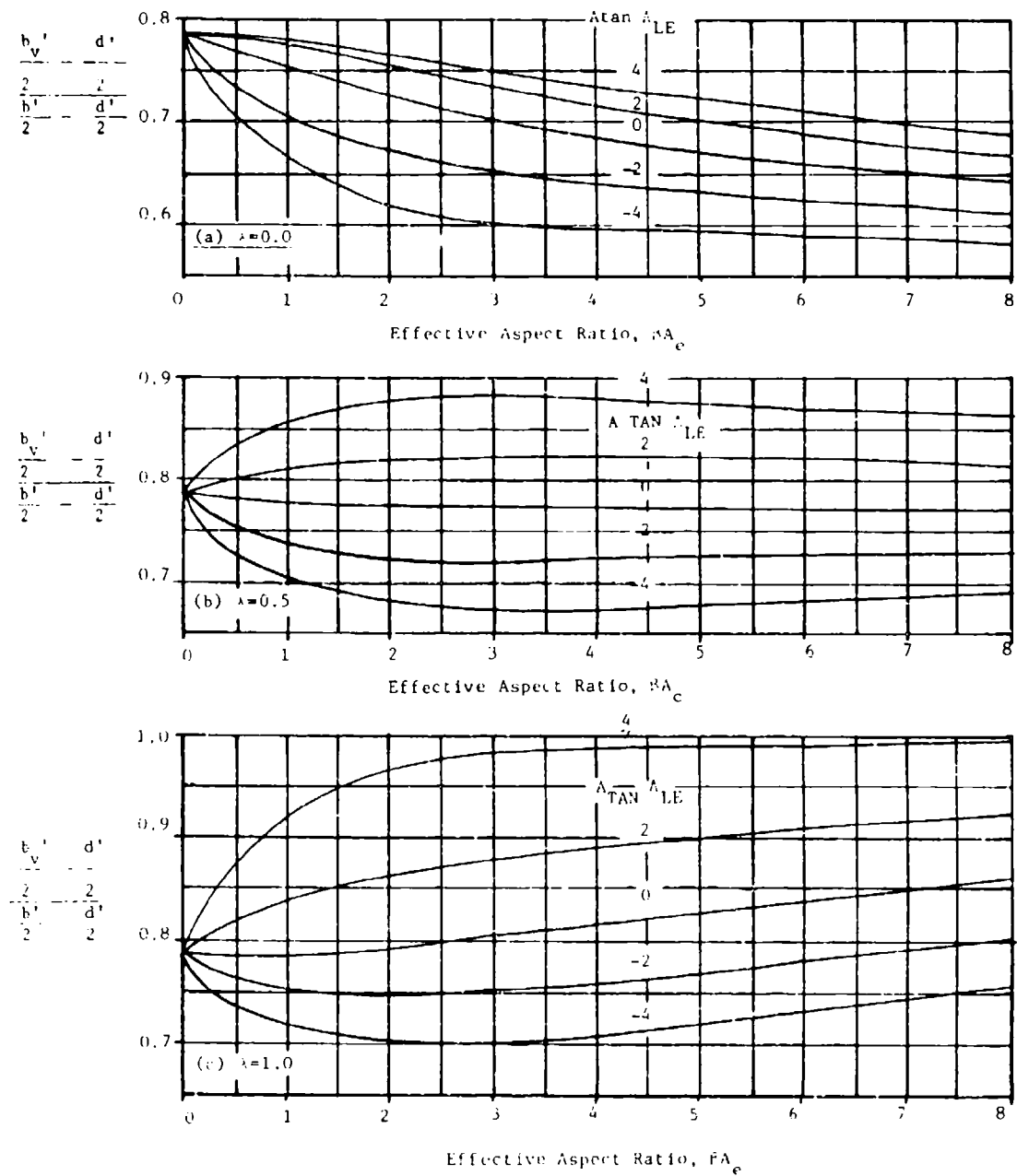


Figure 11. Wing-Vertex Lateral Positions at Subsonic Speeds

DYNAMIC PRESSURE RATIO

No modifications for this method are necessary.

C. Supersonic

DOWNWASH

No modifications to Method 1 are required. Method 2 is inapplicable to wings with sweptforward leading edges. However, rectangular wing results could be used as a rough approximation. For Method 3, Datcom Figure 4.4.1-80, "Wing Vortex Lateral Position..." should be replaced with Figure 12 for aft and forward swept wings. Figure 12 was obtained from a supersonic vortex-lattice code.

No data have been found to substantiate the previous modifications. Correlation of Figure 12 and Datcom Figure 4.4.1-80 with aft swept wing data indicates that better accuracy was obtained with values obtained from Figure 12.

DYNAMIC PRESSURE RATIO

No modifications appear to be required for this method.

No data have been found to substantiate this methodology.

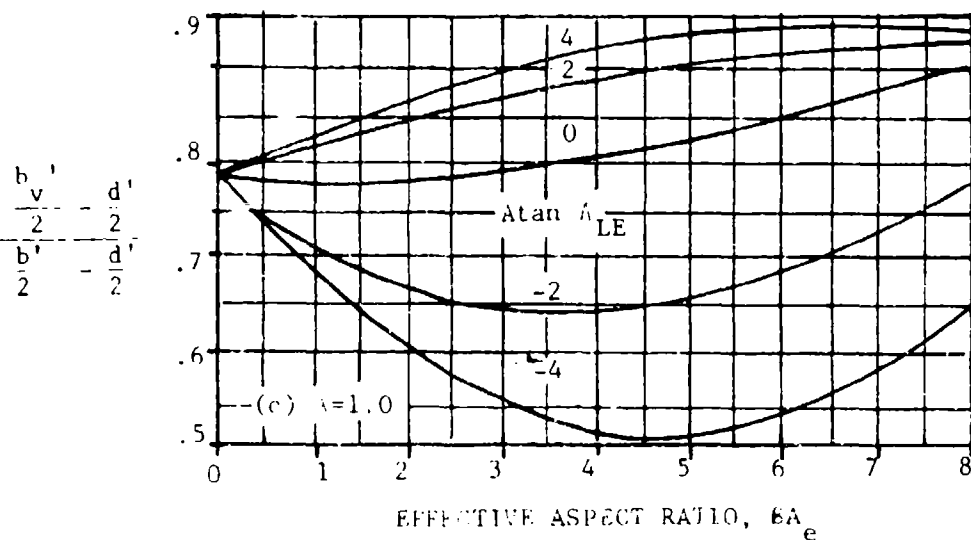
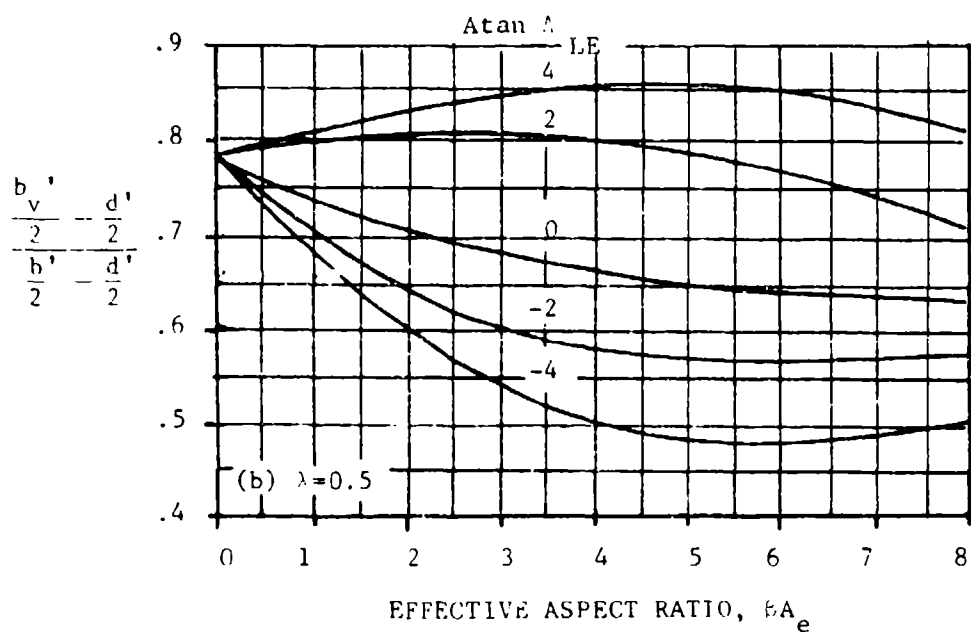
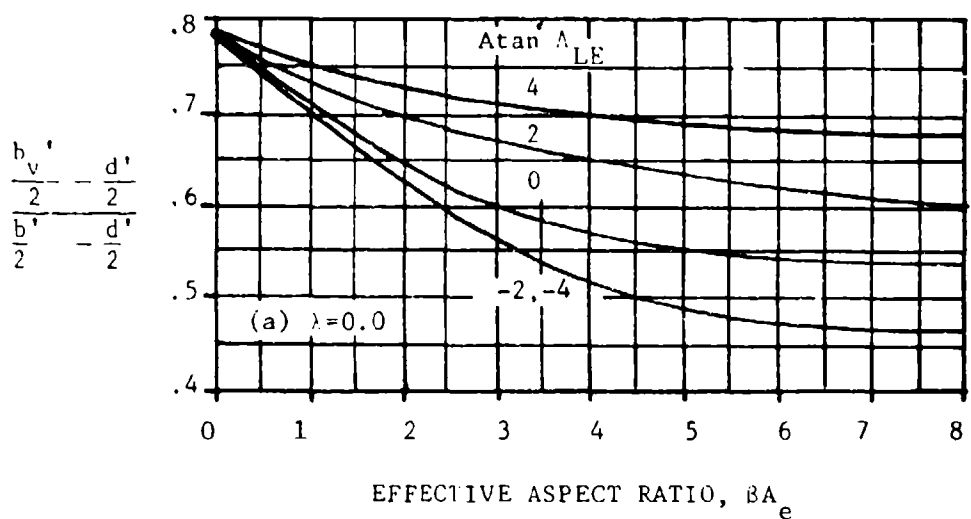


Figure 12. Wing-Vortex Lateral Positions at Supersonic Speeds

4.5 WING-BODY-TAIL COMBINATIONS AT ANGLE OF ATTACK

No correlations between predicted results and test data were performed for wing-body-tail configurations. It was felt that validation of the wing-alone, wing-body, and wing-wing methodologies was sufficient.

4.5.1.1 WING-BODY-TAIL LIFT-CURVE SLOPE

A. All Speeds

No modifications to either method are required other than those described in Sections 4.1.3.2, "Wing Lift-Curve Slope"; 4.3.1.2, "Wing-Body Lift-Curve Slope"; and 4.4.1, "Wing-Wing Combinations at Angle of Attack" in the appropriate speed range.

4.5.1.2 WING-BODY-TAIL LIFT IN THE NONLINEAR ANGLE-OF-ATTACK RANGE

A. All Speeds

No modifications to either method are required other than those described in Sections 4.1.3.2, "Wing Lift-Curve Slope", 4.1.3.3, "Wing Lift in the Nonlinear Angle-of-Attack Range"; 4.1.3.4, "Wing Maximum Lift"; 4.3.1.2 "Wing-Body Lift-Curve Slope"; 4.3.1.3, "Wing-Body Lift in the Nonlinear Angle-of-Attack Range", and 4.4.1, "Wing-Wing Combinations at Angle of Attack" in the appropriate speed range.

4.5.1.3 WING-BODY-TAIL MAXIMUM LIFT

A. All Speeds

No modifications are necessary other than those described in Sections 4.1.4.1, "Wing Pitching-Moment-Curve Slope"; 4.1.4.3, "Wing Pitching Moment in the Nonlinear Angle-of-Attack Range"; 4.3.1.4, "Wing-Body Maximum Lift"; 4.3.2.2, "Wing-Body Pitching-Moment-Curve Slope"; 4.3.3.1, "Wing-Body Zero-Lift Drag"; 4.3.3.2, "Wing-Body Drag at Angle of Attack"; and 4.4.1, "Wing-Wing Combinations at Angle of Attack" in the appropriate speed range.

4.5.2.1 WING-BODY-TAIL PITCHING-MOMENT-CURVE SLOPE

A. All Speeds

No modifications to either method are required other than those described in Sections 4.3.1.2, "Wing-Body Lift-Curve Slope"; 4.3.2.2, "Wing-Body Pitching-Moment-Curve Slope"; 4.3.3.2, "Wing-Body Drag at Angle of Attack"; and 4.4.1, "Wing-Wing Combinations at Angle of Attack" in the appropriate speed range.

4.5.3.1 WING-BODY-TAIL ZERO-LIFT DRAG

A. Subsonic

No modifications are necessary. Datcom drag values should not be used for performance estimation.

B. Transonic

The absolute value of the quarter-chord sweep angle should be used in Datcom Figure 4.5.3.1-19, "Drag Divergence Mach Number Chart". No other modifications are necessary. Datcom drag values should not be used for performance estimation.

C. Supersonic

No modifications are necessary other than those described in Paragraph C of Section 4.3.3.1, "Wing-Body Zero-Lift Drag". Datcom drag values should not be used for performance estimation.

4.5.3.2 WING-BODY-TAIL DRAG AT ANGLE OF ATTACK

A. All Speeds

No modifications are necessary other than those described in Sections 4.1.3.1. "Wing Zero-Lift Angle of Attack"; 4.1.5.1, "Wing Zero-Lift Drag"; 4.3.1.2 "Wing-Body Lift-Curve Slope"; 4.3.2.1, "Wing-Body Zero-Lift Pitching Moment"; 4.3.2.2, "Wing-Body Pitching-Moment-Curve Slope"; 4.3.3.1, "Wing-Body Zero-Lift Drag"; 4.3.3.2, "Wing-Body Drag at Angle of Attack"; and 4.4.1, "Wing-Wing Combinations at Angle of Attack" in the appropriate speed range. Datcom drag values should not be used for performance estimation.

4.6 POWER EFFECTS AT ANGLE OF ATTACK

No modifications are expected other than those described for the power-off coefficients.

No data have been found to substantiate these methodologies.

4.7 GROUND EFFECTS AT ANGLE OF ATTACK

No modifications are expected other than those described for the out-of-ground-effect coefficients.

No data have been found to substantiate these methodologies.

4.8 LOW-ASPECT-RATIO WINGS AND WING-BODY COMBINATIONS AT ANGLE OF ATTACK

This section is based on delta wing shapes and should not be used for analysis of sweptforward planforms.

5.1 WINGS IN SIDESLIP

5.1.1.1 WING SIDESLIP DERIVATIVE C_{Y_B} IN THE LINEAR
ANGLE OF ATTACK RANGE

A. Subsonic

No modifications for this method are required.

Fair accuracy was obtained, as shown in Figure 13, for the planforms analyzed.

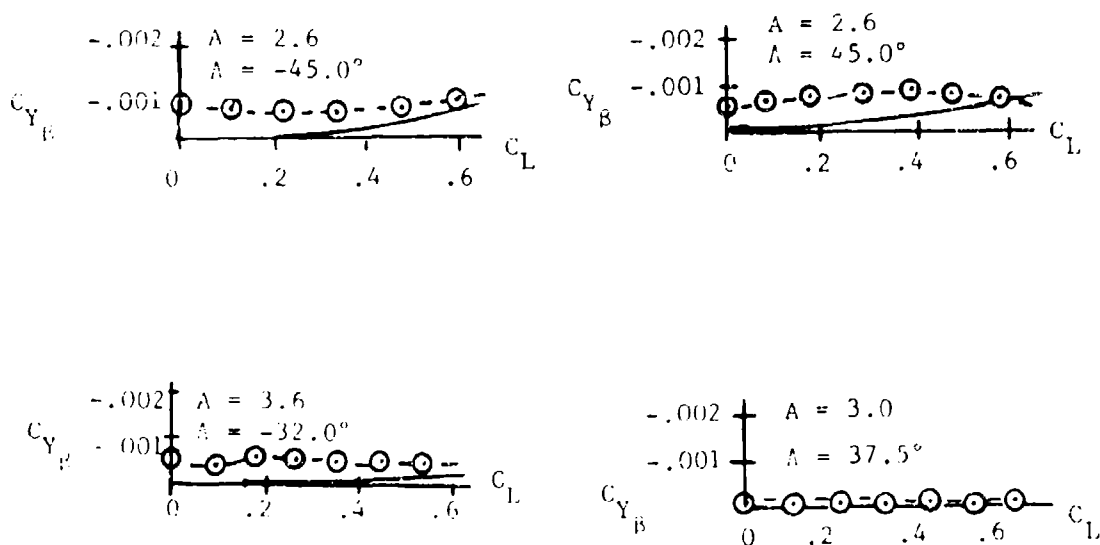


Figure 13. Comparison of Calculated and Experimental Values
of C_{Y_B}

B. Transonic

No method is presented.

C. Supersonic

The existing relations do not account for wings with sweptforward leading edges. The rectangular planform methodology can be used for a first approximation.

5.1.2.1 WING SIDESLIP DERIVATIVE C_{ℓ_B} IN THE LINEAR ANGLE-OF-ATTACK

A. Subsonic

The only modification to this method is in adapting Datcom Figure 5.1.2.1-27, "Wing Sweep Contribution...". That figure, based on work done by Polhamus and Sleeman (Reference 5) was found to be oddly reflexive. Changing the sign of the midchord sweep angle (from positive to negative) results in a change of sign for the sweep contribution factor (from negative to positive) with the magnitude remaining unchanged. To illustrate, for a wing with an aspect ratio of 8.0, a taper ratio of 0.5 and a midchord sweep angle of 40 degrees, the sweep contribution factor is $-.004$ (Figure 14). For the same wing swept forward 40 degrees at the midchord point, its sweep contribution factor is $.004$. The sweep factor is then used in Datcom Equation 5.1.2.1-a just as the aft-swept sweep correction factor would be used.

Good agreement was noted between test and predicted rolling moments (Figure 15).

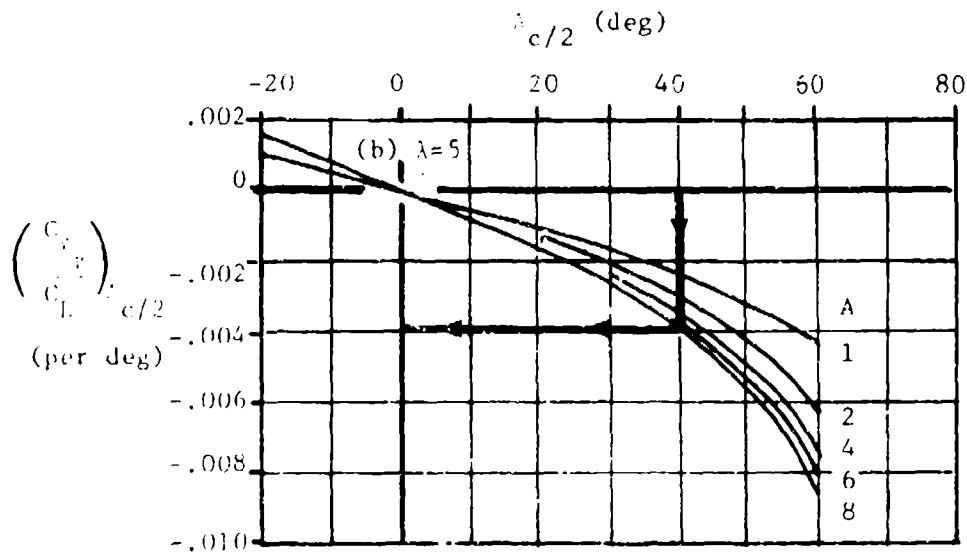


Figure 14. Datcom Figure 5.1.2.1-27, "Wing Sweep Contribution to C_{ℓ_B} "; (b) $\lambda = .5$

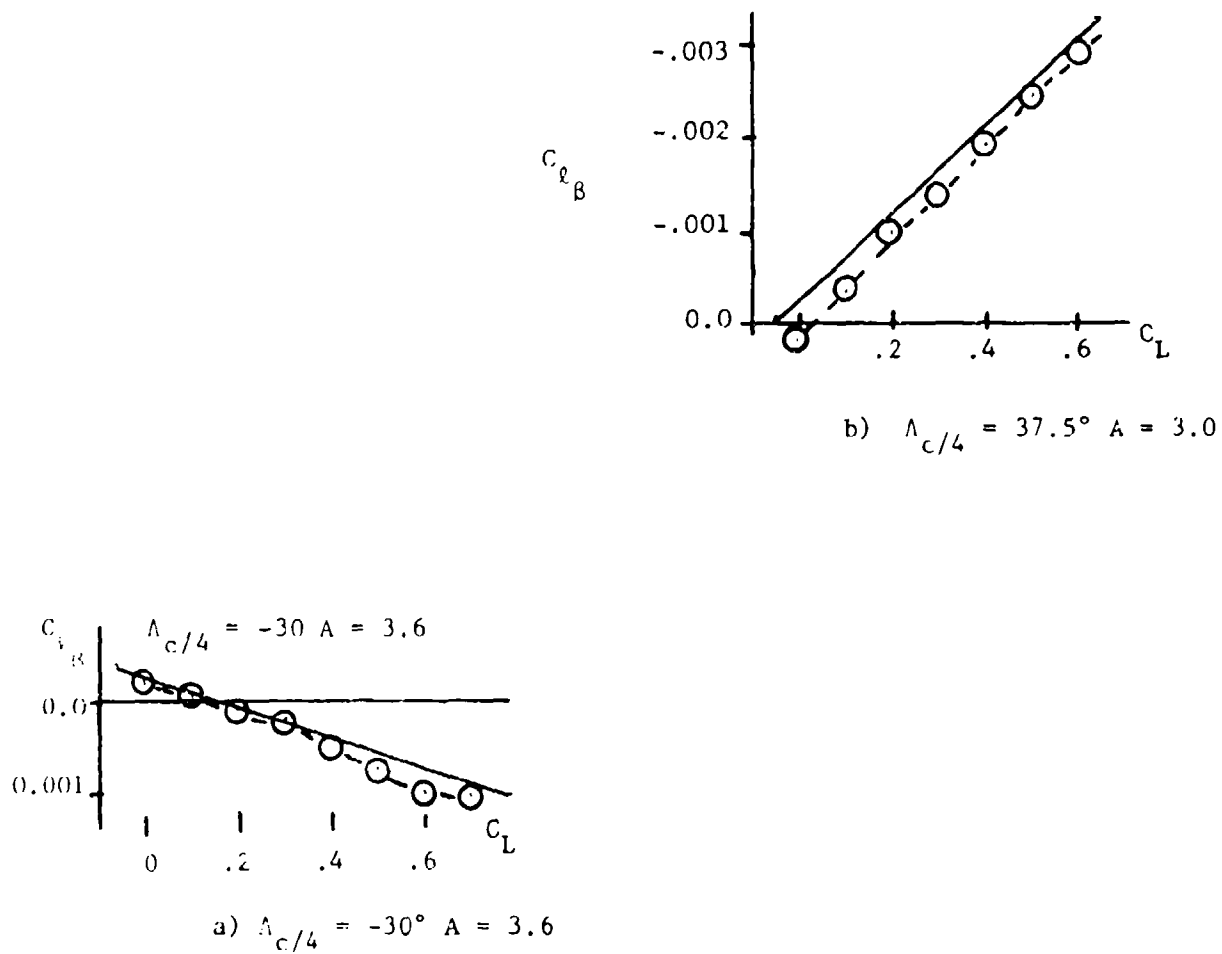


Figure 15. Comparison of Calculated and Experimental Values of C_{l_B}

B. Transonic

No modifications to this method are required other than those described in Paragraphs A and C of this section and in Paragraph B of Section 4.1.3.2, "Wing Lift-Curve Slope".

While no wing-alone data were found at this speed, good agreement (average difference = .000879) was noted between test and predicted wing-body results. Table 23 contains a summary of the planforms analyzed, their parameters, and test and predicted results.

C. Supersonic

No modifications are necessary other than those described in Paragraph C of Sections 4.1.3.2, "Wing Lift-Cover Slope" and 7.1.2.2, "Wing Rolling Derivative C_{ξ_p} ".

Good agreement (average difference = .000116) was noted between test and predicted wing-body values. No wing-alone data were found at this speed. Table 24 contains a summary of the planforms analyzed, their parameters, and test and predicted values.

5.1.2.2 WING ROLLING-MOMENT COEFFICIENT C_l AT ANGLE OF ATTACK

A. All Speeds

No modifications are necessary.

5.1.3.1 WING SIDESLIP DERIVATIVE $C_{n\beta}$ IN THE LINEAR ANGLE-OF-ATTACK RANGE β

A. Subsonic

No modifications to the methodologies are necessary. Good agreement (Figure 16) was noted between test and predicted results.

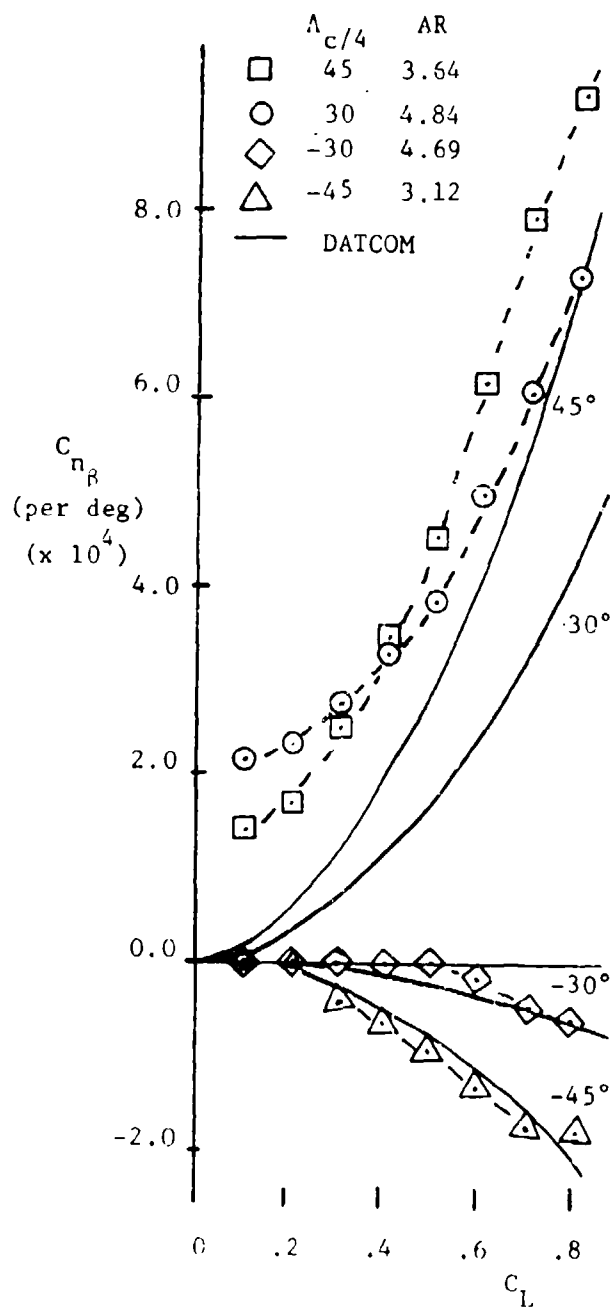


Figure 16. Comparison of Calculated and Experimental Values of $C_{n\beta}$

B. Transonic

No method is presented.

C. Supersonic

The comments in Paragraph C of Section 5.1.1.1 are appropriate here.

5.2 WING-BODY COMBINATIONS IN SIDESLIP

5.2.1.1 WING-BODY SIDESLIP DERIVATIVE $C_{Y\beta}$ IN THE LINEAR ANGLE-OF-ATTACK RANGE

A. All Speeds

No modifications are necessary as the methodologies are independent of sweep angle.

No substantiation was performed.

5.2.1.2 WING-BODY SIDE-FORCE COEFFICIENT C_Y AT ANGLE OF ATTACK

A. All Speeds

No modifications are necessary.

5.2.2.1 WING-BODY SIDESLIP DERIVATIVE $C_{l\beta}$ IN THE LINEAR ANGLE-OF-ATTACK RANGE

A. Subsonic

No modifications are required other than those described in Paragraph A of Section 5.1.2.1, "Wing Sideslip Derivative $C_{l\beta}$ ".

Good agreement (average difference = .000211) was noted between test and predicted values. Table 25 contains a summary of the planforms analyzed, their parameters, and the test and predicted results.

B. Transonic

No modifications are necessary other than those described in Paragraph B of Section 5.1.2.1, "Wing Sideslip Derivative $C_{l\beta}$...".

Good agreement (average difference = .00038) was noted between test and predicted results. Table 23 contains a summary of the planforms analyzed, their parameters, and test and predicted results.

C. Supersonic

No modifications are necessary other than those described in Paragraph C of Section 5.1.2.1, "Wing Sideslip Derivative $C_{l\beta}$...".

Good agreement (average difference = .00012) was noted between test and predicted values. Table 24 contains a summary of the planforms analyzed, their parameters, and test and predicted values.

5.2.3.1 WING-BODY SIDESLIP DERIVATIVE $C_{n\beta}$ IN THE
LINEAR ANGLE-OF-ATTACK RANGE

A. All Speeds

The comments in Paragraph A of Section 5.2.1.1, "Wing-Body Sideslip Derivative $C_{Y\beta}$...", are appropriate here.

5.2.3.2 WING-BODY YAWING-MOMENT COEFFICIENT $C_{n\alpha}$ AT
ANGLE OF ATTACK

A. Subsonic

The comments in Paragraph A of Section 5.2.1.1, "Wing-Body Sideslip Derivative $C_{Y\beta}$..." are appropriate here.

B. Transonic

No method is presented.

C. Supersonic

The comments in Paragraph A of this section are appropriate here.

5.3 TAIL-BODY COMBINATIONS IN SIDESLIP

5.3.1.1 TAIL-BODY SIDESLIP DERIVATIVE C_Y IN THE LINEAR ANGLE-OF-ATTACK RANGE β

A. Subsonic

No modifications are required. At this time, no sweptforward vertical tail data have been found to substantiate the methodologies.

B. Transonic

No method is presented.

C. Supersonic

No modifications are required other than those described in Paragraph C of Section 4.1.3.2, "Wing Lift-Curve Slope".

No sweptforward vertical tail data were found to substantiate the methodologies.

D. Hypersonic

The comments in Paragraph C of this section are appropriate here.

5.3.1.2 TAIL-BODY SIDE-FORCE COEFFICIENT C_Y AT ANGLE
OF ATTACK

A. Subsonic

The comments in Paragraph A of Section 5.3.1.1, "Tail-Body Sideslip Derivative C_{Y_β} ..." are appropriate here.

B. Transonic

No method is presented.

C. Supersonic

The comments in Paragraph C of Section 5.3.1.1, "Tail-Body Sideslip Derivative C_{Y_β} ..." are appropriate here.

5.3.2.1 TAIL-BODY SIDESLIP DERIVATIVE $C_{\ell\beta}$ IN THE
LINEAR ANGLE-OF-ATTACK RANGE

A. Subsonic

No modifications are required.

No sweptforward vertical tail data were found to substantiate the methodology.

B. Transonic

No method is presented.

C. Supersonic

The comments in Paragraph C of Section 5.3.1.1, "Tail-Body Sideslip Derivative $C_{Y\beta}$..." are appropriate here.

D. Hypersonic

The comments in Paragraph C of this section are appropriate here.

5.3.3.1 TAIL-BODY SIDESLIP DERIVATIVE $C_{n\beta}$ IN THE
LINEAR ANGLE-OF-ATTACK RANGE

A. Subsonic

No modifications are required other than those described in Paragraph A of Section 4.1.4.2, "Wing Pitching-Moment-Curve Slope".

No sweptforward vertical tail data were found to substantiate the methodologies.

B. Transonic

No method is presented.

C. Supersonic

No modifications are necessary other than those described in Paragraph C of Sections 4.1.4.2, "Wing Pitching-Moment-Curve Slope" and 5.3.1.1, "Tail-Body Sideslip Derivative $C_{Y\beta}$

No sweptforward vertical tail data were found to substantiate the methodologies.

5.3.3.2 TAIL-BODY YAWING-MOMENT COEFFICIENT C_n AT
ANGLE OF ATTACK

A. Subsonic

The comments in Paragraph A of Section 5.3.3.1, "Tail-Body Sideslip Derivative C_{n_β} ..." are appropriate here.

B. Transonic

No method is presented.

C. Supersonic

No modifications are necessary other than those described in Paragraph C of Section 5.3.1.2. "Tail-Body Side-Force Coefficient C_Y at Angle of Attack".

5.4 FLOW FIELDS IN SIDESLIP

5.4.1 WING-BODY WAKE AND SIDEWASH IN SIDESLIP

A. Subsonic

No modifications are required.

No data were found to substantiate the methodology.

B. Transonic

No method is presented.

C. Supersonic

No method is presented.

5.5 LOW-ASPECT-RATIO WINGS AND WING-BODY COMBINATIONS IN SIDESLIP

The comments in Section 4.8 "Low-Aspect-Ratio Wings and Wing-Body Combinations..." are appropriate here.

5.6 WING-BODY-TAIL COMBINATIONS IN SIDESLIP

5.6.1.1 WING-BODY-TAIL SIDESLIP DERIVATIVE $C_{Y\beta}$ IN THE LINEAR ANGLE-OF-ATTACK RANGE

A. Subsonic

No modifications are required.

No substantiation was performed.

B. Transonic

No method is presented.

C. Supersonic

The comments in Paragraph C of Section 5.3.1.1, "Tail-Body Sideslip Derivative $C_{Y\beta}$ " are appropriate here.

5.6.1.2 WING-BODY-TAIL SIDE-FORCE COEFFICIENT C_Y AT
ANGLE OF ATTACK

A. Subsonic

The comments in Paragraph A of Section 5.6.1.1, "Wing-Body-Tail Sideslip Derivative C_Y ..." are appropriate here.

B. Transonic

No method is presented.

C. Supersonic

No modifications are required other than those described in Paragraph C of Section 5.3.1.2, "Tail-Body Side-Force Coefficient C_Y at Angle of Attack".

No substantiation was performed.

5.6.2.1 WING-BODY-TAIL SIDESLIP DERIVATIVE C_{l_β} IN THE
LINEAR ANGLE-OF-ATTACK RANGE

A. Subsonic

No modifications are required.

Good agreement (average difference = .000750) was noted between test and predicted values. Table 26 contains a summary of the planforms analyzed, their parameters, and test and predicted results.

B. Transonic

No method is presented.

C. Supersonic

No modifications are required other than described in Paragraph C of Section 5.3.1.1, "Tail-Body Sideslip Derivative C_{Y_β} ...".

No substantiation was performed.

5.6.3.1 WING-BODY-TAIL SIDESLIP DERIVATIVE $C_{n\beta}$ IN THE
LINEAR ANGLE-OF-ATTACK RANGE

A. Subsonic

No modifications are necessary.

No substantiation was performed.

B. Transonic

No method is presented.

C. Supersonic

The comments in Paragraph A of this section are appropriate here.

5.6.3.2 WING-BODY-TAIL YAWING-MOMENT COEFFICIENT C_n AT
ANGLE OF ATTACK

A. Subsonic

The comments in Paragraph A of Section 5.6.3.1, "Wing-Body-Tail Sideslip Derivative $C_{n\beta}$..." are appropriate here.

B. Transonic

No method is presented.

C. Supersonic

No modifications are necessary other than those described in Paragraph C of Section 5.6.1.2, "Wing-Body-Tail Side-Force Coefficient C_Y at Angle of Attack".

No substantiation was performed.

6.1 SYMMETRICALLY DEFLECTED FLAPS AND CONTROL DEVICES ON WING-BODY AND TAIL-BODY COMBINATIONS

6.1.4.1 CONTROL DERIVATIVE $C_{L\dot{\alpha}}$ OF HIGH-LIFT AND CONTROL DEVICES

A. Subsonic

No modifications to any of the method are required.

To obtain increased accuracy from split flap analyses, multiply the lift increment by the cosine of the sweep angle:

$$(\Delta C_{L\dot{\alpha}})_{\text{Split Flap}} = (\Delta C_{L\dot{\alpha}})_{\text{Datcom}} \cos \Lambda_c/4 \quad (8)$$

The average difference between test and predicted results was reduced from .1229 (using Datcom Equation 6.1.4.1-a) to .0506 (using Equation 8). The average difference between test and predicted single and double-slotted flap results was .0170 and .0740, respectively. Data for only one plain flap configuration was found; its average difference was .0273. Leading-edge device prediction results consistently overestimated in magnitude the test values. The average difference between nose flap test and predicted value was .0159. Slat and Krueger flap average difference was .0344 and .0150, respectively. No data were found for either internally- or internally-blown-flap configurations. Table 27 contains a summary of the planforms analyzed, their parameters, and test and predicted results.

B. Transonic

No modifications are required.

No substantiation was performed.

C. Supersonic

No modifications are required.

No substantiation was performed.

6.1.4.2 WING LIFT-CURVE SLOPE WITH HIGH-LIFT AND CONTROL
DEVICES

A. All Speeds

No modifications are required.

Good agreement (4.33% average error) was noted between subsonic test and predicted values for both leading- and trailing-edge devices. No jet flap data were found. Transonic and supersonic substantiation was not performed. Table 28 contains a summary of the planforms analyzed, their parameters, and test and predicted results.

6.1.4.3 WING MAXIMUM LIFT WITH HIGH-LIFT AND CONTROL DEVICES

Datcom Figure 6.1.4.3-10, "Planform Correction Factor - Trailing-Edge Flaps" should be replaced with Figure 17 of this report as the Datcom figure was found to cause increasing error with increasing sweep angle. Figure 17 is based on the Datcom figure but includes the modifications suggested by J. W. Martin, Jr. of NASC as described in Reference 6. No other modifications are necessary.

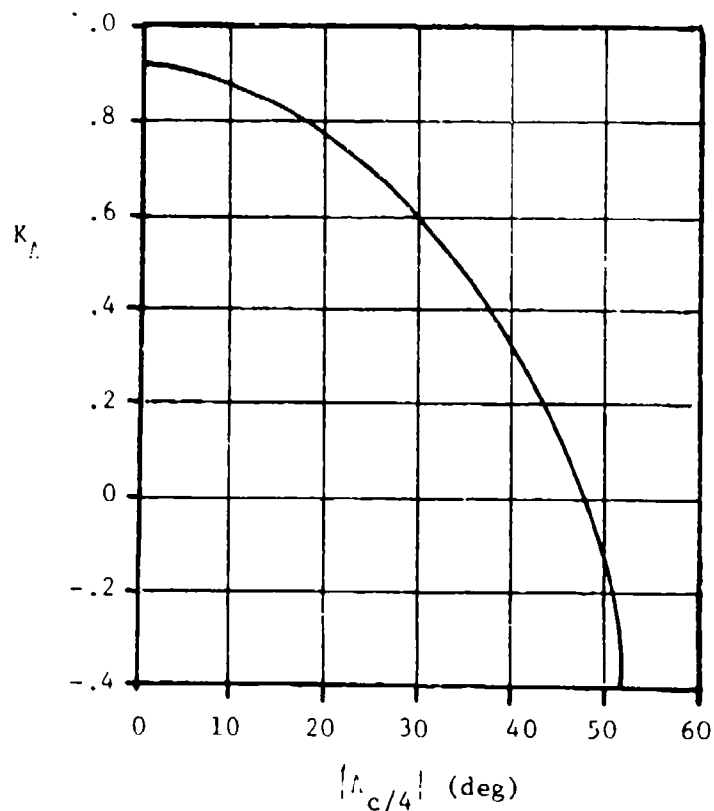


Figure 17. Planform Correction Factor - Trailing-Edge Flaps (Replaces Datcom Figure 6.1.4.3-10)

Correlation of test data with results from Method 1 (trailing-edge flaps) shows the improvement in accuracy gained in using Figure 17 in place of Datcom Figure 6.1.4.3-10. For split flaps, the average difference was reduced from .1998 to .0569. Also, average difference decreased from .2685 to .1040 for single-slotted flaps and from .2864 to .06577 for double-slotted flaps. Method 2, for leading-edge slats, gave fair agreement with an average difference between test and predicted results of .07833. No data were found for jet flap correlation (Method 3).

Table 29 contains a summary of the planforms analyzed, their parameters, and test results compared with both the existing and proposed method results.

6.1.5.1 PITCHING-MOMENT INCREMENT AC_m DUE TO HIGH-LIFT AND CONTROL DEVICES

A. Subsonic

No modifications are necessary for the jet-flap and leading-edge device methods, and for Method 1 of the trailing-edge mechanical flap section. For Method 2 of that section, Figure 18 (from Reference 33) should be used to obtain sweptforward wing loading coefficients.

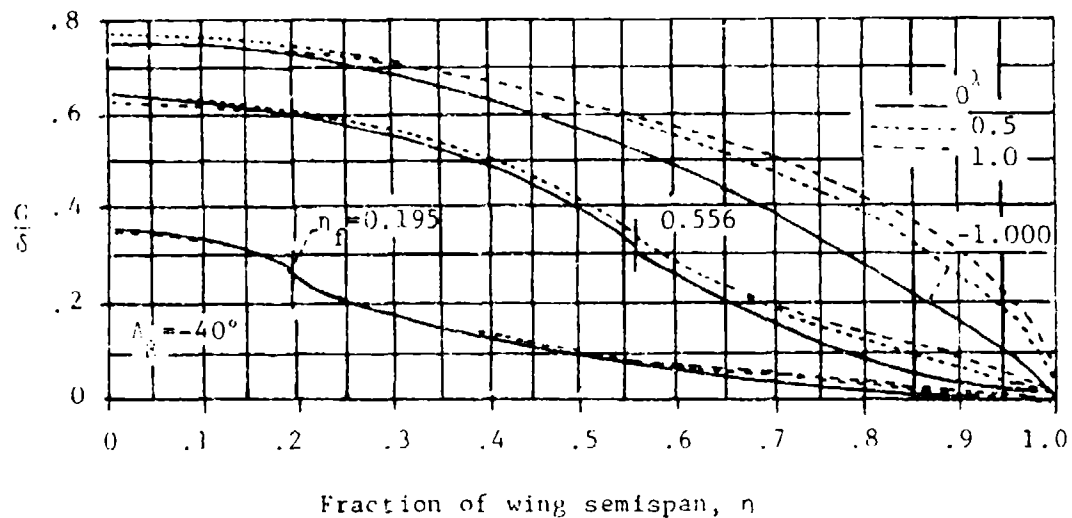
Fair agreement (average difference = .08905) was noted between test and predicted trailing-edge mechanical flap values using Method 1. Method 2 substantiation was not performed. Good agreement (mean difference = .02088) was noted between test and predicted leading edge device increments. No jet flap data were found. Table 30 contains a summary of the planforms analyzed, their parameters, and test and predicted results.

B. Transonic

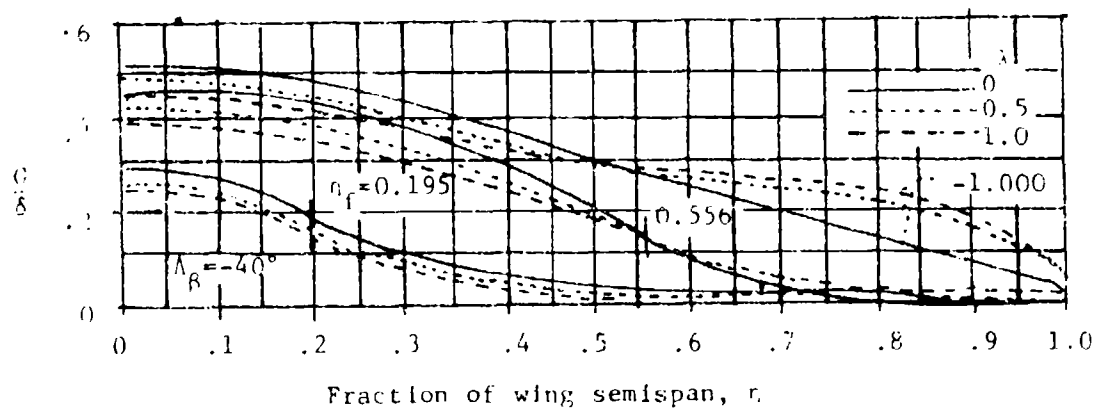
The methodology of this section should not be used to estimate sweptforward wing characteristics. Insufficient data currently exist to validate Datcom Figure 6.1.5.1-69, "Transonic Control-Surface Pitch-Effectiveness Parameters".

C. Supersonic

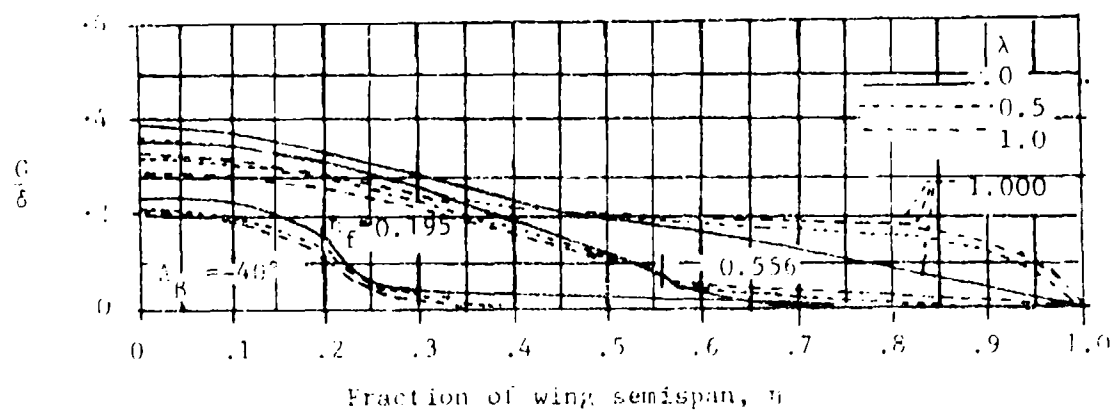
Figure 19 (from Reference 34) should be used for sweptforward wings having untapered controls with the outboard edge coincident with the wingtip.



a) $\frac{BA}{\kappa_{av}} = 2.0$



b) $\frac{BA}{\kappa_{av}} = 6.0$



c) $\frac{BA}{\kappa_{av}} = 10.0$

Figure 18. Spanwise Load Distribution Due to Symmetric Flap Deflection

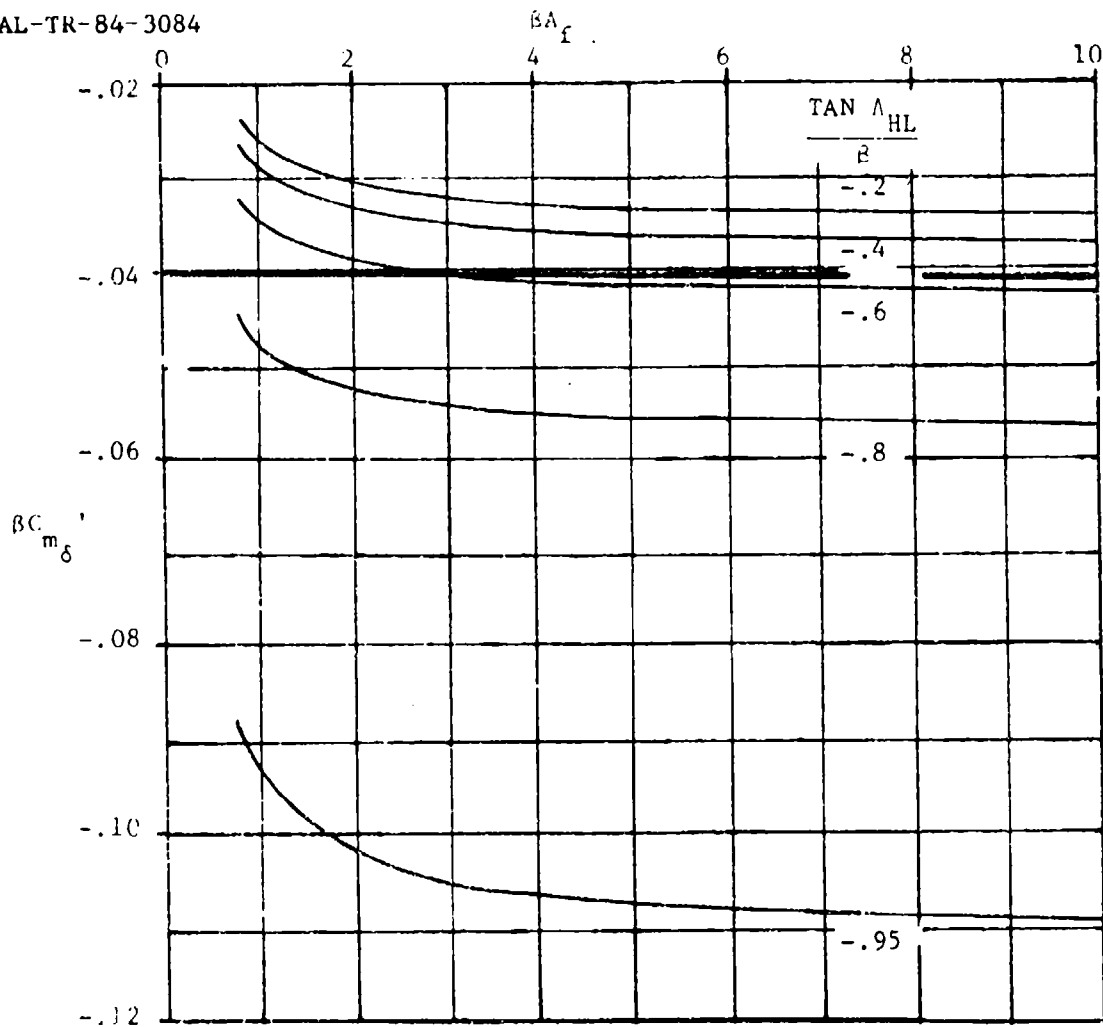
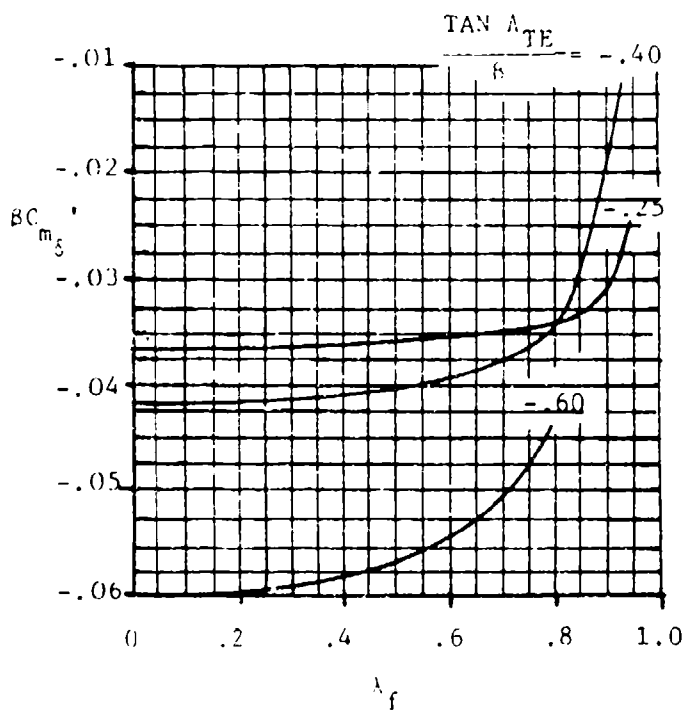


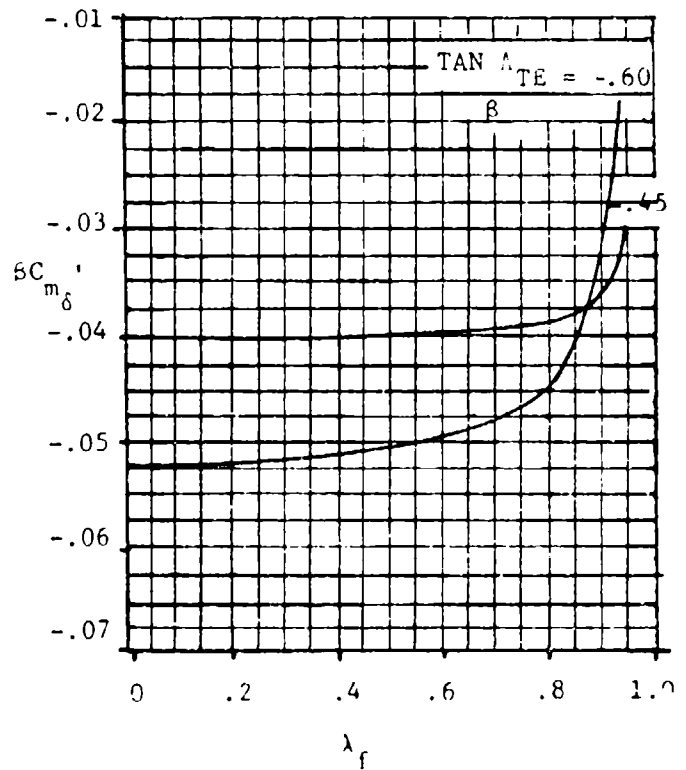
Figure 19. Pitching-Moment Derivative for Untapered Trailing-Edge Control Surfaces located at the Wing Tip

Figure 20 (from Reference 34) should be used for tapered sweptforward controls, again, with the outboard edge coincident with the wingtip. For tapered and untapered controls having the outboard edge not coincident with the wing tip, Datcom Figure 6.1.5.1-73a, "Pitching Moment Derivative...", can be used with no modifications. No other modifications are necessary other than those described in Paragraph C of Section 6.2.1.1, "Rolling Moment Due to Control Deflection".

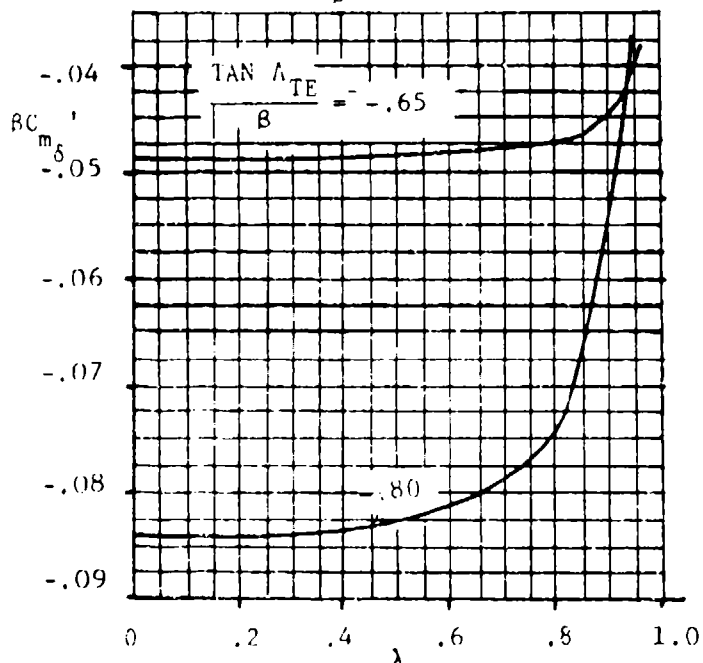
No substantiation was performed.



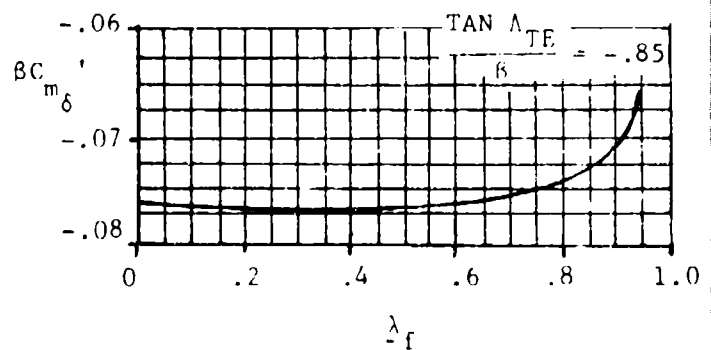
a) $\frac{TAN \Lambda_{HL}}{\beta} = -0.20$



b) $\frac{TAN \Lambda_{HL}}{\beta} = -0.40$



c) $\frac{TAN \Lambda_{HL}}{\beta} = -0.60$



d) $\frac{TAN \Lambda_{HL}}{\beta} = -0.80$

Figure 20. Pitching-Moment Derivative for Tapered Trailing-Edge Control Surfaces Having Outboard Edge Coincident with Wing Tip

6.1.5.2 WING DERIVATIVE $C_{n_{\dot{\alpha}}}$ WITH HIGH-LIFT AND CONTROL
DEVICES

A. All Speeds

No modifications are necessary.

No substantiation was performed.

6.1.6.1 HINGE-MOMENT DERIVATIVE $C_{h\alpha}$ OF HIGH-LIFT AND CONTROL DEVICES

A. Subsonic

No modifications are necessary.

Good agreement (average difference = .11453) was noted between test and predicted values. Table 31 contains a summary of the planforms analyzed, their parameters, and test and predicted results.

B. Transonic

No method is presented.

C. Supersonic

No guidance was found in open literature to evaluate this term for sweptforward wing planforms. It is recommended that treating the control surface be analyzed as if it were on a sweptback wing having a taper ratio equal to the reciprocal of the sweptforward wing taper ratio. The modifications necessary include using the absolute value of the various sweep angles and altering the control surface description as follows (primed values denote the pseudo-aft swept wing):

$$A'_{LE} = |A_{LE}|$$

$$A'_{HL} = |A_{HL}|$$

$$A'_{TE} = |A_{TE}|$$

$$C'_r = C_t$$

$$C'_t = C_r$$

$$C'_{f_r} = C_{f_t}$$

$$C'_{f_t} = C_{f_r}$$

(9)

$$Y'_i = b/2 = Y_o$$

$$Y'_o = b/2 - Y_i$$

No substantiation was performed.

6.1.6.2 HINGE-MOMENT DERIVATIVE $C_{h\delta}$ OF HIGH-LIFT AND
CONTROL DEVICES

A. Subsonic

No modifications are necessary.

Insufficient data were found to allow substantiation; however, good correlation ($\Delta C_{h\delta} = .00124$) was noted between the test and predicted values for the configuration found.

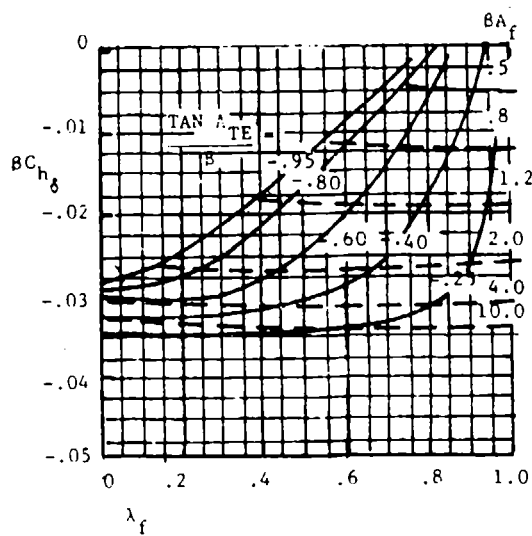
B. Transonic

No method is presented.

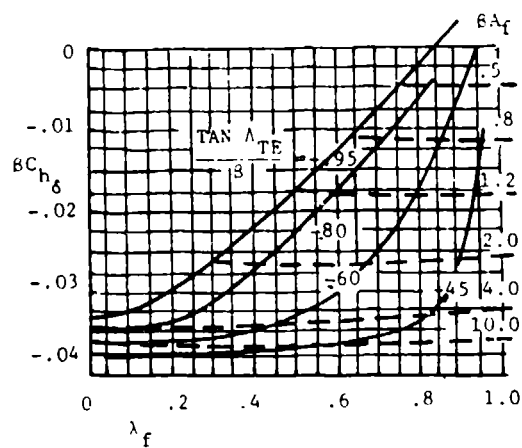
C. Supersonic

Figure 21 (from Reference 34) should be used in place of Datcom Figure 6.1.6.2-17, "Supersonic Theoretical Hinge-Moment Derivative $C_{h\delta}$ ", for planforms having sweptforward hinge line sweep angles. No other modifications are necessary.

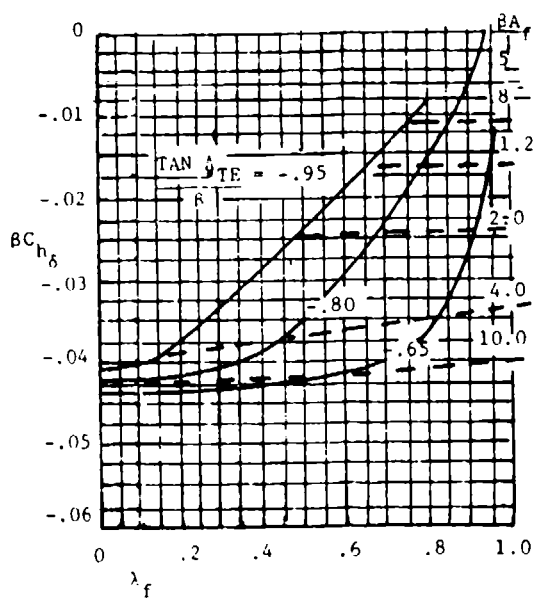
No substantiation was performed.



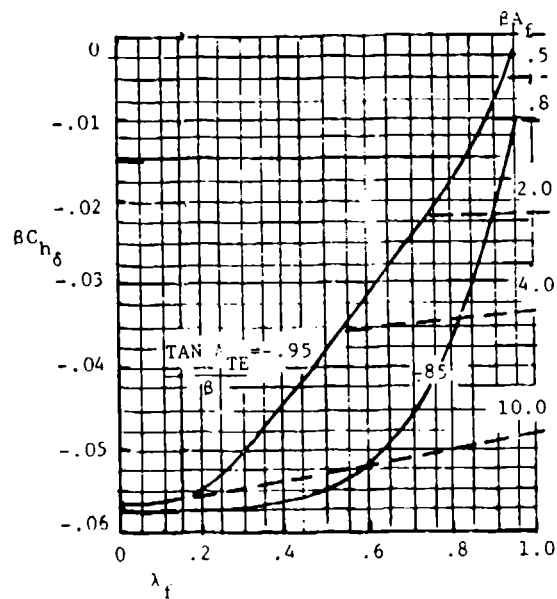
a) $\frac{TAN \Lambda_{HL}}{\beta} = -.20$



b) $\frac{TAN \Lambda_{HL}}{\beta} = -.40$



c) $\frac{TAN \Lambda_{HL}}{\beta} = -.60$



d) $\frac{TAN \Lambda_{HL}}{\beta} = -.80$

Figure 21. Supersonic Theoretical Hinge-Moment Derivative $BC_{h\delta}$

6.1.7 DRAG OF HIGH-LIFT AND CONTROL DEVICES

A. Subsonic

No modifications are required.

No substantiation was performed.

B. Transonic

No method is presented.

C. Supersonic

No modifications are required.

No substantiation was performed.

6.2 ASYMMETRICALLY DEFLECTED CONTROLS ON WING-BODY AND TAIL-BODY COMBINATIONS

6.2.1.1 ROLLING MOMENT DUE TO CONTROL DEFLECTION

A. Subsonic

No modifications are required.

Fair agreement was noted between test and predicted values for plain-trailing-edge flaps (average difference = .06475) and spoilers (average difference = .00257). Table 32 contains a summary of the planforms analyzed, their parameters, and test and predicted results.

B. Transonic

No modifications are necessary other than those described in Paragraph B of Section 4.1.3.2, "Wing Lift-Curve Slope".

No substantiation was performed.

C. Supersonic

Figures 22 through 25 (from Reference 34) should be used as described for the following control surface configurations:

- a. Tapered control surfaces with outboard edge coincident with wing tip: use Figure 22.
- b. Tapered control surface with outboard edge not coincident with wing tip: use Figure 23.
- c. Untapered control surface with outboard edge coincident with wing tip: use Figure 24.

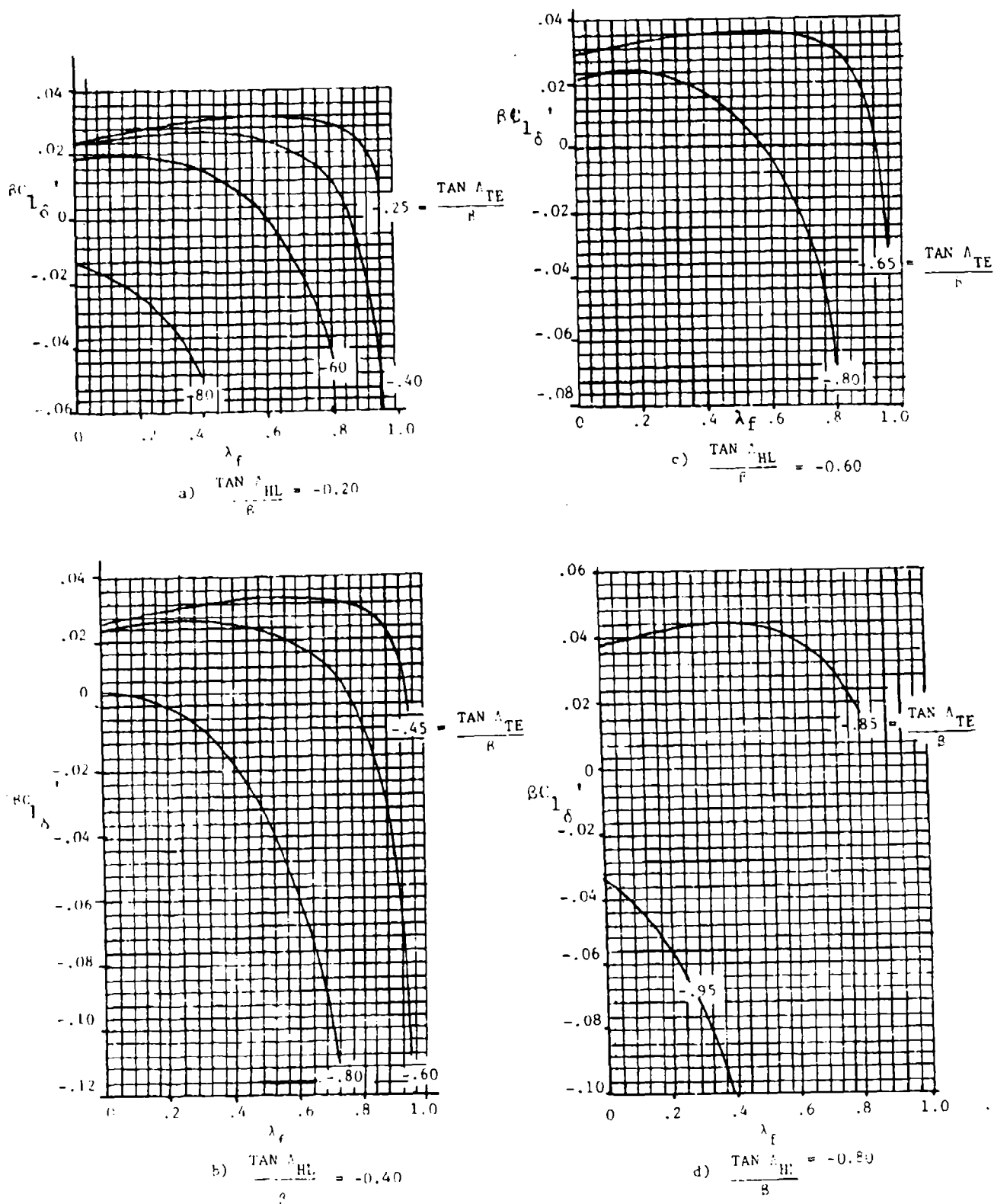


Figure 22. Rolling-Moment Derivative for Tapered Control Surfaces Having Outboard Edge Coincident with Wing Tip

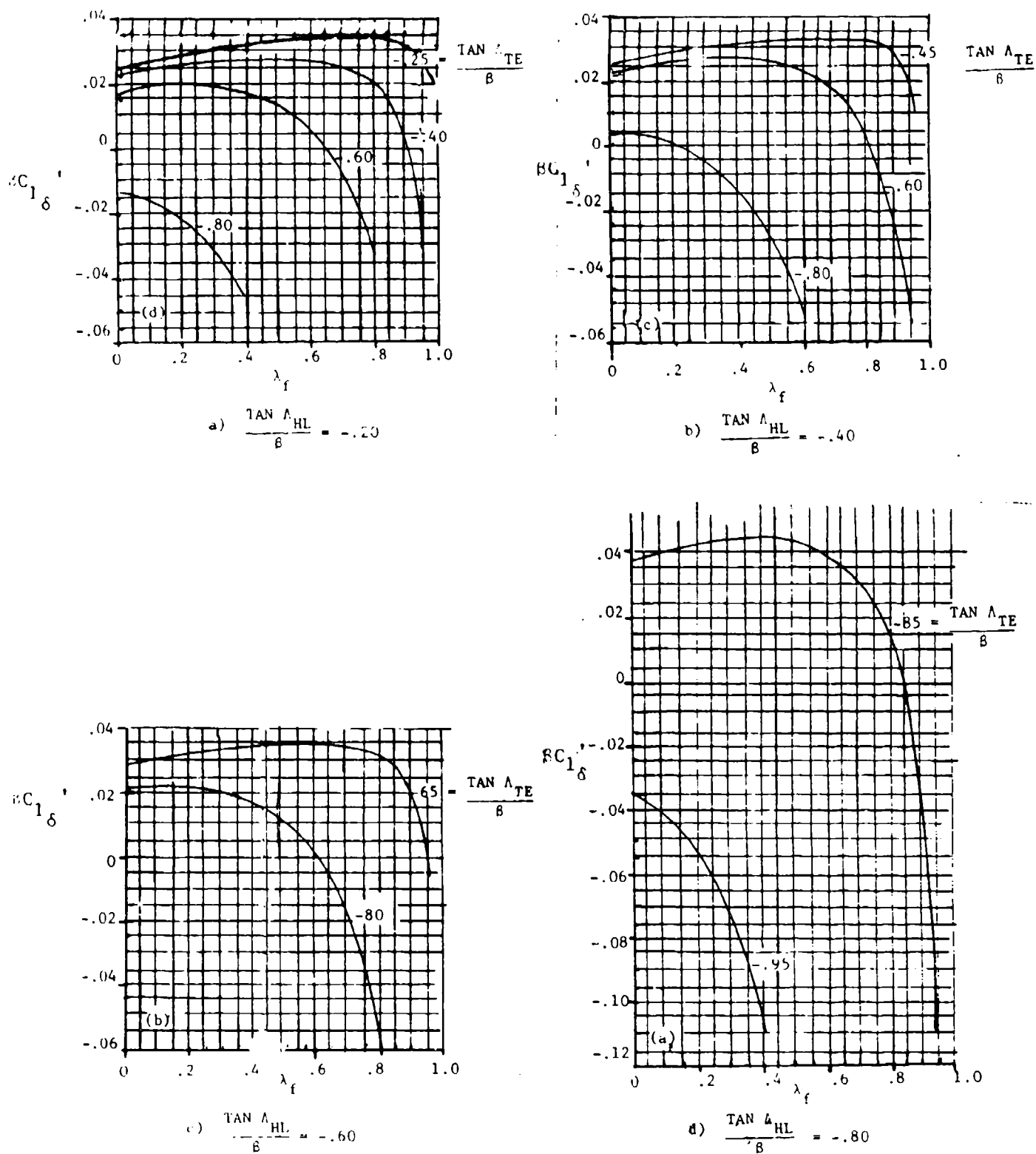


Figure 23. Rolling-Moment Derivative for Tapered Control Surfaces Having Outboard Edge Not Coincident with Wing-Tip

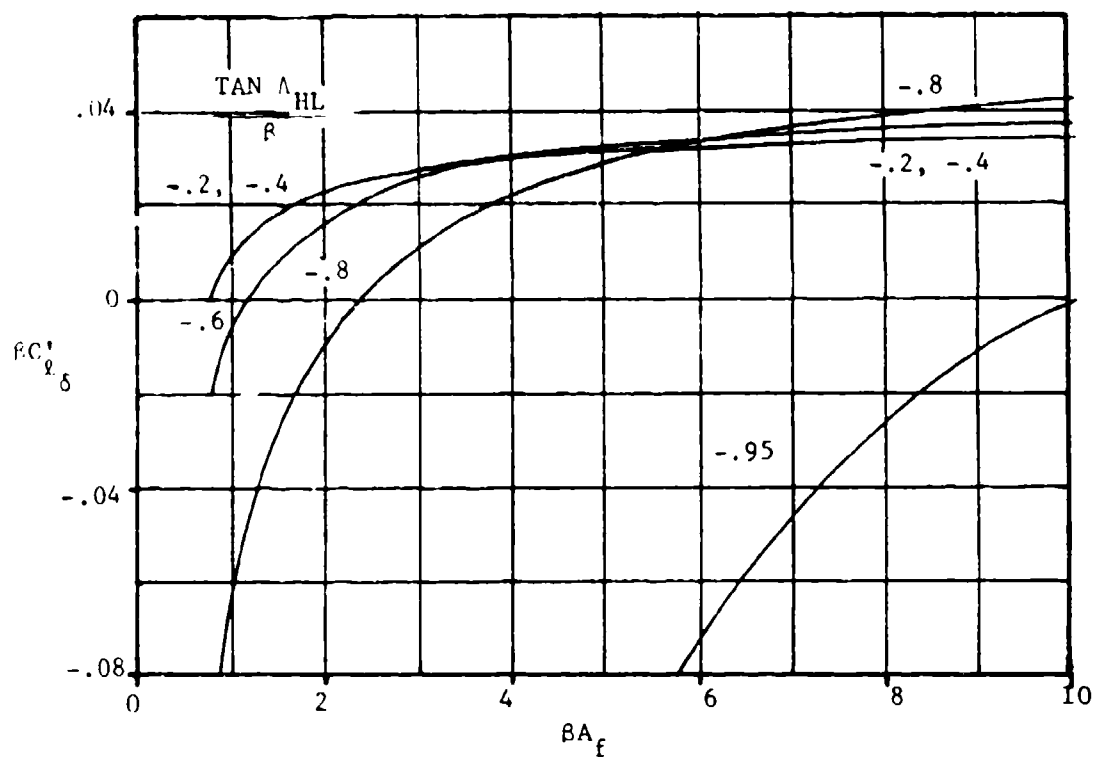


Figure 24. Rolling-Moment Derivative for Untapered Control Surfaces Having Outboard Edge Coincident with Wing Tip

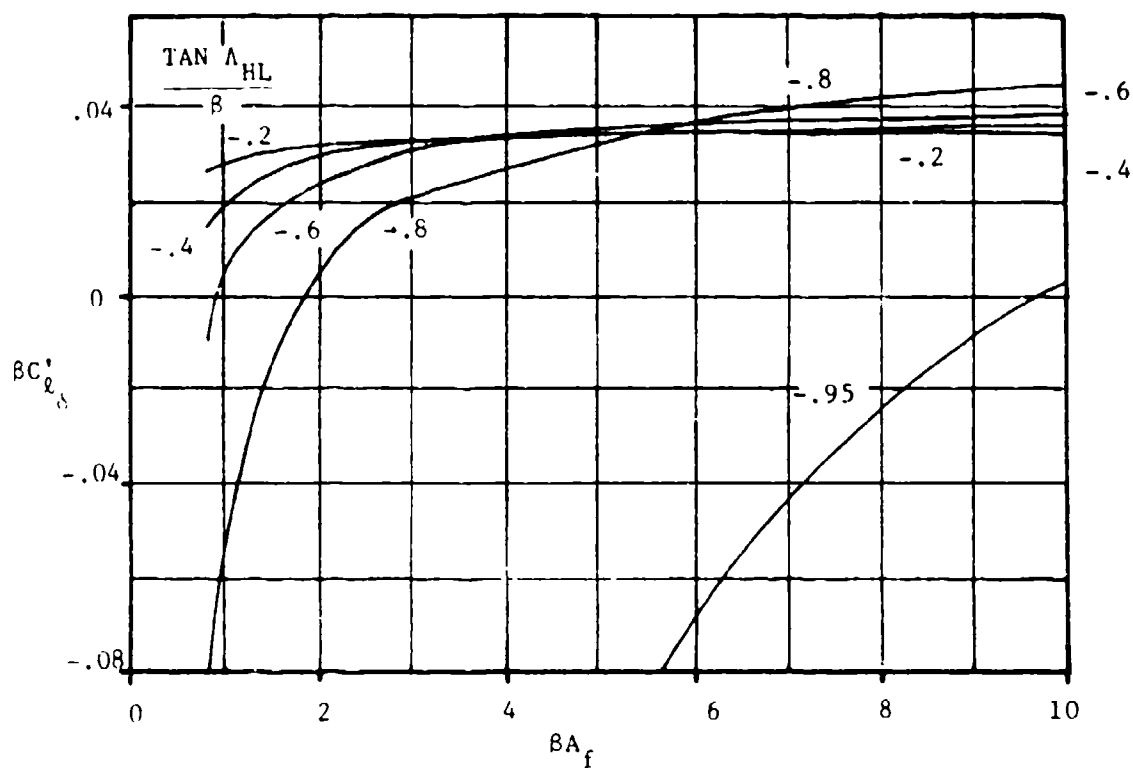


Figure 25. Rolling Moment Derivative for Untapered Control Surfaces Having Outboard Edge Not Coincident with Wing Tip

d. Untapered control surface with outboard edge not coincident with wing tip: use Figure 25.

Also, the absolute value of the quarter-chord sweep angle should be used in Datcom Figure 6.2.1.1-30, "Spoiler Rolling Moments...".

No substantiation was performed.

6.2.1.2 ROLLING-MOMENT DUE TO A DIFFERENTIALLY DEFLECTED
HORIZONTAL STABILIZER

A. Subsonic

No modifications are required other than those described in Paragraph A of Sections 4.3.1.3, "Wing-Body Lift in the Nonlinear Angle-of-Attack Range" and 4.4.1 "Wing-Wing Combinations at Angle of Attack".

No substantiation was performed.

B. Transonic

No modifications are required other than those described in Paragraph B of Sections 4.1.3.2, "Wing Lift-Curve Slope"; 4.3.1.3, "Wing-Body Lift in the Nonlinear Angle-of-Attack Range"; and 4.4.1 "Wing-Wing Combinations at Angle of Attack". The comments in Paragraphs A and C of this section are also applicable here.

No substantiation was performed.

C. Supersonic

No modifications are required other than those described in Paragraph C of Sections 4.1.3.2, "Wing Lift-Curve Slope"; 4.3.1.2, Wing-Body Lift-Curve Slope"; and 4.3.1.3, "Wing-Body Lift in the Nonlinear Angle-of-Attack Range".

No substantiation was performed.

6.2.2.1 YAWING MOMENT DUE TO CONTROL DEFLECTION

A. Subsonic

No modifications are necessary other than the use of the absolute value of the leading-edge sweep angle in Datcom Figure 6.2.2.2-11, "Yawing Moment Due to Spoiler...".

Fair agreement was noted between test and predicted values for plain flap (average difference = .00111) and spoiler configurations (average difference = .00365). Table 33 contains a summary of the planforms analyzed, their parameters, and test and predicted results.

B. Transonic

No modifications are necessary other than those described in Paragraph A of this section and Paragraph B of Section 4.1.3.2, "Wing Lift-Curve Slope".

No substantiation was performed.

C. Supersonic

The absolute value of the midchord sweep angle should be used in Datcom Figure 6.2.2.1-13, "Yawing Moment Due to Aileron Deflection...". Also, the modifications described in Paragraph C of Sections 4.1.3.2, "Wing Lift-Curve Slope" and 6.2.1.1, "Rolling Moment Due to Control Deflection" are appropriate here. No other modifications are necessary.

No substantiation was performed.

6.3 SPECIAL CONTROL METHODS

No modifications are required.

No substantiation was performed.

7.1 WING DYNAMIC DERIVATIVES

7.1.1.1 WING PITCHING DERIVATIVE C_{Lq}

A. Subsonic

No modifications are required other than those described in Paragraph A of Section 4.1.4.2, "Wing Pitching-Moment-Curve Slope".

Good agreement (5.13% error) was noted between test and predicted results for the single sweptforward planform found. Table 34 contains a summary of the planforms analyzed, their parameters, and test and predicted results.

B. Transonic

No method is presented.

C. Supersonic

Based on the reversibility theorem, the relation

$$(C_{Lq})_{FSW} = 2(C_{m\alpha})_{ASW} \quad (10)$$

should be used to obtain sweptforward wing characteristics, using an aft swept wing identical in planform to the forward swept wing in reverse flow. Care must be taken with respect to the moment reference center location, as the root quarterchord location for the sweptback planform is the three-quarter chord location for the sweptforward planform. Also, the modifications described in Paragraph C of Section 4.1.3.2, "Wing Lift-Curve Slope" are relevant here as well.

Analyses were performed using twice the sweptforward pitching-moment-curve slope value (using methods described in this report) to obtain the sweptback value of C_{Lq} . The values derived from using reversibility theorem assumptions were then compared to results obtained from this section with fair correlation (an average of 14%) was noted.

7.1.1.2 WING PITCHING DERIVATIVE C_{n_q}

A. Subsonic

No modifications are required other than those described in Paragraph A of Section 4.1.4.2, "Wing Pitching-Moment-Curve Slope".

An error of 16.12% was noted between test and predicted results for the single sweptforward planform found. Table 35 contains a summary of the planforms analyzed, their parameters, and test and predicted results.

B. Transonic

No modifications are required other than those described in Paragraphs A and C of this section and Paragraphs B and C of Section 4.1.3.2, "Wing Lift-Curve Slope".

No substantiation was performed.

C. Supersonic

The reversibility theorem states that

$$(C_{m_q})_{FSW} = (C_{m_q})_{ASW} \quad (11)$$

Hence, to obtain values of this derivative use the absolute value of the trailing-edge sweep angle. Also, the modifications described in Paragraph C of Sections 7.1.1.1, "Wing Pitching Derivative C_{L_q} " and 4.1.4.2, "Wing Pitching-Moment-Curve Slope" are applicable here.

No substantiation was performed.

7.1.1.3 WING PITCHING DERIVATIVE C_{D_q}

A. Subsonic

Other than using the absolute value of the leading-edge sweep angle, no modifications are necessary.

B. Transonic

No method is presented.

C. Supersonic

No method is presented.

7.1.2.1 WING ROLLING DERIVATIVE C_{Y_p}

A. Subsonic

No modifications are required.

Good agreement (average $\Delta C_{Y_p} = .0145$) was noted between test and predicted values. Table 36 contains a summary of the planforms analyzed, their parameters, and test and predicted results.

B. Transonic

No method is presented.

C. Supersonic

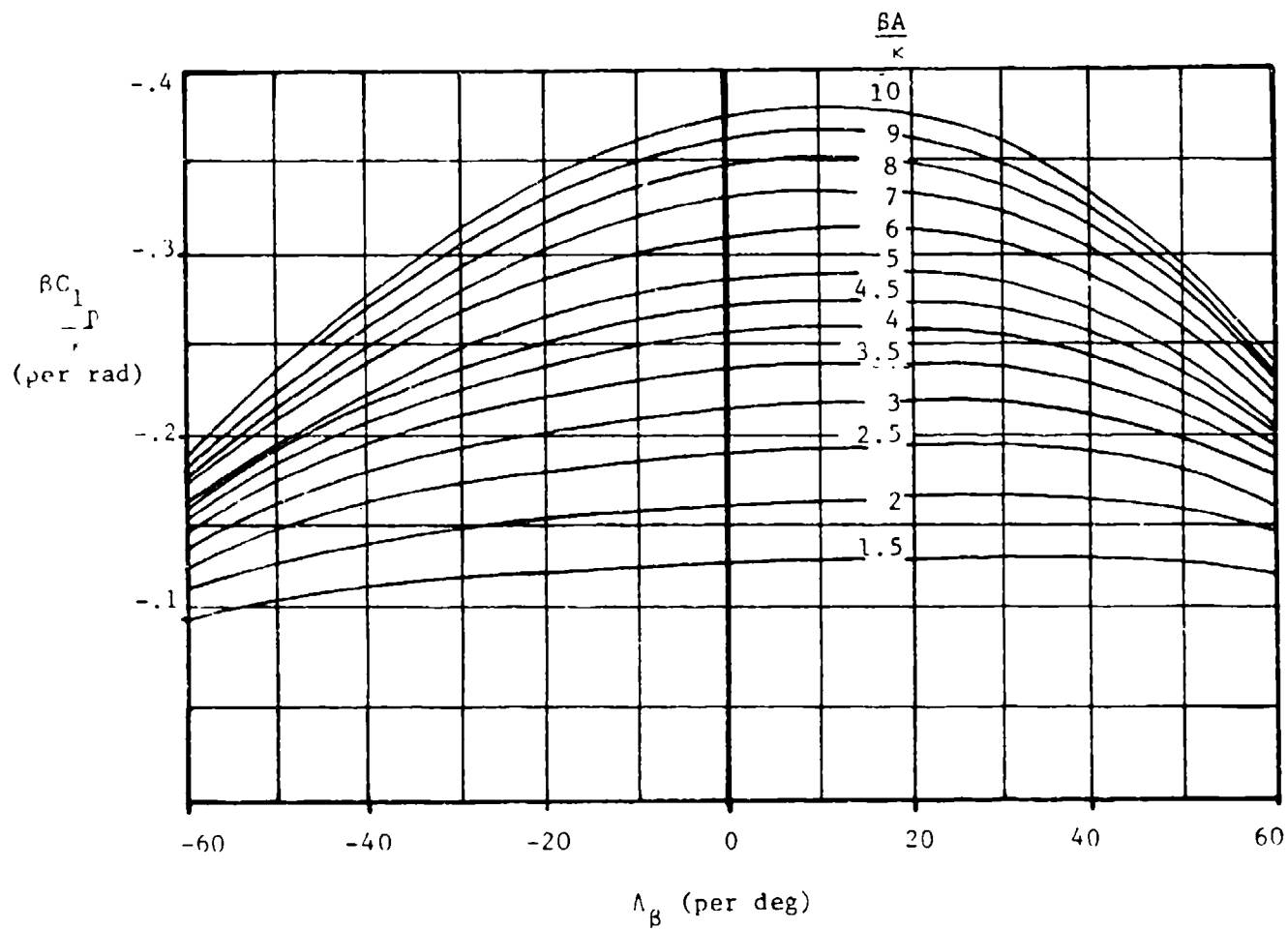
The methodology of this section is unsuited for sweptforward planforms. No method is presented to determine forward swept wing characteristics.

7.1.2.2 WING ROLLING DERIVATIVE C_{ℓ_p}

A. Subsonic

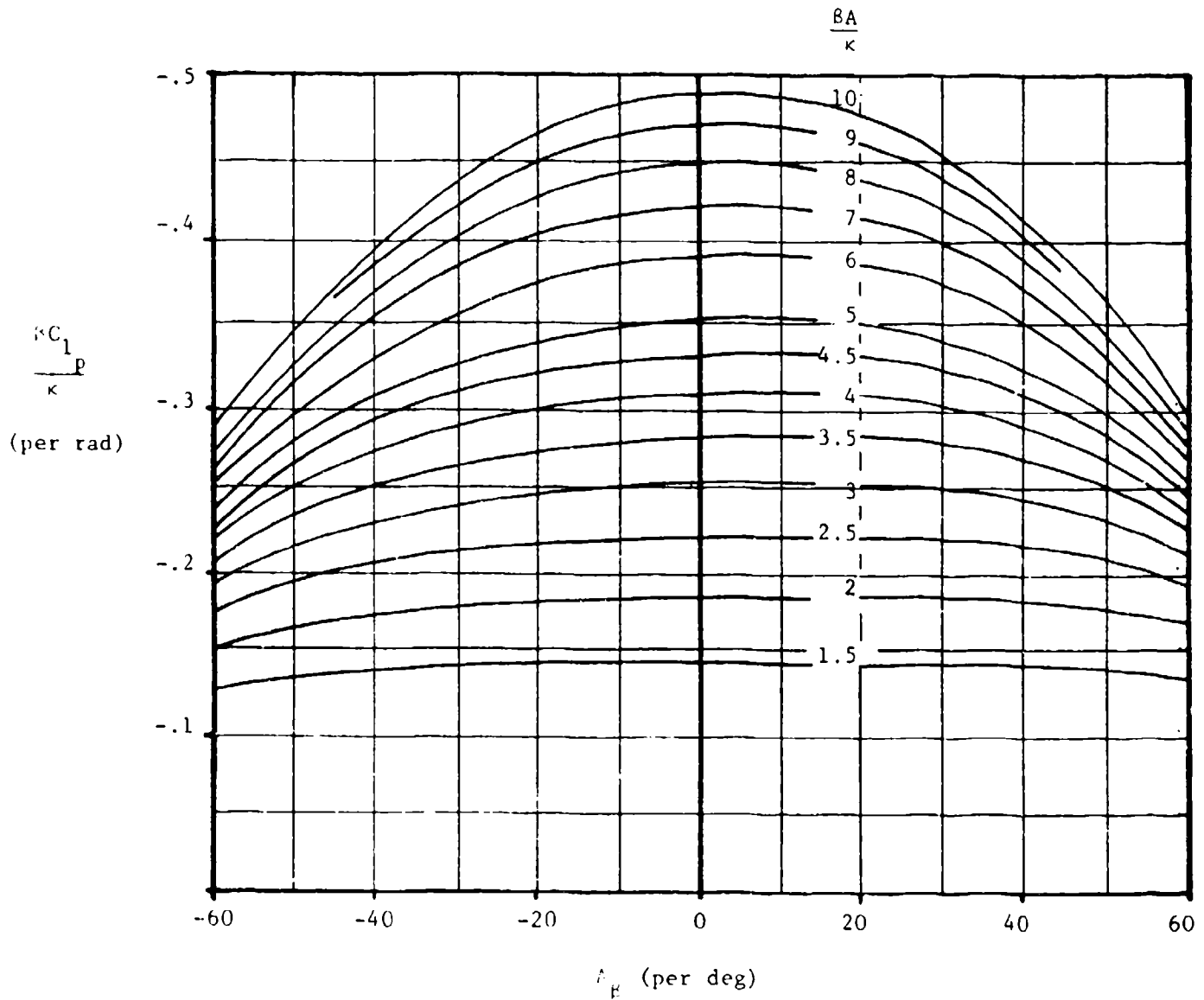
Figure 26 (from Reference 35) should be used in place of Datcom Figure 7.1.2.2-20, "Rolling-Damping Parameter at Zero Lift". The absolute value of the quarter-chord sweep angle should be used in Datcom Figure 7.1.2.2.-24, "Drag-Due-To-Lift Roll-Damping Parameter". Also, the modifications discussed in Paragraph A of Sections 4.1.5.1, "Wing Zero-Lift Drag", 4.1.3.3; "Wing Lift in the Nonlinear Angle-of-Attack Range"; and 4.1.3.2, "Wing Lift-Curve Slope" are appropriate here.

Good agreement (9.08% average error) was noted between test and predicted results. Table 37 contains a summary of the planforms analyzed, their parameters, and test and predicted values.



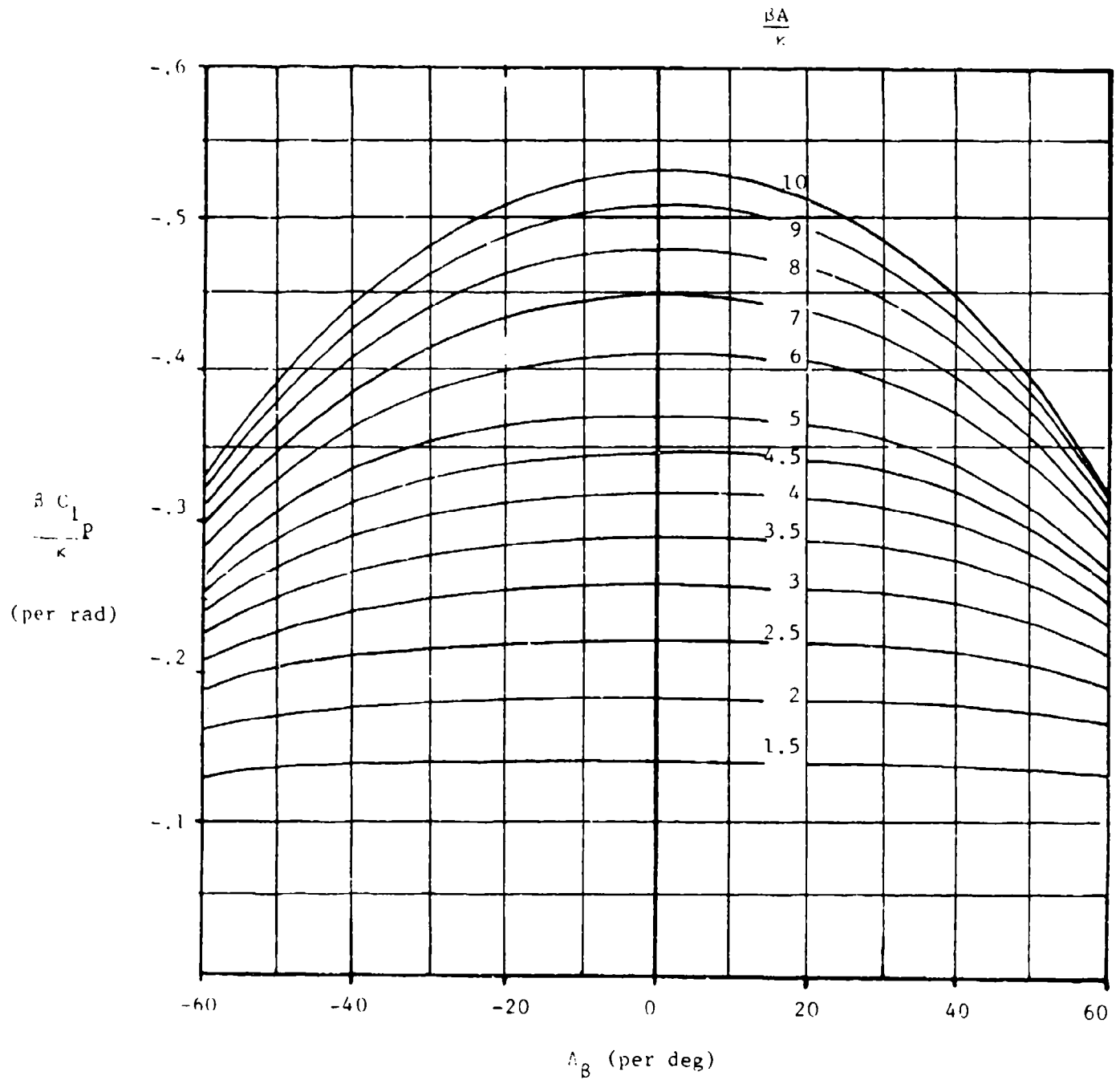
a. Taper Ratio = 0.0

Figure 26. Roll-Damping Parameter at Zero Lift



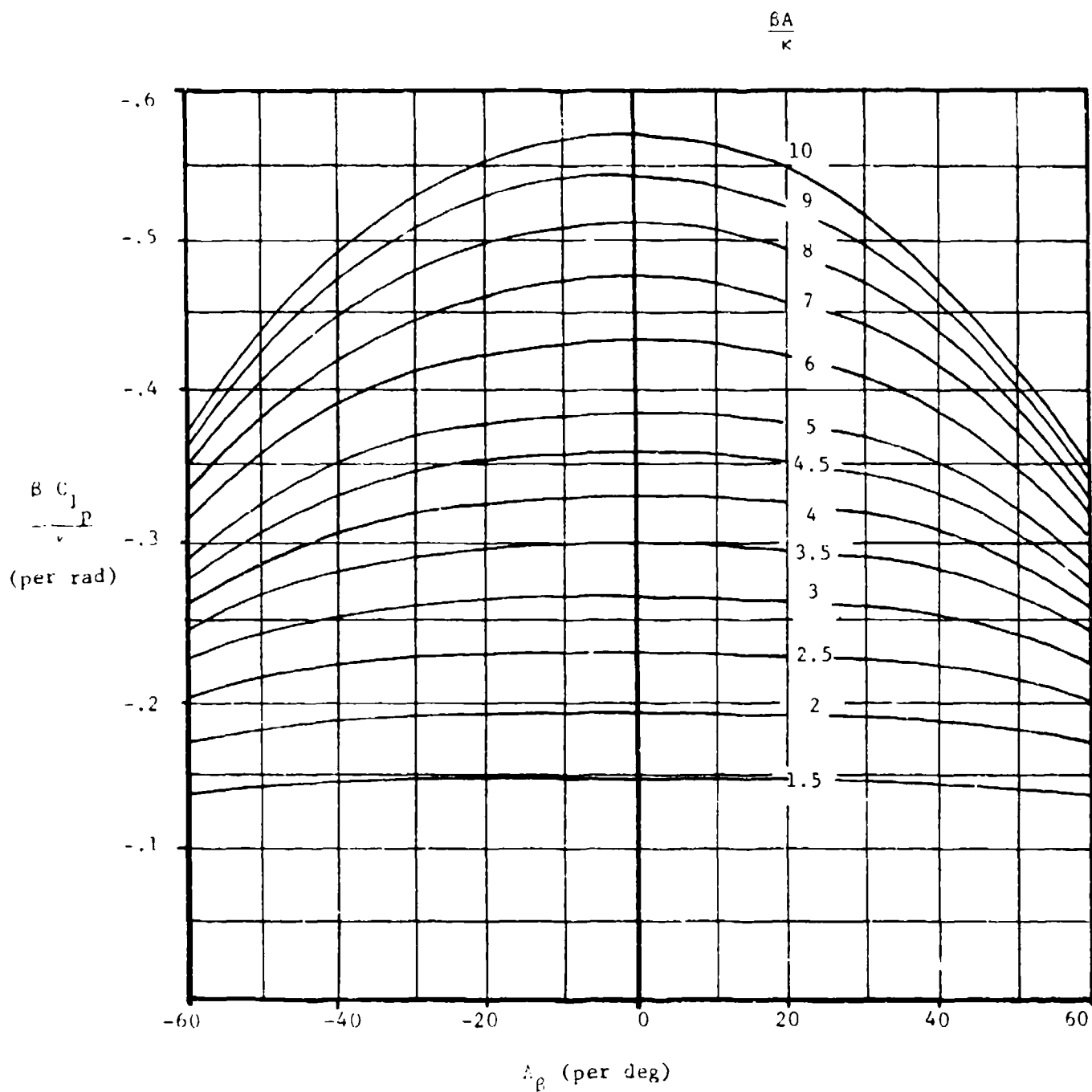
b) Taper Ratio = 0.25

Figure 26. Roll-Damping Parameter at Zero Lift



c) Taper Ratio = 0.5

Figure 26. Poll-Damping Parameter at Zero Lift



d) Taper Ratio = 1.0

Figure 26. Roll-Damping Parameter at Zero Lift

B. Transonic

No method is presented.

C. Supersonic

The absolute value of the designated sweep angle should be used in Datcom Figures 7.1.2.2-25, "Roll-Damping Parameter" and 7.1.2.2-27, "Damping-In-Roll Correction Factor for Sonic-Leading-Edge Region". No other modifications are necessary.

No substantiation was performed.

7.1.2.3 WING ROLLING DERIVATIVE C_{n_p}

A. Subsonic

No modifications are necessary other than those discussed in Paragraph A of Sections 7.1.2.2, "Wing Rolling Derivative C_{ℓ_p} "; 4.1.5.1, "Wing Zero-Lift Drag"; and 4.1.5.2, "Wing Drag at Angle of Attack".

B. Transonic

No method is presented.

C. Supersonic

The comments in Paragraph C of Section 7.1.2.1, "Wing Rolling Derivative C_{Y_p} " are appropriate here.

7.1.3.1 WING YAWING DERIVATIVE C_{Y_r}

A. All Speeds

No method is presented.

7.1.3.2 WING YAWING DERIVATIVE C_{l_r}

A. Subsonic

Insufficient data currently exist to validate this section. Existing data indicate using the unswept quarter-chord line in Datcom Figure 7.1.3.2-10, "Wing Yawing Derivative C_{l_r} " to obtain approximations for sweptforward wing planforms.

B. Transonic

No method is presented.

C. Supersonic

No method is presented.

7.1.3.3 WING YAWING DERIVATIVE C_{n_r}

A. Subsonic

Figure 27 should be used in lieu of Datcom Figure 7.1.3.3-6, "Low-Speed Drag-Due-To-Lift Yaw-Damping Parameter". Figure 28 should be used in lieu of Datcom Figure 7.1.2.2-7, "Low-Speed Profile-Drag-Yaw-Damping Parameter". These new figures are based on work done by Toll and Queijo (Reference 7).

No substantiation was performed.

B. Transonic

No method is presented.

C. Supersonic

No method is presented.

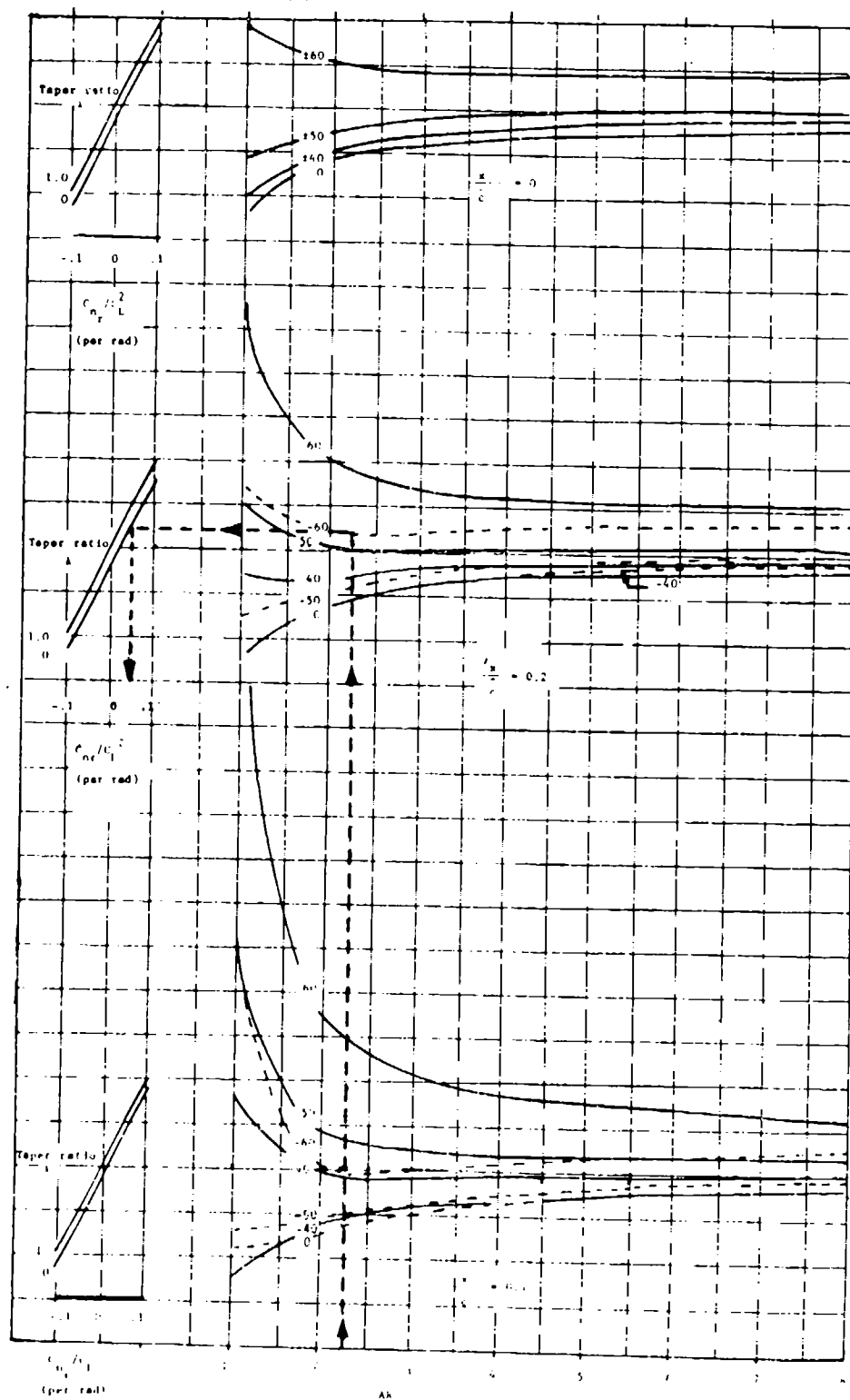


Figure 27. Low-Speed Drag-Due-To-Lift Yaw-Damping Parameter

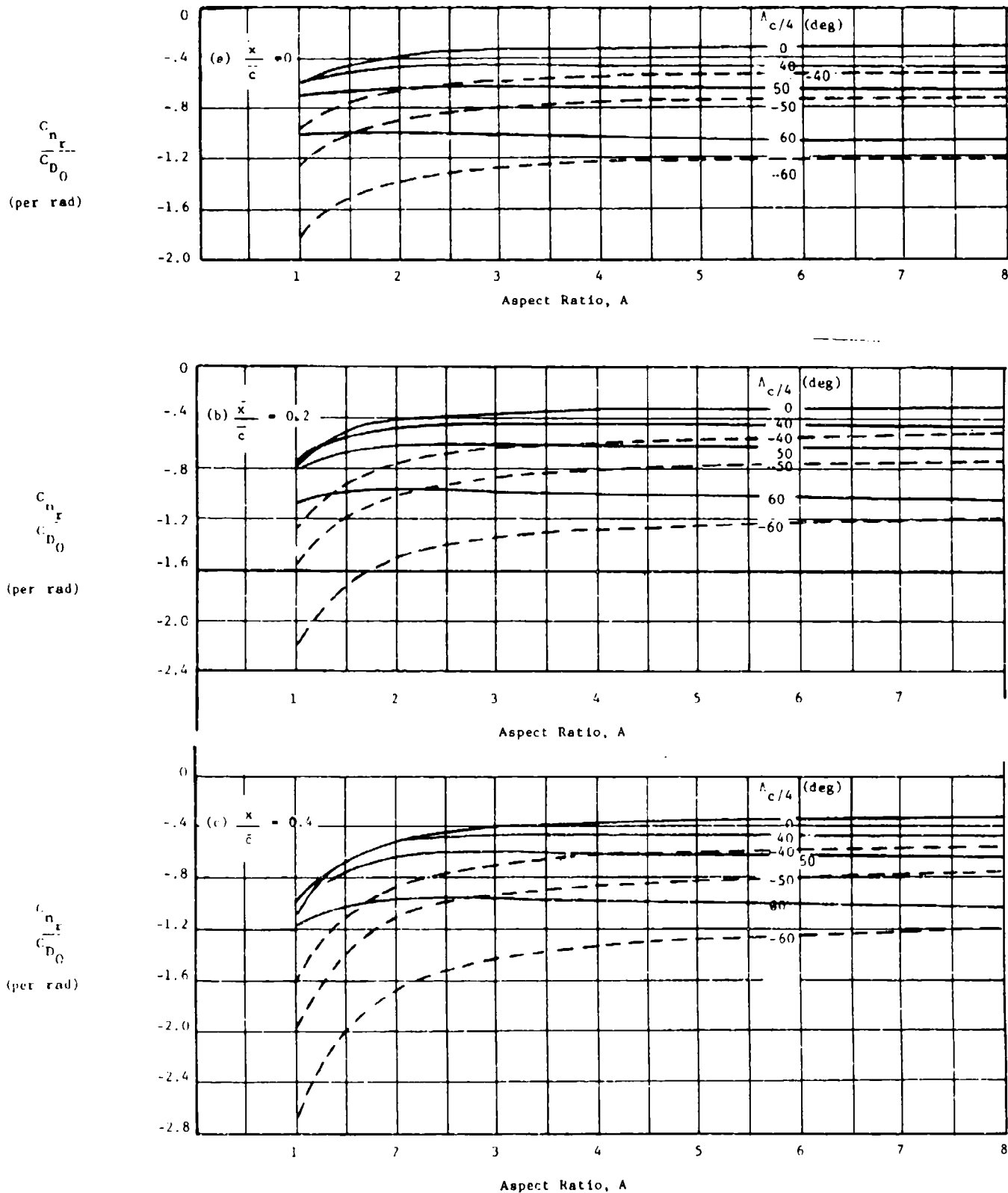


Figure 28. low-Speed Profile-Drag Yaw-Damping Parameter

7.1.4.1 WING ACCELERATION DERIVATIVE $C_{L_{\dot{\alpha}}}$

A. Subsonic

No modifications are necessary other than those described in Paragraph A of Section 4.1.4.2, "Wing Pitching-Moment-Curve Slope".

No substantiation was performed.

B. Transonic

The comments of Paragraph A of this section are applicable here.

No substantiation was performed.

C. Supersonic

The reversibility theorem states that this derivative is identical whether in forward or reverse flight. Use the absolute value of the trailing-edge sweep angle to obtain forward swept wing characteristics.

No substantiation was performed.

7.1.4.2 WING ACCELERATION DERIVATIVE $C_{m_{\dot{\alpha}}}$

A. Subsonic

The comments of Paragraph A of Section 7.1.4.1, "Wing Acceleration Derivative $C_{L_{\dot{\alpha}}}$ " are appropriate here.

No substantiation was performed.

B. Transonic

The comments of Paragraph B of Section 7.1.4.1, "Wing Acceleration Derivative $C_{L_{\dot{\alpha}}}$ " are appropriate here.

No substantiation was performed.

C. Supersonic

No guidance was found in literature. The author suggests using the absolute value of the trailing-edge sweep angle to obtain forward-swept-wing characteristics.

No substantiation was performed.

7.1.4.3 WING DERIVATIVE C_{D_α}

A. Subsonic

No modifications are necessary.

No substantiation was performed.

B. Transonic

No method is presented.

C. Supersonic

No method is presented.

7.3 WING-BODY DYNAMIC DERIVATIVES

7.3.1.1 WING-BODY PITCHING DERIVATIVE C_{Lq}

A. All Speeds

No modifications to either method are necessary other than those described in Sections 7.1.1.1, "Wing Pitching Derivative C" and 4.3.1.2, "Wing-Body Lift-Curve Slope" in the appropriate speed range.

No substantiation was performed.

7.3.1.2 WING-BODY PITCHING DERIVATIVE C_{m_q}

A. All Speeds

No modifications to either method are necessary other than those described in Sections 7.1.1.2, "Wing Pitching Derivative C_{m_q} ", and 4.3.1.2, "Wing-Body Lift-Curve Slope".

No substantiation was performed.

7.3.2.1 WING-BODY ROLLING DERIVATIVE C_{Y_P}

A. Subsonic

No modifications are necessary.

No substantiation was performed.

B. Transonic

No method is presented.

C. Supersonic

No method is presented.

7.3.2.2 WING-BODY ROLLING DERIVATIVE $C_{\ell p}$

A. Subsonic

No modifications are necessary other than those described in Paragraph A of Section 7.1.2.2, "Wing Rolling Derivative $C_{\ell p}$ ".

No substantiation was performed.

B. Transonic

No method is presented.

C. Supersonic

The absolute value of the leading-edge sweep angle should be used in Datcom Figure 7.3.2.2-13, "Effect of the Fuselage on Roll Damping". Also, the modifications described in Paragraph C of Section 7.1.2.2, "Wing Rolling Derivative $C_{\ell p}$ " should be incorporated.

7.3.2.3 WING-BODY ROLLING DERIVATIVE C_{n_p}

A. Subsonic

No modifications are necessary other than those described in Paragraph A of Section 7.1.2.3, "Wing Rolling Derivative C_{n_p} ".

No substantiation was performed.

B. Transonic

No method is presented.

C. Supersonic

No method is presented.

7.3.3.1 WING-BODY ROLLING DERIVATIVE C_{Y_r}

A. All Speeds

No methods are presented.

7.3.3.2 WING-BODY ROLLING DERIVATIVE C_{ℓ_r}

A. Subsonic

No modifications are necessary other than those described in Paragraph A of Section 7.1.3.2, "Wing Rolling Derivative C_{ℓ_r} ".

No substantiation was performed.

B. Transonic

No method is presented.

C. Supersonic

No method is presented.

7.3.3.3 WING-BODY ROLLING DERIVATIVE C_{n_r}

A. Subsonic

The comments of Paragraph A of Section 7.1.3.3, "Wing Rolling Derivative C_{n_r} " are appropriate here.

No substantiation was performed.

B. Transonic

No method is presented.

C. Supersonic

No method is presented.

7.3.4.1 WING-BODY ACCELERATION DERIVATIVE $C_{L_{\alpha}}$

A. All Speeds

No modifications to either method are necessary other than those at the appropriate speed of Sections 7.1.4.1, "Wing Acceleration Derivative $C_{L_{\alpha}}$ " and 4.3.1.2, "Wing-Body Lift-Curve Slope".

No substantiation was performed.

7.3.4.2 WING-BODY ACCELERATION DERIVATIVE $C_{m_{\alpha}}$

A. All Speeds

No modifications to either method are necessary other than those at the appropriate speed of Sections 4.3.1.2, "Wing-Body Lift-Curve Slope" and 7.1.4.2, "Wing Acceleration Derivative $C_{n_{\alpha}}$ ".

No substantiation was performed.

7.4 WING-BODY-TAIL DYNAMIC DERIVATIVES

7.4.1.1 WING-BODY-TAIL PITCHING DERIVATIVE C_{Lq}

A. All Speeds

No modifications are necessary for either method other than those described at the appropriate speed in Sections 7.3.1.1, "Wing-Body Pitching Derivative C_{Lq} "; 4.4.1, "Wing-Wing Combinations at Angle of Attack"; 4.3.1.2, "Wing-Body Lift-Curve Slope"; and 4.1.3.2, "Wing Lift-Curve Slope".

No substantiation was performed.

7.4.1.2 WING-BODY-TAIL PITCHING DERIVATIVE C_{mq}

A. All Speeds

No modifications are necessary for either method other than those described at the appropriate speed in Sections 7.3.1.2, "Wing-Body Pitching Derivative C_{mq} "; 4.4.1, "Wing-Wing Combinations at Angle of Attack"; 4.3.1.2, "Wing-Body Lift-Curve Slope"; and 4.1.3.2, "Wing Lift-Curve Slope".

No substantiation was performed.

7.4.1.3 WING-BODY-TAIL PITCHING DERIVATIVE C_{Dq}

A. Subsonic

Other than use of the absolute value of the leading-edge sweep angle in Datcom Figure 7.4.1.3 -4, "Variation in Downwash with Pitch Rate", no modifications are necessary.

No substantiation was performed.

B. Transonic

No method is presented.

C. Supersonic

No method is presented.

7.4.2.1 WING-BODY-TAIL ROLLING DERIVATIVE C_{Yp}

A. Subsonic

No modifications are necessary for either method.

No substantiation was performed.

B. Transonic

No method is presented.

C. Supersonic

No method is presented.

7.4.2.2 WING-BODY-TAIL ROLLING DERIVATIVE $C_{\ell p}$

A. Subsonic

No modifications are necessary for either method other than those described in Paragraph A of Section 7.1.2.2, "Wing Rolling Derivative $C_{\ell p}$...".

No substantiation was performed.

B. Transonic

No method is presented.

C. Supersonic

No method is presented.

7.4.2.3 WING-BODY-TAIL ROLLING DERIVATIVE C_{n_p}

A. Subsonic

No modifications are necessary for either method other than those described in Paragraph A of Section 7.3.2.3, "Wing-Body Rolling Derivative C_{n_p} ".

No substantiation was performed.

B. Transonic

No method is presented.

C. Supersonic

No method is presented.

7.4.3.1 WING-BODY-TAIL YAWING DERIVATIVE C_{Y_r}

A. Subsonic

No modifications are required.

No substantiation was performed.

B. Transonic

No method is presented.

C. Supersonic

No method is presented.

7.4.3.2 WING-BODY-TAIL YAWING DERIVATIVE C_{ℓ_r}

A. Subsonic

No modifications are required other than those described in Paragraph A of Section 7.3.3.2, "Wing-Body Yawing Derivative C_{ℓ_r} ".

No substantiation was performed.

B. Transonic

No method is presented.

C. Supersonic

No method is presented.

7.4.3.3 WING-BODY-TAIL YAWING DERIVATIVE C_{n_r}

A. Subsonic

No modifications are required other than those described in Paragraph A of Section 7.3.3.3, "Wing-Body Yawing Derivative C_{n_r} ".

No substantiation was performed.

B. Transonic

No method is presented.

C. Supersonic

No method is presented.

7.4.4.1 WING-BODY-TAIL ACCELERATION DERIVATIVE $C_{L_{\dot{\alpha}}}$

A. All Speeds

No modifications to either method are necessary other than those described at the appropriate speed of Sections 7.3.4.1, "Wing-Body Acceleration Derivative $C_{L_{\dot{\alpha}}}$ "; 4.4.1, "Wing-Wing Combinations at Angle of Attack"; 4.3.1.2, "Wing-Body Lift-Curve Slope"; and 4.1.3.2, "Wing Lift-Curve Slope".

No substantiation was performed.

7.4.4.2 WING-BODY-TAIL ACCELERATION DERIVATIVE $C_{m_{\dot{\alpha}}}$

A. All Speeds

No modifications to either method are necessary other than those described at the appropriate speeds of Sections 7.3.4.2, "Wing-Body Acceleration Derivative C "; 4.4.1, "Wing-Wing Combinations at Angle of Attack"; 4.3.1.2, "Wing-Body Lift-Curve Slope"; and 4.1.3.2, "Wing Lift-Curve Slope".

No substantiation was performed.

7.4.4.3 WING-BODY-TAIL DERIVATIVE $C_{D\alpha}$

A. Subsonic

No modifications are necessary other than those described in Paragraph A of Section 4.4.1, "Wing-Wing Combinations at Angle of Attack".

No substantiation was performed.

B. Transonic

No method is presented.

C. Supersonic

No method is presented.

7.4.4.4 WING-BODY-TAIL DERIVATIVE $C_{Y\beta}$

A. Subsonic

The absolute value of the vertical tail leading-edge sweep angle should be used in Datcom Figures 7.4.4.4-6, "Sidewash Contribution Due to Angle of Attack"; 7.4.4.4 - 22, "Sidewash Contribution Due to Dihedral"; 7.4.4.4-26, "Sidewash Contribution Due to Wing Twist"; and 7.4.4.4-42, "Sidewash Contribution Due to Body Effect".

No substantiation was performed.

B. Transonic

No method is presented.

C. Supersonic

No method is presented.

7.4.4.5 WING-BODY-TAIL DERIVATIVE $C_{\dot{\beta}}$

A. Subsonic

No modifications are necessary other than those described in Paragraph A of Section 7.4.4.4, "Wing-Body-Tail Derivative $C_{Y\dot{\beta}}$ ".

No substantiation was performed.

B. Transonic

No method is presented.

C. Supersonic

No method is presented.

7.4.4.6 WING-BODY-TAIL DERIVATIVE $C_{n\dot{\beta}}$

All Speeds

The comments of Section 7.4.4.5 at the appropriate speed are relevant here.

No substantiation was performed.

APPENDIX - SUMMARY OF METHODOLOGY MODIFICATIONS

SECTION	DERIVATIVE	MODIFICATIONS
4.1	WINGS AT ANGLE OF ATTACK	
4.1.3.1	α_o	<p>Subsonic: Use Equation 2 in place of Datcom Equation 4.1.3.1-b. Use Figure 2 to obtain FSW Twist Effect Factors.</p> <p>Transonic: NDM</p> <p>Supersonic: NDM</p>
4.1.3.2	C_{L_α}	<p>Subsonic: No modifications are required for Method 1. Method 2 should not be used.</p> <p>Transonic: Use $\Lambda_{c/2}$ in Datcom Figure 4.1.3.2-53b.</p> <p>Supersonic: In Datcom Figure 4.1.3.2-56a through -56f use Λ_{TE} in place of Λ_{LE}. Use Λ_{LE} in Datcom Figure 4.1.3.2-60.</p> <p>Hypersonic: Supersonic comments are applicable here.</p>
4.1.3.3	$C_L @ \alpha$	<p>Subsonic: Use Λ_{LE} in Datcom Equation 4.1.3.3-e. See report text if planform parameter $J > 1$.</p> <p>Transonic: Use Λ_{LE} in all equations and charts.</p> <p>Supersonic: Use Λ_{LE} in all equations and charts. See modifications, Section 4.1.3.2, Supersonic.</p> <p>Hypersonic: See modifications, this section and 4.1.3.2, Supersonic.</p>
4.1.3.4	$C_{L_{max}}$ & $\alpha_{C_{L_{max}}}$	<p>Subsonic: Method 1: No modifications are necessary.</p> <p>Method 2: Use Λ_{LE} in Datcom Figures 4.1.3.4-21a, -21b and -22. See modifications, Section 4.1.3.1, Subsonic.</p> <p>Method 3: Use Λ_{LE} in Datcom Figures 4.1.3 24a and -25b.</p>

<u>SECTION</u>	<u>DERIVATIVE</u>	<u>MODIFICATIONS</u>
4.1.3.4 con't		<p>Transonic: Use A_{LE} in Datcom Figures 4.1.3.4-24a, -25b and -26b.</p> <p>Supersonic: See Modifications, Sections 4.1.3.2 and 4.1.3.3, Supersonic</p> <p>Hypersonic: See Modifications, Sections 4.1.3.2 and 4.1.3.3, Supersonic</p>
4.1.4.1	C_{m_o}	<p>Subsonic: Method 1: Use Figure 5 to obtain FSW twist effect factor Method 2: Do not use</p> <p>Transonic: NDM</p> <p>Supersonic: NDM</p>
4.1.4.2	$\frac{dC_m}{dC_L}$	<p>Subsonic: Use Figure 6 to obtain FSW aerodynamic-center locations.</p> <p>Transonic: No sweptforward wing method presented. Do not use existing Datcom method.</p> <p>Supersonic: Use Figure 6 to obtain FSW aerodynamic-center locations.</p> <p>Hypersonic: Use Figure 6 to obtain FSW aerodynamic-center locations.</p>
4.1.4.3	$C_m @ \alpha$	<p>All speeds: No sweptforward wing method presented. Do not use existing Datcom methods. However, Datcom Figure 4.1.4.3-25 can be used to determine pitch-up/down trend by use of $A_{c/4}$.</p>
4.1.5.1	C_{D_o}	<p>All speeds: No modifications necessary. Do not use results for performance estimation.</p>
4.1.5.2	C_{D_L}	<p>Subsonic: Use A_{LE} in Datcom Figures 4.1.5.2-53a and -53b. Use $A_{c/4}$ in Datcom Figure 4.1.5.2-48. Use Figure 8 in place of Datcom Figure 4.1.5.2-4Z for sweptforward wing planforms. Do not use results for performance estimation.</p>

SECTION	DERIVATIVE	MODIFICATIONS
4.1.5.2 con't		<p>Transonic: Use A_{LE} in Datcom Figure 4.1.5.2-55. Do not use results for performance estimation.</p> <p>Supersonic: No modifications necessary. Do not use results for performance estimation.</p>
4.3	Wing-Body, Tail-Body Combinations at Angle of Attack	
4.3.1.2	$C_{L\alpha}$	<p>Subsonic: No modifications for either method.</p> <p>Transonic: Use A_{TE} for A_{LE} in Datcom Figure 4.3.1.2-11. See modifications Section 4.1.3.2, Transonic.</p> <p>Supersonic: Use A_{TE} for A_{LE} in Datcom Figure 4.3.1.2-11. See Section 4.1.3.2, Supersonic.</p>
4.3.1.3	$C_L @ \alpha$	<p>Subsonic: See Sections 4.1.3.3 and 4.4.1, Subsonic.</p> <p>Transonic: See Sections 4.1.3.2, 4.1.3.3, 4.3.1.2, and 4.4.1, Transonic.</p> <p>Supersonic: See Sections 4.1.3.2, 4.1.3.3, 4.3.1.2 and 4.4.1, Supersonic.</p>
4.3.1.4	$C_{L_{max}} @ \alpha C_{L_{max}}$	<p>Subsonic: Method 1: No modifications necessary. Method 2: Use Figure 9a in place of Datcom Figure 4.3.1.4-12b and Figure 9b in place of Datcom Figure 4.3.1.4-12c.</p> <p>Transonic: NDM</p> <p>Supersonic: Method 1: See Sections 4.1.3.4 and 4.3.1.2, Supersonic. Method 2: See Section 4.3.1.3</p>
4.3.2.1	$C_{m\alpha}$	<p>Subsonic: Method 1: See Section 4.1.4.1, Method 1, Subsonic. Method 2: Do not use.</p> <p>Transonic: Method 1: Section 4.1.4.1, Method 1, Subsonic Method 2: Do not use.</p> <p>Supersonic: No sweptforward wing method presented. Do not use existing Datcom method.</p>

<u>SECTION</u>	<u>DERIVATIVE</u>	<u>MODIFICATIONS</u>
4.3.2.2	$\frac{dC_m}{dC_L}$	<p>Subsonic: See Section 4.1.4.2, Subsonic.</p> <p>Transonic: No sweptforward wing method presented. Do not use existing Datcom method.</p> <p>Supersonic: Use A_{LE} in Datcom Figures 4.3.2.2-36b and 4.3.2.2-37. See Sections 4.1.3.2, 4.1.4.2, and 4.3.1.2, Supersonic.</p>
4.3.3.1	C_{D_o}	<p>Subsonic: No modifications necessary. Do not use results for performance estimation.</p> <p>Transonic: No modifications necessary. Do not use results for performance estimation.</p> <p>Supersonic: Use A_{LE} in all equations and figures in this speed range. Do not use results for performance estimation.</p>
4.3.3.2	$C_D @ \alpha$	<p>All speeds: Method 1: Do not use.</p> <p>Method 2: See section 4.1.5.2 in the appropriate speed range. Do not use results for performance estimation.</p>
4.4	Wing-Wing Combinations at Angle of Attack	
4.4.1	Downwash	<p>Subsonic: Method 1: Use Figure 10 in place of Datcom Figure 4.4.1-66, use $A_{C/4}$ in Datcom Figure 4.4.1-67. See Sections 4.1.3.1 and 4.1.3.4, Subsonic. See text to increase accuracy of this method.</p> <p>Method 2: No modifications.</p> <p>Method 3: Use Figure 11 in place of Datcom Figure 4.4.1-71. See Section 4.3.1.3, Subsonic.</p>
	Downwash due to flap deflection	No modifications necessary.
	Upwash	Method unsuited for swept wings. No method presented.
	Dynamic pressure ratio	No modifications necessary.

<u>SECTION</u>	<u>DERIVATIVE</u>	<u>MODIFICATIONS</u>
	Downwash	Transonic: See Sections 4.1.3.2 and 4.1.3.3, Transonic.
	Dynamic pressure ratio	No modifications necessary.
	Downwash	Supersonic: Method 1: No modifications necessary. Method 2: Applicable to rectangular and sweptback planforms only. Method 3: Use Figure 12 in place of Datcom Figure 4.4.1-80.
	Dynamic pressure ratio	No modifications necessary.
<hr/>		
4.5	Wing-Body Tail Combinations at Angle of Attack	
4.5.1.1	$C_{L_{\alpha}}$	All speeds: For both methods, see Sections 4.1.3.2, 4.3.1.2, and 4.4.1 in the appropriate speed range.
4.5.1.2	$C_L @ \alpha$	All speeds: For both methods, see Sections 4.1.3.2, 4.1.3.3, 4.1.3.4, 4.3.1.2, 4.3.1.3, and 4.4.1 in the appropriate speed range.
4.5.1.3	$C_{L_{max}} @ \alpha_{C_{L_{max}}}$	All speeds: See Sections 4.1.4.2, 4.1.4.3, 4.3.1.4, 4.3.2.2, 4.3.3.1, 4.3.3.2, and 4.4.1 in the appropriate speed range.
4.5.2.1	$C_{m_{\alpha}}$	All speeds: See Sections 4.3.1.2, 4.3.2.2, 4.3.3.2, and 4.4.1 in the appropriate speed range.
4.5.3.1	C_{D_0}	Subsonic: No modifications necessary. Do not use results for performance estimation. Transonic: Use $ A_{c/4} $ in Datcom Figure 4.5.3.1-19. Do not use results for performance estimation. Supersonic: See Section 4.3.3.1, Supersonic. Do not use results for performance estimation.

<u>SECTION</u>	<u>DERIVATIVE</u>	<u>MODIFICATIONS</u>
4.5.3.2	$C_{D_{\alpha}}$	All speeds: See Sections 4.1.3.1, 4.1.5.1, 4.3.1.2, 4.3.2.1, 4.3.2.2, 4.3.3.1, 4.3.3.2, and 4.4.1 in the appropriate speed range. Do not use results for performance estimation.
4.6	Power effects at Angle of Attack	No modifications are expected other than those described for power-off coefficients.
4.7	Ground effects at angle of attack	No modifications are expected other than those described for out-of-ground-effect coefficients.
4.8	Low-Aspect-Ratio Wings and Wing-Body Combination at Angle of Attack	This section is unsuited for sweptforward wing applications and should not be used.
5.1	Wings in Sideslip	
5.1.1.1	$C_{Y_{\beta}}$	Subsonic: No modifications are necessary. Transonic: NDM Supersonic: Method applicable to rectangular planforms only.
5.1.2.1	$C_{L_{\beta}}$	Subsonic: See text for modified use of Datcom Figure 5.1.2.1-27. Transonic: See Section 4.1.3.2, Transonic. Supersonic: See Sections 4.1.3.2 and 7.1.2.2, Supersonic.
5.1.3.1	$C_{n_{\beta}}$	Subsonic: No modifications necessary Transonic: NDM Supersonic: See Sections 5.1.1.1, Supersonic.
5.2	Wing-Body Combinations in Sideslip	

<u>SECTION</u>	<u>DERIVATIVE</u>	<u>MODIFICATIONS</u>
5.2.1.1	$C_{y_{\beta}}$	All speeds: No modifications necessary
5.2.2.1	$C_{\ell_{\beta}}$	All speeds: See Section 5.1.2.1 in the appropriate speed range.
5.2.3.1	$C_{n_{\beta}}$	All speeds: No modifications necessary.
5.3	Tail-Body Combinations in Sideslip	
5.3.1.1	$C_{y_{\beta}}$	Subsonic: No modifications necessary. Transonic: NDM Supersonic: See Section 4.1.3.2, Supersonic. Hypersonic: See Section 4.1.3.2, Hypersonic.
5.3.2.1	$C_{\ell_{\beta}}$	Subsonic: No modifications required. Transonic: NDM Supersonic: See Section 5.3.1.1, Supersonic.
5.3.3.1	$C_{n_{\beta}}$	Subsonic: See Section 4.1.4.2, Subsonic. Transonic: NDM Supersonic: See Sections 4.1.4.2 and 5.3.1.1, Supersonic.
5.4	Flow Fields in Sideslip	
5.4.1	Wake and Sidewash	Subsonic: No modifications necessary. Transonic: NDM Supersonic: NDM
5.5	Low-Aspect-Ratio Wings and Wing-Body Combinations in Sideslip	This section is unsuited for swept-forward wing applications and should not be used.

SECTION	DERIVATIVE	MODIFICATIONS
5.6	Wing-Body-Tail Combinations in Sideslip	
5.6.1.1	C_{y_β}	Subsonic: No modifications necessary. Transonic: NDM Supersonic: See Section 5.3.1.1, Supersonic.
5.6.2.1	C_{ℓ_β}	Subsonic: No modifications necessary. Transonic: NDM Supersonic: See Section 5.3.1.1, Supersonic.
5.6.3.1	C_{n_β}	Subsonic: No modifications necessary. Transonic: NDM Supersonic: No modifications necessary
6.1	Symmetrically Deflected Flaps and Control Devices on Wing-Body and Tail-Body Combinations	
6.1.4.1	C_{L_δ}	All speeds: No modifications necessary. See text to obtain increased accuracy at subsonic speeds.
6.1.4.2	$(C_{L_\alpha})_\delta$	All speeds: No modifications necessary.
6.1.4.3	Maximum Lift with High-Lift and Control Devices	Use Figure 17 in place of Datcom Figure 6.1.4.3-10.
6.1.5.1	C_{m_δ}	Subsonic: No modifications are necessary, to the jet-flap methods and leading-edge device and to Method 1, for trailing-edge mechanical flaps. Figure 18 should be used to obtain sweptforward wing estimates in Method 2 for trailing-edge mechanical flaps. Transonic: Existing methodologies should not be used for FSW estimation. No method is presented.

<u>SECTION</u>	<u>DERIVATIVES</u>	<u>MODIFICATIONS</u>
6.1.5.1 con't		Supersonic: Use Figure 19 in place of Datcom Figure 6.1.5.1-70 for sweptforward wings. Use Figure 20 in place of Datcom Figure 6.1.5.1-73 for sweptforward wings. See Section 6.2.1.1, Supersonic.
6.1.5.2	$(C_{m_{\alpha}})_{\delta}$	All speeds: No modifications necessary.
6.1.6.1	$C_{h_{\alpha}}$	Subsonic: No modifications necessary. Transonic: NDM Supersonic: Treat sweptforward control as if on sweptback wing with inverse taper. See text for notation modifications.
6.1.6.2	$C_{h_{\delta}}$	Subsonic: No modifications necessary. Transonic: NDM Supersonic: Use Figure 21 in place of Datcom Figure 6.1.6.2-17.
6.1.7	$(C_D)_{\delta}$	Subsonic: No modifications necessary. Transonic: NDM Supersonic: No modifications necessary.
6.2	Asymmetrically Deflected Controls on Wing-Body and Tail-Body Combinations	
6.2.1.1	$C_{\ell_{\delta}}$	Subsonic: No modifications necessary. Transonic: See Section 4.1.3.2, Transonic. Supersonic: Use $ A_{c/4} $ in Datcom Figure 6.2.1.1-30. Use Figure 22 in place of Datcom Figure 6.2.1.1-27 for sweptforward wings. Use Figure 23 in place of Datcom Figure 6.2.1.1-28 for sweptforward wings.

SECTION	DERIVATIVE	MODIFICATIONS
6.2.1.1 (Cont'd)		Use Figure 24 in place of Datcom Figure 6.2.1.1-29a for sweptforward wings. Use Figure 25 in place of Datcom Figure 6.2.1.1-29b for sweptforward wings.
6.2.1.2	$(C_\ell)_{H.S.}$	<p>Subsonic: See Sections 4.3.1.3 and 4.4.1, Subsonic.</p> <p>Transonic: See Sections 4.1.3.2, 4.3.1.3, and 4.4.1, Transonic.</p> <p>Supersonic: See Sections 4.1.3.2, 4.3.1.2, and 4.3.1.3, Supersonic.</p>
6.2.2.1	C_{n_δ}	<p>Subsonic: Use Λ_{LE} in Datcom Figure 6.2.2.1-11.</p> <p>Transonic: See Section 4.1.3.2, transonic</p> <p>Supersonic: Use $\Lambda_{c/2}$ in Datcom Figure 6.2.2.1-13. See Sections 4.1.3.2 and 6.2.1.1, Supersonic.</p>
6.3	Special Control Methods	No modifications necessary.
7.1	Wing Dynamic Derivatives	
7.1.1.1	C_{l_q}	<p>Subsonic: See Section 4.1.4.2, Subsonic.</p> <p>Transonic: NDM</p> <p>Supersonic: Use the equation,</p> $(C_{l_q})_{FSW} = 2(C_{m_\alpha})_{ASW}$ <p>See text for details. See also Section 4.1.3.2, Supersonic.</p>
7.1.1.2	C_{m_q}	<p>Subsonic: See Section 4.1.4.2, Subsonic.</p> <p>Transonic: See Section 4.1.3.2, Transonic.</p> <p>Supersonic: Use Λ_{TE} for Λ_{LE} in all equations and charts. See Sections 4.1.4.2 and 7.1.1.1, Supersonic.</p>

<u>SECTION</u>	<u>DERIVATIVES</u>	<u>MODIFICATIONS</u>
7.1.1.3	C_{D_q}	<p>Subsonic: Use Λ_{LE} in all equations and charts.</p> <p>Transonic: NDM</p> <p>Supersonic: NDM</p>
7.1.2.1	C_{Y_p}	<p>Subsonic: No modifications necessary.</p> <p>Transonic: NDM</p> <p>Supersonic: The methodology of this section is unsuited for sweptforward wings and should not be used. No method is presented.</p>
7.1.2.2	C_{ℓ_p}	<p>Subsonic: Use Figure 26 in place of Datcom Figure 7.1.2.2-20, use $\Lambda_{c/4}$ in Datcom Figure 7.1.2.2-24. See Sections 4.1.3.3 and 4.1.5.1, Subsonic.</p> <p>Transonic: NDM</p> <p>Supersonic: Use $\Lambda_{c/2}$ in Datcom Figure 7.1.2.2-25 and Λ_{LE} in Datcom Figure 7.1.2.2-27.</p>
7.1.2.3	C_{n_p}	<p>Subsonic: See Sections 4.1.5.1, 4.1.5.2, and 7.1.2.2, Subsonic.</p> <p>Transonic: NDM</p> <p>Supersonic: The methodology of this section is unsuited for sweptforward wings and should not be used. No method is presented.</p>
7.1.3.1	C_{Y_r}	All speeds: NDM
7.1.3.2	C_{ℓ_r}	<p>Subsonic: Section not validated due to lack of data. For all sweptforward planforms, use unswept quarter-chord line in Datcom Figure 7.1.3.2-10.</p> <p>Transonic: NDM</p> <p>Supersonic: NDM</p>

<u>SECTION</u>	<u>DERIVATIVES</u>	<u>MODIFICATIONS</u>
7.1.3.3	C_{n_r}	<p>Subsonic: Use Figure 27 in place of Datcom Figure 7.1.3.3-6 and Figure 28 in place of Datcom Figure 7.1.3.3-7.</p> <p>Transonic: NDM</p> <p>Supersonic: NDM</p>
7.1.4.1	$C_{L_{\dot{\alpha}}}$	<p>Subsonic: See Section 4.1.4.2, Subsonic.</p> <p>Transonic: See Sections 4.1.3.2, Transonic and 4.1.4.2, Subsonic.</p> <p>Supersonic: Use Λ_{TE} whenever Λ_{LE} is called for.</p>
7.1.4.2	$C_{m_{\dot{\alpha}}}$	<p>Subsonic: See Section 4.1.4.2, Subsonic.</p> <p>Transonic: See Sections 4.1.3.2, Transonic and 4.1.4.2, Subsonic.</p> <p>Supersonic: Use Λ_{TE} whenever Λ_{LE} is called for.</p>
7.1.4.3	$C_{D_{\dot{\alpha}}}$	<p>Subsonic: No modifications necessary.</p> <p>Transonic: NDM</p> <p>Supersonic: NDM</p>
7.3	Wing-Body Dynamic Derivatives	
7.3.1.1	C_{L_q}	All speeds: See Sections 7.1.1.1 and 4.3.1.2 in the appropriate speed range.
7.3.1.2	C_{m_q}	All speeds: See Sections 7.1.1.2 and 4.3.1.2 in the appropriate speed range.
7.3.2.1	C_{Y_P}	<p>Subsonic: No modifications necessary.</p> <p>Transonic: NDM</p> <p>Supersonic: NDM</p>
7.3.2.2	C_{l_P}	<p>Subsonic: See Section 7.1.2.2, subsonic.</p> <p>Transonic: NDM</p> <p>Supersonic: Use Λ_{LE} in Datcom figure 7.3.2.2-13. See Section 7.1.2.2, Supersonic.</p>

<u>SECTION</u>	<u>DERIVATIVES</u>	<u>MODIFICATIONS</u>
7.3.2.3	C_{n_p}	Subsonic: See Section 7.1.2.3, Subsonic. Transonic: NDM Supersonic: NDM
7.3.3.1	C_{Y_r}	All speeds: NDM
7.3.3.2	C_{ℓ_r}	Subsonic: See Section 7.1.3.2, Subsonic. Transonic: NDM Supersonic: NDM
7.3.3.3	C_{n_r}	Subsonic: See Section 7.1.3.3, Subsonic. Transonic: NDM Supersonic: NDM
7.3.4.1	$C_{L_{\dot{\alpha}}}$	All speeds: See Sections 4.3.1.2 and 7.3.1.1 in the appropriate speed range.
7.3.4.2	$C_{m_{\dot{\alpha}}}$	All speeds: See Sections 4.3.1.2 and 7.3.1.1 in the appropriate speed range.
7.4	Wing-Body-Tail Dynamic Derivatives	
7.4.1.1	C_{L_q}	All speeds: See Sections 4.1.3.2, 4.3.1.2, 4.4.1, and 7.3.1.1 in the appropriate speed range.
7.4.1.2	C_{m_q}	All speeds: See Sections 4.1.3.2, 4.3.1.2, 4.4.1, and 7.3.1.2 in the appropriate speed range.
7.4.1.3	C_{D_q}	Subsonic: Use $ A_{LE} $ in Datcom Figure 7.4.1.4. Transonic: NDM Supersonic: NDM

<u>SECTION</u>	<u>DERIVATIVES</u>	<u>MODIFICATIONS</u>
7.4.2.1	C_{Y_p}	Subsonic: No modifications necessary. Transonic: NDM Supersonic: NDM
7.4.2.2	C_{ℓ_p}	Subsonic: See Section 7.1.2.2, Subsonic. Transonic: NDM Supersonic: NDM
7.4.2.3	C_{n_p}	Subsonic: See Section 7.3.2.3, Subsonic. Transonic: NDM Supersonic: NDM
7.4.3.1	C_{Y_r}	Subsonic: No modifications necessary. Transonic: NDM Supersonic: NDM
7.4.3.2	C_{ℓ_r}	Subsonic: See Section 7.3.3.2, Subsonic Transonic: NDM Supersonic: NDM
7.4.3.3	C_{n_r}	Subsonic: See Section 7.3.3.3, Subsonic. Transonic: NDM Supersonic: NDM
7.4.4.1	$C_{L_{\dot{\alpha}}}$	All speeds: See Sections 4.1.3.2, 4.3.1.2, 4.4.1, and 7.3.4.1 in the appropriate speed range.
7.4.4.2	$C_{m_{\dot{\alpha}}}$	All speeds: See Sections 4.1.3.2, 4.3.1.2, 4.4.1, and 7.3.4.2 in the appropriate speed range.

<u>SECTION</u>	<u>DERIVATIVE</u>	<u>MODIFICATIONS</u>
7.4.4.3	$C_{D_{\alpha}}$	<p>Subsonic: See Section 4.4.1.</p> <p>Transonic: NDM</p> <p>Supersonic: NDM</p>
7.4.4.4	$C_{Y_{\beta}}$	<p>Subsonic: Use A_{LE} in Datcom Figures 7.4.4.4-6, 7.4.4.4-22, 7.4.4.4-26, and 7.4.4.4-42.</p> <p>Transonic: NDM</p> <p>Supersonic: NDM</p>
7.4.4.5	$C_{L_{\beta}}$	<p>Subsonic: See Section 7.4.4.4, Subsonic.</p> <p>Transonic: NDM</p> <p>Supersonic: NDM</p>
7.4.4.6	$C_{n_{\beta}}$	<p>Subsonic: See Section 7.4.4.4, Subsonic.</p> <p>Transonic: NDM</p> <p>Supersonic: NDM</p>

REFERENCES

1. "USAF Stability and Control Datcom", Project Engineer: D. E. Hoak; Flight Control Division, Flight Dynamics Laboratory, Wright-Patterson Air Force Base, Ohio, October 1960 (Revised April 1978).
2. DeYoung, John and Harper, Charles W., "Theoretical Symmetric Span Loading at Subsonic Speeds for Wings Having Arbitrary Plan Form", NACA Report 921, 1948.
3. Williams, J. E. and Vukelich, S. R., Analysis of Datcom Methods as Applied to Modern Configurations, McDonnell Douglas Corporation, MDC E2265, 1980.
4. Lundry, Jerry L., "Charts for Obtaining Subsonic Inviscid Induced Drag of Twisted Swept Wings", Douglas Aircraft Company, Report LB-31689, 1964.
5. Polhamus, Edward C. and Sleeman, William C., Jr., "The Rolling Moment Due to Sideslip of Swept Wings at Subsonic and Transonic Speeds", NASA TN D-209, 1960.
6. Bauer, C. R., Anderson, A.K., Jr., and Lee, R.F., "Investigation of USAF Stability and Control Datcom Prediction Methods and Related Data", McDonnell Douglas Corporation, Report MDC J8328, 1978.
7. Toll, Thomas A., and Queijo, M. J., "Approximate Relations and Charts for Low-Speed Stability Derivatives of Swept Wings", NACA TN 1581, 1948.
8. Sharpes, D. G., "Validation of USAF Stability and Control Datcom Methodologies for Sweptforward Wing Planforms - Subsonic Wing Lift", AFWAL-TM-219-FIGC, 1982.
9. Martina, Albert P. and Deters, Owen J., "Maximum Lift and Longitudinal Stability Characteristics at Reynolds Number Up to 7.8×10^6 of a 35° Sweptforward Wing Equipped with High-Lift and Stall-Control Devices, Fuselage, and Horizontal Tail", NACA RM L9H18a, 1950.
10. McCormack, Gerald M. and Cook, Woodrow L., "Effects of Several Leading-Edge Modifications on the Stalling Characteristics of a 45° Swept-Forward Wing", NACA RM A9D29, 1949.
11. Parser, Paul E. and Spearman, M. Leroy, "Wing-Tunnel Tests at Low Speed of Swept and Yawed Wings Having Various Plan Forms", NACA RM L7D23, 1947.
12. Feigenbaum, David and Goodman, Alex, "Preliminary Investigation at Low Speeds of Swept Wings in Rolling Flow", NACA RM L7E09, 1947.
13. Paniszczyn, T. F. and Paulovich, K. F., "Summary Report, Tests of 1/10-Scale XB-53 Complete Model, Galtit 10-ft Tunnel", Consolidated Vultee Aircraft Corp., Report No. FZT-112-007, 1946.

14. Vincenti, Walter G., Van Dyke, Milton D., and Matteson, Frederick H., "Investigation of Wing Characteristics at a Mach Number of 1.53. II - Swept Wings of Taper Ratio 0.5", NACA RM A8E05, 1948.
15. Hopkins, Edward J., "Lift, Pitching Moment, and Span Load Characteristics of Wings at Low Speed as Affected by Variations of Sweep and Aspect Ratio", NACA TN 2284, 1950.
16. McCormack, Gerald M. and Stevens, Victor I., Jr., "An Investigation of the Low-Speed Stability and Control Characteristics of Swept-Forward and Swept-Back Wings in the Ames 40- by 80-Foot Wind Tunnel", NACA RM A6K15, 1947.
17. Cahill, Jones F. and Gottlieb, Stanley M., "Low-Speed Aerodynamic Characteristics of a Series of Swept Wings Having NACA 65A006 Airfoil Sections", NACA RM L50F16, 1951.
18. Savage, Paul W., "Experimental Analysis of the Effects of Sweep and Aspect Ratio on Incompressible Flow About Forward Swept Wings", Master's Thesis, AFIT/GAE/AA/81D-26, 1981.
19. Hieser, Gerald and Whitcomb, Charles F., "Investigation of the Effects of a Nacelle on the Aerodynamic Characteristics of a Swept Wing and the Effects of Sweep on a Wing Alone", NACA TN 1709, 1948.
20. Mendelsohn, Robert A. and Brewer, Jack D., "Comparison Between the Measured and Theoretical Span Loadings on a Moderately Swept-Forward and a Moderately Swept-Back Semispan Wing", NACA TN 1351, 1946.
21. Conner, D. William and Cancro, Patrick A., "Low-Speed Characteristics in Pitch of a 34° Sweptforward Wing with Circular-Arc Airfoil Sections", NACA RM L7F04a, 1948.
22. Alexander, Sidney R., "Drag Measurements of a 34° Swept- Forward and Swept-Back NACA 65-009 Airfoil of Aspect Ratio 2.7 as Determined by Flight Tests at Supersonic Speeds", NACA RM L6I11, 1946.
23. Paulovich, K. F., "Summary Report, Ge it Power-Off Wind Tunnel Tests on a Revised 1/10-Scale XA-44 Complete Model", Consolidated Vultee Aircraft Corp., Report No. ZT-001a, 1946.
24. McCormack, Gerald M. and Cook, Woodrow L., "Effects of Boundary-Layer Control on the Longitudinal Characteristics of a 45° Swept-Forward Wing-Fuselage Combination", NACA RM A9K02a, 1950.
25. Graham, Robert R., "Lateral-Control Investigation at a Reynolds Number of 5,300,000 of Wing Aspect Ratio 5.8 Sweptforward 32° at the Leading Edge", NACA RM L9H18, 1950.

26. Spearman, M. Leroy and Comisarow, Paul, "An Investigation of the Low-Speed Static Stability Characteristics of Complete Models Having Sweptback and Sweptforward Wings", NACA RM L8H31, 1948.
27. Tolhurst, William H., Jr., "An Investigation of the Downwash and Wake Behind Large-Scale Swept and Unswept Wings", NACA RM A7L05, 1948.
28. Hoggard, H. Page, Jr. and Hagerman, John R., "Downwash and Wake Behind Untapered Wings of Various Aspect Ratios and Angles of Sweep", NACA TN 1703, 1948.
29. Paulovich, K. F., "Tests of Revised 1/10-Scale XA-44 Complete Model (Modified Wing No. 10) in Galcit 10-ft. Tunnel - Summary Report", Consolidated Vultee Aircraft Corp. Report No. FZT-112-005, 1946.
30. Luoma, Arvo A., Bielat, Ralph P., and Whitcomb, Richard T., "High-Speed Wind-Tunnel Investigation of the Lateral Control Characteristics of Plain Ailerons on a Wing with Various Amounts of Sweep", NACA RM L7I15, 1947.
31. MacLachlan, Robert and Fisher, Lewis R., "Wind-Tunnel Investigation at Low Speeds of the Pitching Derivatives of Untapered Swept Wings", NACA RM L8G19, 1948.
32. Maggin, Bernard and Bennett, Charles, "Low-Speed Stability and Damping-in-Roll Characteristics of Some High Swept Wings", NACA TN 1286, 1946.
33. DeYoung, J., "Theoretical Symmetric Span Loading Due to Flap Deflection for Wings of Arbitrary Plan Form at Subsonic Speeds", NACA Rept. 1071, 1952.
34. Goin, K. L., "Equations and Charts for the Rapid Estimation of Hinge-Moment and Effectiveness Parameters for Trailing Edges Swept Ahead of the Mach Lines", NACA Rept. 1041, 1951.
35. DeYoung, J., "Theoretical Antisymmetric Span Loading for Wings of Arbitrary Plan Form at Subsonic Speeds", NACA Rept. 1056, 1951.

TABLE 1. SUBSONIC WING-ALONE LIFT-CURVE SLOPE
DATA SUMMARY AND SUBSTANTIATION

REF	A	$\Lambda_{c/2}$	CALC	$C_{L\alpha}$ TEST	E percent error
9	5.8	-38	.0628	.0630	-0.3
10	3.6	-47	.0468	.0488	-4.1
11	2.6	60	.0346	.0380	-8.9
	4.5	30	.0588	.0550	6.9
	6.0	0	.0726	.0730	-0.5
	4.5	-30	.0588	.0530	10.9
	2.1	-52	.0358	.0400	-10.5
12	2.6	45	.0431	.0400	7.8
	2.6	-45	.0431	.0480	-10.2
28	3.0	60	.0353	.0380	-7.1
	3.0	-60	.0353	.0350	0.9
13	4.1	-33	.0588	.0600	-2.0

$$\text{average error} = \frac{\sum |E|}{n} = 5.85$$

TABLE 2. SUPERSONIC WING-BODY NORMAL-FORCE-CURVE SLOPE
DATA SUMMARY AND SUBSTANTIATION

REF	$\Lambda_{c/2}$	A	d/b	M	$C_{N\alpha}$ CALC	$C_{N\alpha}$ TEST	E percent error
14	-30	3.5	.067	1.53	.0592	.0585	1.2
	-43	2.9	.073	1.53	.0580	.0550	5.5
	-60	2.0	.088	1.53	.0390	.0365	6.8
Unpub.	-38	4.0	.164	1.40	.0813	.0760	7.0
				1.50	.0745	.0720	3.5

$$\text{average error} = \frac{\sum |E|}{n} = 4.79$$

TABLE 3.

SUBSONIC WING-ALONE LIFT VARIATION
WITH ANGLE OF ATTACK
DATA SUMMARY AND SUBSTANTIATION

REF	Λ_{LE}	A	J	$C_{L_{max}}$	$\alpha_{C_{L_{max}}}$	α	CALC C_L	TEST C_L	E percent error
9	-32	5.8	7.6	0.945	19.04	6	0.3905	0.418	-6.58
						8	0.5242	0.545	-3.82
						12	0.7855	0.770	2.01
						16	0.9318	0.915	1.84
						18	0.9525	0.960	-0.78
10	-42	3.5	2.4	1.015	25.58	6	0.3095	0.310	-0.16
						8	0.4231	0.420	0.74
						12	0.6594	0.620	6.35
						16	0.8826	0.780	13.15
						20	1.0114	0.920	9.93
						24	1.0545	1.000	5.45
15	46	3.4	3.0	1.000	25.05	6	0.3412	0.375	-9.01
						8	0.4622	0.470	-1.66
						12	0.7087	0.720	-1.57
						16	0.9515	0.870	9.37
						20	1.0560	0.960	10.00
						24	1.0384	0.980	5.96
	46	2.8	2.6	0.970	25.50	6	0.3070	0.360	-14.72
						8	0.4191	0.460	-8.89
						12	0.6516	0.670	-2.74
						16	0.8860	0.820	8.05
						20	0.9801	0.960	2.09
						24	0.9880	0.990	-0.20
	-37	4.2	4.9	1.083	23.19	6	0.3569	0.385	-7.30
						8	0.4862	0.495	-1.78
						12	0.7530	0.697	8.03
						16	0.9899	0.855	15.78
						20	1.0981	0.980	12.05
						22	1.0979	1.010	8.70
	-37	3.4	3.8	0.975	23.61	6	0.3314	0.370	-10.43
						8	0.4509	0.480	-6.06
						12	0.6967	0.720	-3.24
						16	0.9369	0.845	10.88
						20	1.0388	0.970	7.09
						22	1.0378	0.990	4.83
	-37	2.8	3.0	0.860	22.50	6	0.3099	0.360	-13.92
						8	0.4230	0.460	-8.04
						12	0.6578	0.670	-1.82
						16	0.8529	0.820	4.01
						20	0.9217	0.955	-3.49

TABLE 3. CONTINUED

REF	Λ_{LE}	A	J	C_{Lmax}	αC_{Lmax}	α	CALC C_L	TEST	E percent error
16	-41	3.1	2.3	1.085	27.60	6	0.3000	0.290	3.45
						8	0.3837	0.380	0.97
						12	0.6524	0.580	12.48
						16	0.8798	0.789	11.51
						20	1.0192	0.920	10.78
						24	1.1036	1.040	6.12
	-26	3.6	5.2	1.261	23.21	6	0.3890	0.405	-3.95
						8	0.5310	0.530	0.19
						12	0.8260	0.780	5.90
						16	1.0900	0.990	10.10
						20	1.2230	1.145	6.81
	5	4.6	0.9	1.352	21.09	6	0.4255	0.445	-4.38
						8	0.5761	0.580	-0.67
						12	0.8642	0.845	2.27
						16	1.1350	1.110	2.25
						20	1.3178	1.340	-1.66
	48	3.6	2.9	1.053	25.89	6	0.3301	0.360	-8.31
						8	0.4494	0.460	-2.30
						12	0.6954	0.680	2.26
						16	0.9291	0.895	3.81
						20	1.0585	1.090	-2.89
						22	1.0852	1.145	-5.22
						24	1.0862	1.180	-7.95
	33	4.8	7.1	1.075	23.70	6	0.3916	0.440	-11.00
						8	0.5261	0.565	-6.88
						12	0.7938	0.820	-3.20
						16	1.0678	1.070	-0.21
						20	1.1200	1.280	-12.50
						22	1.1087	1.220	-9.12
17	-47	4.0	2.6	1.075	28.03	6	0.3292	0.315	4.51
						8	0.4482	0.430	4.23
						12	0.6935	0.685	1.24
						16	0.9410	0.840	12.02
						20	1.0966	0.930	17.91
						24	1.1527	0.980	17.62
						26	1.1592	0.980	18.29
	4	4.0	7.2	0.862	15.14	6	0.4065	0.380	6.97
						8	0.5473	0.500	9.46
						10	0.6786	0.620	9.45
						12	0.7765	0.705	10.14
						14	0.8403	0.730	15.11

TABLE 3. CONCLUDED

REF	Λ_{LE}	A	J	$C_{L_{max}}$	$^{\alpha}C_{L_{max}}$	α	CALC	TEST	E percent error
17	43	4.0	2.5	1.051	27.30	6	0.3384	0.360	-6.00
						8	0.4585	0.495	-7.37
						12	0.7029	0.705	-0.30
						16	0.9457	0.875	8.08
						20	1.0789	0.970	11.23
						24	1.1110	1.040	6.83
						26	1.0969	1.010	8.60

$$\text{average error} = \frac{\sum |E|}{n} = 6.67$$

TABLE 4: MAXIMUM LIFT AND ANGLE OF ATTACK FOR MAXIMUM LIFT
FOR WING-ALONE CONFIGURATIONS
AT SUBSONIC SPEEDS

AT SUBSONIC SPEEDS								E	
REF	ASPECT RATIO * CLASS	Λ_{LE}	$Re \times 10^{-6}$ over M.A.C.	$C_{L_{max}}$		$\alpha C_{L_{max}}$		percent error	
				CALC	TEST	CALC	TEST	$C_{L_{max}}$	$\alpha C_{L_{max}}$
9	H	-32	7.00	0.945	0.96	19.22	18.8	-1.6	2.2
10	B	48	10.62	1.035	1.05	26.00	28.0	-1.0	-7.1
15	H	-37	1.99	1.125	1.05	23.62	24.6	7.1	-4.0
	B	-37	2.07	0.975	1.03	24.03	24.5	-5.4	-1.9
	L	-37	2.16	0.860	1.02	22.50	24.5	-15.7	-8.2
16	H	-26	4.92	1.261	1.18	23.21	22.6	6.9	2.7
	H	5	4.03	1.352	1.37	20.90	21.0	-1.3	-4.6
	B	-41	8.08	1.085	1.08	27.13	27.6	0.5	-1.7
17	B	48	5.83	1.053	1.22	25.84	28.0	-13.7	-7.7
	H	4	6.00	0.782	0.73	13.78	13.4	7.1	2.8
	B	-47	6.00	1.030	0.98	27.76	24.8	5.1	11.9
	B	43	6.00	0.983	1.06	25.11	24.4	-7.3	2.9

<p>* H - High Aspect Ratio</p> <p>L - Low Aspect Ratio</p> <p>B - Borderline Aspect Ratio</p>	<p>average error = $\frac{\sum E }{n} =$</p> <p>High Aspect Ratio = 4.80 2.45</p> <p>Low Aspect Ratio = 15.70 8.20</p> <p>Borderline Aspect Ratio = 5.55 5.55</p>
---	--

TABLE 5. WING-ALONE ZERO-LIFT PITCHING MOMENT
DATA SUMMARY AND SUBSTANTIATION

REF	$\Lambda_{c/4}$	Λ	CALC	C_{m_0} TEST	ΔC_{m_c}
9	-35	5.8	-.0030	-.0025	-.0005
10	-45	3.6	-.0068	-.0086	.0018
15	45	3.4	-.0152	-.0149	-.0003
	45	2.8	-.0146	-.0201	.0055
	-40	4.2	-.0189	-.0229	.0040
	-40	3.4	-.0178	-.0242	.0064
	-40	2.8	-.0167	-.0252	.0085
16	45	3.6	-.0014	-.0039	.0025
	30	4.8	-.0027	-.0074	.0047
	0	4.6	-.0045	.0005	-.0050
	-30	4.7	-.0044	-.0023	-.0021
	-45	3.1	-.0030	-.0025	-.0005
17	45	4.0	0	0	0
	0	4.0	0	.0005	-.0005
	-45	4.0	0	.0020	-.0020

$$\text{average difference} = \frac{\sum |\Delta C_{m_0}|}{n} = .0030$$

TABLE 6\ SUBSONIC WING-ALONE
AERODYNAMIC-CENTER LOCATION
DATA SUMMARY AND SUBSTANTIATION

REF	$\Lambda_{c/4}$	A	M	$\frac{x_{ac}}{c_r}$		Δx_{ac}
				CALC	TEST	
9	-36	5.8	.19	-.3332	-.3157	-.0175
10	-45	3.6	.14	-.3073	-.2968	-.0105
11	-30	5.2	.10	-.4110	-.4476	.0366
	-30	4.5		-.3260	-.3713	.0453
	-30	3.6		-.2130	-.4446	.2316
	-32	3.6		-.0839	-.1111	.0272
	-30	3.5		-.0334	-.0567	.0233
	-45	2.1		-.2120	-.2587	.0467
	-47	2.1		-.0998	.0558	-.1556
	-45	2.2		-.0597	-.1267	.0670
	-60	3.0		-.8240	-.8696	.0456
	-60	1.5		-.2900	-.3225	.0325
12	-45	2.6	.17	-.3120	-.3466	.0346
15	-40	5.3	.16	-.3935	-.2519	-.1416
		4.2		-.3225	-.2081	-.1144
		3.4		-.2522	-.1735	-.0787
		2.8		-.1886	-.1424	-.0462
	-30	6.8		-.3378	-.2052	-.1326
		5.3		-.2496	-.1276	-.1220
		4.2		-.1760	-.1037	-.0723
		3.4		-.1275	-.0614	-.0661
	-45	3.1	.12	-.2046	-.2303	.0257
	-30	4.7		-.1542	-.1545	.0003
	-15	4.8	.14	-.0480	-.0649	.0169
18		4.3		-.0220	-.0501	.0281
		3.8		.0060	-.0136	.0196
	-30	3.9		-.2450	-.3077	.0627
		3.5		-.1970	-.2625	.0655
		3.2		-.1660	-.2140	.0480
	-45	2.6		-.3020	-.3985	.0965
		2.3		-.2520	-.3434	.0914
		2.1		-.2020	-.3081	.1061
	-45	2.7	.20	-.1800	-.1290	-.0510
			.30	-.1825	-.1319	-.0506
			.40	-.1820	-.1264	-.0556
19			.51	-.1830	-.1269	-.0561
			.56	-.1850	-.1279	-.0571
			.61	-.1850	-.1306	-.0544
			.66	-.1860	-.1230	-.0630
			.70	-.1840	-.1247	-.0593
	-12	6.1	.26	.0620	.0563	.0057

$$\text{average difference} = \frac{\sum |\Delta x_{ac}|}{n} = .0625$$

TABLE 7. SUPERSONIC WING-BODY
AERODYNAMIC-CENTER LOCATION
DATA SUMMARY AND SUBSTANTIATION

REF	$\lambda_{c/2}$	A	d/b	CALC.	$\frac{x_{ac}}{c_r}$	Δx_{ac}
					TEST	
14	-60	2.0	.088	-.1997	.0148	-.2145
	-43	2.9	.073	.0193	-.0104	.0297
	-30	3.5	.067	.1394	.1013	.0381
Unpub.	-34	4.0	.164	-.0914	-.2208	.1293

$$\text{average error} = \frac{\sum |\Delta x_{ac}|}{n} = .1029$$

TABLE 8. ZERO-LIFT DRAG
DATA SUMMARY AND SUBSTANTIATION

REF	$\Lambda_{c/4}$	A	PLANFORM*	M	CD ₀ CALC	CD ₀ TEST	ΔCD_0
9	-35	5.8	W	0.19	.00919	.00893	.00026
10	-45	3.6	W	0.14	.00770	.01222	-.00452
11	30	5.2	W	0.12	.01169	.01884	-.00715
	-30	5.2	W	0.12	.01169	.01986	-.00817
	58	2.1	W	0.12	.00829	.01224	-.00395
	-47	2.1	W	0.12	.00902	.01486	-.00584
16	45	3.6	W	0.16	.00786	.02296	-.01510
	30	4.8	W	0.16	.00846	.02583	-.01737
	-30	4.7	W	0.16	.00848	.02581	-.01733
	-45	3.1	W	0.16	.00741	.01990	-.01249
17	-45	4.0	W	0.20	.00699	.00507	.00192
Unpub.	-12	5.6	WB	0.80	.01744	.0561	-.03866
				0.90	.01974	.0676	-.04786
				0.95	.02684	.0762	-.04936
				1.05	.04524	.0969	-.05166
	-33	4.0	WB	0.80	.01845	.0364	-.01795
				0.90	.01845	.0375	-.01905
				0.95	.01845	.0402	-.02175
				1.05	.03635	.0551	-.01875
	-54	1.9	WB	0.80	.02252	.0194	.00312
				0.90	.02252	.0193	.00322
				0.95	.02252	.0213	.00122
				1.05	.03112	.0343	-.00318
22	34	2.7	W	1.20	.07476	.02643	.04833
				1.25	.06877	.02492	.04385
				1.30	.06326	.02580	.03746
	-34	2.7	W	1.20	.07476	.03550	.03926
				1.25	.06877	.03342	.03535
				1.30	.06326	.03121	.03205

*W - Wing-Alone
WB - Wing-Body

$$\text{average difference} = \frac{|\Delta CD_0|}{n}$$

Subsonic = .00855
Transonic = .02298
Supersonic = .03938

TABLE 9. SUBSONIC WING-ALONE DRAG DUE TO LIFT
DATA SUMMARY AND SUBSTANTIATION

REF	$\Lambda_{c/4}$	A	C_L	CALC	C_{D_L}	TEST	ΔC_{D_L} ($\times 10^4$)
9	-35	5.8	.1	.00084	-.00012		9.6
			.2	.00324	.00197		12.7
			.3	.00718	.00749		-3.1
			.4	.01266	.01374		-10.8
			.5	.01970	.02179		-20.9
			.6	.02828	.04316		-148.8
10	-45	3.6	.1	.00095	.00081		1.4
			.2	.00382	.00398		-1.6
			.3	.00859	.00891		-3.2
			.4	.01527	.01877		-35.0
			.5	.02386	.02954		-56.8
			.6	.03436	.05028		-159.2
11	-47	2.1	.1	.00187	-.00019		20.6
			.2	.00746	.00285		46.1
			.3	.01679	.01162		51.7
			.4	.02985	.02362		62.3
			.5	.04665	.04266		39.9
			.6	.06717	.07371		-65.4
	-30	5.2	.1	.00078	.00143		-6.5
			.2	.00314	.00598		-28.4
			.3	.00706	.01159		-45.3
			.4	.01255	.01869		-61.4
			.5	.01961	.02717		-75.6
			.6	.02824	.04178		-135.4
16	-45	3.1	.1	.00107	.00065		4.2
			.2	.00423	.00323		10.0
			.3	.00950	.00933		1.7
			.4	.01687	.01881		-19.4
			.5	.02635	.03333		-69.8
			.6	.03793	.05397		-160.4
	-30	4.7	.1	.00074	0		7.4
			.2	.00294	.00022		27.2
			.3	.00660	.00135		52.5
			.4	.01172	.00484		68.8
			.5	.01831	.01352		47.9
			.6	.02635	.02064		57.1
17	-45	4.0	.1	.00132	.00019		11.3
			.2	.00527	.00332		19.5
			.3	.01185	.01117		6.8
			.4	.02106	.02523		-41.7
			.5	.03291	.05399		-210.8
			.6	.04739	.09157		-441.8

TABLE 9. CONCLUDED

REF	$\Lambda_{c/4}$	A	C_L	CALC	C_{DL} TEST	ΔC_{DL} ($\times 10^4$)
21	-36	3.9	.1	.00271	.00078	19.3
			.2	.01082	.00867	21.5
			.3	.02435	.02500	-6.5
			.4	.04330	.04571	-24.1
			.5	.06765	.07965	-120.0
			.6	.09741	.12698	-295.7

$$\text{average difference} = \frac{\sum |\Delta C_{DL}|}{n} = 58.2$$

TABLE 10.

TRANSONIC WING-BODY DRAG DUE TO LIFT
DATA SUMMARY AND SUBSTANTIATION

REF	$\Lambda_{c/4}$	A	d/b	M	C_L	C_{DL}	TEST	ΔC_{DL} ($\times 10^4$)
Unpub.	-12	5.6	.133	0.80	.009	.00001	.00072	-7.1
					.084	.00069	-.00910	97.9
					.164	.00262	-.01692	195.4
					.332	.01077	-.01535	261.2
					.674	.04447	.00817	363.0
					.735	.05295	.02415	288.0
					.772	.05839	.03375	246.4
					.207	.00486	-.01390	187.6
					.372	.01569	-.00662	223.1
					.518	.03045	.01445	160.0
					.579	.03796	.02928	86.8
					.613	.04252	.03850	40.2
				0.90	.704	.05610	.05854	-24.4
					.325	.01332	-.00733	206.5
					.484	.02947	.00751	219.6
					.550	.03808	.02672	113.6
					.577	.04192	.03652	54.0
					.612	.04714	.04733	-1.9
				0.95	.670	.05652	.06694	-104.2
					.101	.00149	-.00673	82.2
					.271	.01067	-.00701	176.8
					.459	.03063	.01365	169.8
					.530	.04087	.02148	193.9
					.564	.04631	.02845	178.6
					.595	.05153	.03909	124.4
					.677	.06280	.06038	24.2
				1.05	.059	.00056	-.00539	59.6
					.138	.00310	-.00961	127.1
					.214	.00743	-.01083	182.6
					.383	.02371	-.00467	283.8
					.536	.04647	.00850	379.7
					.698	.07881	.03106	477.5
					.771	.09623	.04545	577.8
					.021	.00007	-.00169	17.6
					.109	.00198	-.00765	96.3
					.193	.00617	-.00980	159.7
					.374	.02321	-.00371	269.2
					.537	.04791	.01217	357.4
				0.90	.690	.07922	.03744	417.8
					.825	.11332	.07430	390.2
					.101	.00173	-.00701	87.4
					.185	.00586	-.00916	150.2
					.360	.02226	-.00472	269.8
					.523	.04682	.01192	349.0
					.692	.08201	.04116	408.5
					.762	.09954	.05737	421.7
				0.95	.840	.12093	.07819	427.4
	-33	4.0	.153	0.80	.059	.00056	-.00539	59.6
					.138	.00310	-.00961	127.1
					.214	.00743	-.01083	182.6
					.383	.02371	-.00467	283.8
					.536	.04647	.00850	379.7
					.698	.07881	.03106	477.5
					.771	.09623	.04545	577.8
					.021	.00007	-.00169	17.6
					.109	.00198	-.00765	96.3
					.193	.00617	-.00980	159.7
					.374	.02321	-.00371	269.2
					.537	.04791	.01217	357.4
				0.90	.690	.07922	.03744	417.8
					.825	.11332	.07430	390.2
					.101	.00173	-.00701	87.4
					.185	.00586	-.00916	150.2
					.360	.02226	-.00472	269.8
					.523	.04682	.01192	349.0
					.692	.08201	.04116	408.5
					.762	.09954	.05737	421.7
					.840	.12093	.07819	427.4
				0.95				

TABLE 10. CONCLUDED

REF	$\lambda_{c/4}$	A	d/b	M	C_L	C_{DL}	TEST	ΔC_{DL} (x 10 ⁴)	
Unpub.	-33	4.0	.153	1.05	.093	.00154	-.00320	47.4	
					.277	.01380	-.00182	156.2	
					.474	.04046	.01317	272.9	
					.662	.07882	.04022	386.0	
					.743	.09922	.05611	431.1	
					.824	.12199	.07623	457.6	
					.905	.14727	.09898	482.9	
					-54	1.9	.206	0.80	.026
	.081	.00197	-.00065	26.2					
	.179	.00970	.00334	63.6					
	.290	.02552	.01355	119.7					
	.403	.04913	.03114	179.9					
	.465	.06542	.04431	211.1					
	.525	.08356	.06063	229.3					
	.075	.00165	.00044	12.1					
	0.90	.174	.00877	.00409				46.8	
		.282	.02320	.01474				84.6	
		.401	.04685	.03420				126.5	
		.458	.06105	.04743				136.2	
		.522	.07927	.06465				146.2	
		.578	.09709	.08348				136.1	
		0.95	.082	.00196				-.00004	20.0
			.189	.01051				.00414	63.7
	.304		.02711	.01577				113.4	
	.422		.05221	.03599				162.2	
	.485		.06883	.05041				184.2	
	.547		.08768	.06662				210.6	
	.601		.10586	.08603				198.3	
	1.05		.068	.00131				-.00064	19.5
		.184	.00950	.00349				60.1	
		.312	.02715	.01600				111.5	
		.437	.05327	.03622				170.5	
		.509	.07242	.05064				217.8	
		.571	.09102	.06665				243.7	
		.634	.11250	.08546				270.4	

$$\text{average difference} = \frac{\sum |\Delta C_{DL}|}{n} = 188.8$$

TABLE 11. SUPERSONIC WING-BODY DRAG DUE TO LIFT
DATA SUMMARY AND SUBSTANTIATION

REF	$\Lambda_{c/4}$	A	d/b	M	C_L	CALC C_{DL}	TEST	ΔC_{DL} ($\times 10^4$)
Unpub.	-12	5.6	.133	1.2	-.070	.00095	.0067	-57.5
					.081	.00201	.0009	11.1
					.205	.01012	.0025	76.2
					.348	.02734	.0157	116.4
					.424	.03996	.0275	124.6
					.502	.05545	.0461	93.5
					.577	.07296	.0691	38.6
				1.3	-.078	.00139	.0063	-49.1
					.070	.00189	.0009	9.9
					.185	.01000	.0013	87.0
					.307	.02606	.0133	127.6
					.372	.03773	.0251	126.3
					.438	.05186	.0336	182.6
					.502	.06791	.0532	147.1
	-33	4.0	.153	1.2	.044	.00046	.0024	-19.4
					.211	.00951	.0028	67.1
					.380	.03077	.0150	157.7
					.554	.06557	.0393	262.7
					.633	.08602	.0554	306.2
					.720	.11158	.0749	366.8
					.796	.13713	.0955	416.3
				1.3	.036	.00038	.0012	-8.2
					.187	.00885	.0019	69.5
					.340	.02913	.0136	155.3
					.503	.06376	.0371	266.6
					.579	.08478	.0520	327.8
					.656	.10920	.0703	389.0
	-54	1.9	.206	1.2	.731	.13614	.0906	455.4
					.058	.00135	.0006	7.5
					.174	.01224	.0040	82.4
					.285	.03321	.0156	176.1
					.407	.06814	.0349	332.4
					.473	.09218	.0480	441.8
					.539	.11996	.0636	563.6
					.602	.15012	.0816	685.2
				1.3	.060	.00145	.0003	11.5
					.169	.01171	.0036	81.1
					.284	.03335	.0151	182.5
					.403	.06763	.0351	325.3
					.467	.09101	.0481	429.1
					.530	.11755	.0636	539.5
					.597	.14942	.0811	683.2

$$\text{average difference} = \frac{\sum |\Delta C_{DL}|}{n} = 215.6$$

TABLE 12. SUBSONIC WING-BODY LIFT-CURVE SLOPE
DATA SUMMARY AND SUBSTANTIATION

<u>REF</u>	<u>$\Lambda_{c/2}$</u>	<u>A</u>	<u>d/b</u>	<u>CALC</u>	C_{L_α} <u>TEST</u>	<u>E</u> <u>percent</u> <u>error</u>
13	-33	4.1	.127	.06744	.06408	
23	-17	6.0	.108	.07631	.07772	-1.81
Unpub.	-36	4.0	.164	.07542	.07000	7.74
24	-48	3.6	.142	.05400	.04950	9.09
25	-38	5.8	.120	.06893	.06830	0.92
26	-18	6.6	.143	.08233	.07754	6.18
	-33	5.1	.160	.06893	.06427	7.25
	-48	3.2	.197	.05007	.05414	-7.52

$$\text{average error} = \frac{\sum |\%E|}{n} = 5.72$$

TABLE 13. SUBSONIC WING-BODY LIFT VARIATION
WITH ANGLE OF ATTACK
DATA SUMMARY AND SUBSTANTIATION

REF	$\Lambda_{c/4}$	d/b	J	$C_{L_{max}}$	$\alpha_{C_{L_{max}}}$	α	METHOD C_L		TEST	E percent error	
							1	2		1	2
9	-35	.120	3.4	1.070	20.53	7	0.442	0.465	0.382	15.7	21.7
						9	0.634	0.598	0.540	17.4	10.7
						11	0.784	0.731	0.592	32.4	23.5
						13	0.932	0.864	0.692	34.7	24.9
						15	1.045	0.997	0.791	32.1	26.0
						17	1.136	1.130	0.874	30.0	29.3
						19	1.198	1.263	0.929	29.0	36.0
23	-12	.108	7.7	1.008	14.17	7	0.592	0.545	0.52	13.8	4.8
						9	0.763	0.700	0.67	13.9	4.5
						11	0.940	0.856	0.79	19.0	8.4
						13	1.116	1.012	0.81	37.8	24.9
24	-45	.142	2.0	1.057	28.24	7	0.379	0.334	0.382	-0.8	-12.6
						9	0.429	0.429	0.485	-11.5	-11.5
						11	0.487	0.524	0.592	-17.7	-11.5
						13	0.556	0.619	0.692	-19.7	-10.5
						15	0.636	0.715	0.791	-19.6	-9.6
						17	0.727	0.810	0.874	-16.8	-7.3
						19	0.832	0.905	0.929	-10.4	-2.6
						21	0.950	1.001	0.977	-2.8	2.5
						23	1.083	1.096	1.031	5.0	6.3
						25	1.232	1.191	1.064	15.8	11.9
						27	1.398	1.286	1.085	28.8	18.5

$$\text{average error} = \frac{\sum |\%E|}{n} = 19.3 \quad 14.5$$

TABLE 14. SUBSONIC WING-BODY MAXIMUM LIFT
DATA SUMMARY AND SUBSTANTIATION

REF	$\Lambda_{c/4}$	A	d/b	$C_{L_{max}}$		$\alpha C_{L_{max}}$		E percent error	
				CALC	TEST	CALC	TEST	C_L	α
9	-35	5.8	.120	1.070	1.21	20.53	26.0	-11.6	-21.0
13	-26	4.1	.127	0.976	0.90	18.75	21.6	8.4	-13.2
23	-12	6.0	.108	1.008	0.82	14.17	12.4	22.9	14.3
24	-45	3.6	.142	1.025	1.10	24.45	30.3	-6.8	-19.3
average error = $\frac{\sum \%E }{n} = 12.4$									17.0

TABLE 15. SUBSONIC WING-BODY
AERODYNAMIC CENTER LOCATION

REF	$\Lambda_{c/4}$	A	d/b	$\frac{X_{ac}}{c_r}$		ΔX_{ac}
				CALC	TEST	
26	-15	6.6	.143	-.41399	-.39027	-.0237
	-30	5.1	.160	-.28243	-.30655	.0241
	-45	3.2	.197	-.09601	-.16497	.0690
Unpub.	-34	4.0	.164	-.41386	-.44400	.0301
average difference = $\frac{\sum \Delta X_{ac} }{n} = .0367$						

TABLE 16. SUBSONIC WING-BODY ZERO-LIFT DRAG
DATA SUMMARY AND SUBSTANTIATION

REF	$\Lambda_{c/4}$	A	d/b	C_{D_0}		ΔC_{D_0}
				CALC	TEST	
9	-35	5.8	.120	.01096	.01673	-.00577
13	-30	4.1	.127	.01339	.01002	.00337
21	-36	3.9	.123	.00943	.00979	-.00036
23	-12	6.0	.108	.01423	.01128	.00295
24	-45	3.6	.142	.01000	.01895	-.00895
Unpub.	-34	4.0	.197	.01936	.03310	-.01374
average difference = $\frac{\sum \Delta C_{D_0} }{n} = .00586$						

TABLE 17. SUPERSONIC WING-BODY ZERO-LIFT DRAG
DATA SUMMARY AND SUBSTANTIATION

REF	$\Lambda_{c/2}$	A	d/b	M	CD ₀ CALC	CD ₀ TEST	ΔC_{D0}
14	60	2.0	.088	1.53	.01881	.02031	-.00150
	43	2.9	.073		.01977	.02510	-.00533
	30	3.5	.067		.01991	.02474	-.00483
	-30	3.5	.067		.01991	.02540	-.00549
	-43	2.9	.073		.01977	.02722	-.00745
	-60	2.0	.088		.01881	.02110	-.00229

$$\text{average difference} = \frac{\sum |\Delta C_{D0}|}{n} = .00448$$

TABLE 18. SUBSONIC WING-BODY DRAG DUE TO LIFT
DATA SUMMARY AND SUBSTANTIATION

REF	Λ_{LE}	A	d/b	C _L	CD _L CALC	CD _L TEST	ΔC_{DL} (x 10 ⁴)
Unpub.	-7.9	5.6	.133	.239	.00578	0	57.8
				.391	.01352	.00378	97.4
				.540	.02542	.01939	60.3
				.681	.04095	.03536	55.9
				.745	.04960	.03925	103.5
				.820	.06055	.04623	143.2
				.898	.07314	.05795	151.9
	-28.3	4.0	.153	.237	.00853	.00017	83.6
				.378	.02089	.00691	139.8
				.519	.03952	.01847	210.5
				.652	.06337	.03556	278.1
				.720	.07790	.04718	307.2
				.784	.09319	.06162	315.7
				.858	.11233	.08047	318.6
	-48.7	1.9	.206	.080	.00243	.00041	20.2
				.179	.01015	.00423	59.2
				.283	.02493	.01306	118.7
				.398	.04932	.02891	204.1
				.451	.06363	.04034	232.9
				.516	.08327	.05578	274.9
				.578	.10470	.07323	314.7

$$\text{average difference} = \frac{\sum |\Delta C_{DL}|}{n} = 169.0$$

TABLE 19. SUBSONIC DOWNWASH - METHOD 1
DATA SUMMARY AND SUBSTANTIATION

REF	$\Lambda_{c/4}$	A	$\frac{2h_H}{b}$	α	DOWNWASH ANGLE ϵ		$\Delta\epsilon$
					CALC	TEST	
27	45	3.6	0	0.1	0.05	1.50	-1.45
			.20		0.05	0.40	-0.35
			0	12.7	6.50	5.30	1.20
			.20		6.60	6.40	0.20
			0	21.1	10.30	6.00	4.30
			.20		11.01	8.25	2.76
	30	4.8	-.10	-1.0	-0.52	0.49	-1.01
			0		-0.53	1.50	-2.03
			.30		-0.45	0.53	-0.98
			-.10	8.5	4.19	3.45	0.74
			0		4.38	3.82	0.56
			.30		3.96	3.80	0.16
			-.10	15.9	7.50	4.40	3.10
			0		7.93	4.84	3.09
			.30		7.62	6.80	0.82
	-30	4.7	-.10	-1.0	-0.43	-0.20	-0.23
			0		-0.44	0.40	-0.84
			.20		-0.40	0.70	-1.10
			-.10	9.9	3.63	3.60	0.03
			0		4.00	4.20	-0.20
			.20		4.24	4.40	-0.16
			-.10	16.4	5.18	4.80	0.38
			0		6.17	4.95	1.22
			.20		7.03	6.95	0.08
	-45	3.1	-.10	3.3	1.96	2.35	-0.39
			0		2.14	3.00	-0.86
			.20		2.22	3.10	-0.88
			-.10	9.9	4.79	4.70	0.09
			0		5.22	5.00	0.22
			.20		5.84	8.40	-2.56
			.20	16.4	8.38	2.30	6.08
9	-35	5.8	-.11	0.0	0.21	-2.1	2.31
			.25		0.07	1.8	-1.73
			-.11	4.0	1.86	0	1.86
			.25		1.70	4.2	-2.50
			-.11	8.0	3.34	1.8	1.54
			.25		3.43	6.0	-2.57

$$\text{average difference} = \frac{\sum |\Delta\epsilon|}{n} = 1.37$$

TABLE 20. SUBSONIC DOWNWASH GRADIENT
METHOD 2
DATA SUMMARY AND SUBSTANTIATION

REF	$\Lambda_{c/4}$	A	CALC	$\frac{\partial \epsilon}{\partial \alpha}$	TEST	$\Delta \left(\frac{\partial \epsilon}{\partial \alpha} \right)$
9	-35	5.8	.2989		.3654	.0665
26	45	3.7	.4993		.4079	.0914
	30	5.6	.4058		.4000	.0058
	15	7.2	.3488		.3775	-.0287
	-15	7.2	.3407		.4124	-.0717
	-30	5.4	.3922		.4315	-.0393
	-45	3.3	.4607		.4219	.0388
27	30	4.8	.4200		.3911	.0289
	-30	4.7	.4304		.4706	-.0402
	-45	3.1	.4597		.4489	.0108

$$\text{average difference} = \frac{\sum \left| \Delta \left(\frac{\partial \epsilon}{\partial \alpha} \right) \right|}{n} = .0422$$

TABLE 21. DOWNWASH DUE TO FLAP DEFLECTION
DATA SUMMARY AND SUBSTANTIATION

REF	$\Lambda_{c/4}$	A	$\frac{2b_f}{b}$	CALC	$\Delta \epsilon$	TEST	$\Delta(\Delta \epsilon)$
26	45	3.7	.82	1.0535		2.7789	-1.7254
	30	5.6	.87	1.1414		3.6632	-2.5218
	15	7.2	.88	1.1338		3.0316	-1.8978
	-15	7.2	.90	1.0720		3.7474	-2.6754
	-30	5.4	.86	0.9978		3.1421	-2.1443
	-45	3.3	.82	1.0955		2.0632	-0.9677

$$\text{average difference} = \frac{\sum |\Delta(\Delta \epsilon)|}{n} = 1.9887$$

TABLE 22. SUBSONIC DYNAMIC PRESSURE RATIO
DATA SUMMARY AND SUBSTANTIATION

REF	$\Lambda_{c/4}$	A	C_L	CALC	$\frac{q}{q_\infty}$	TEST	$\frac{\Delta q}{q_\infty}$
28	60	3.0	.004	.836		.970	-.134
			.154	.956		.925	.031
	30	5.2	.028	.895		.952	-.057
			.259	.991		.950	.041
	-30	5.2	0	.893		.890	.003
			.231	.994		.949	.045
	-60	3.0	.022	.837		.780	.057
			.162	.957		.900	.057

$$\text{average difference} = \frac{\sum \left| \frac{\Delta q}{q_\infty} \right|}{n} = .053$$

TABLE 23. TRANSONIC WING-BODY ROLLING MOMENT
DUE TO SIDESLIP
DATA SUMMARY AND SUBSTANTIATION

REF	Λ_{LE}	A	d/b	M	C_L	CALC	C_{ℓ_B}	TEST	ΔC_{ℓ_B} (x 10 ³)
Unpub.	-7.9	5.6	.133	0.6	.161	-.000259	.001130		-1.389
					.540	-.000309	.001490		-1.799
				0.9	-.031	-.000237	-.001750		1.513
					.400	-.000245	.000833		-1.078
				1.2	-.150	-.000332	-.001025		0.693
					.218	-.000239	-.000468		0.229
	-28.3	4.0	.153	0.6	.160	.000154	.00134		-1.186
					.519	.000864	.00188		-1.016
				0.9	.122	.000107	.001145		-1.038
					.559	.001075	.001821		-0.746
				1.2	-.026	-.000395	-.000305		-0.090
					.396	.000351	.000597		-0.246
	-48.7	1.9	.206	0.6	.032	-.000235	.000740		-0.975
					.284	.000221	.001060		-0.839
				0.9	.022	-.000253	.000690		-0.943
					.012	-.000412	.000540		-0.952
				1.2	.299	-.000032	.001125		-1.157
	-29.3	4.0	.164	0.6	-.042	.000695	.001060		-0.365
				0.9	-.067	.000632	.001072		-0.440

$$\text{average difference} = \frac{\sum |\Delta C_{\ell_B}|}{n} = 0.879$$

TABLE 24. SUPERSONIC WING-BODY ROLLING MOMENT
DUE TO SIDESLIP
DATA SUMMARY AND SUBSTANTIATION

<u>REF</u>	<u>Λ_{LE}</u>	<u>A</u>	<u>d/b</u>	<u>M</u>	<u>C_N</u>	<u>CALC...</u>	C_{ℓ_B} <u>TEST</u>	ΔC_{ℓ_B} <u>(x 10³)</u>
Unpub.	-29	4.0	.164	1.5	-.113	.000484	.000472	.012
				1.6	-.104	.000505	.000478	.027
					.258	.000844	.000527	.317
				1.8	-.108	.000364	.000436	-.072
					.225	.000801	.000650	.151
average difference = $\frac{\sum \Delta C_{\ell_B} }{n}$.116

TABLE 25. SUBSONIC WING-BODY ROLLING MOMENT
DUE TO SIDESLIP
DATA SUMMARY AND SUBSTANTIATION

REF	$\Lambda_{c/4}$	A	d/b	Γ	C_L	CALC	C_{ℓ_B} TEST	ΔC_{ℓ_B} (x 10 ³)
13	-30	4.0	.112	7	-.019	-.001463	-.001350	-.113
23	-12	6.0	.108	3	.139	-.000989	-.000870	-.119
				5		-.001393	-.001370	-.023
29	-30	4.9	.112	8	-.014	-.001817	-.001175	-.642
Unpub.	-34	4.0	.164	0	-.012	.000755	.000946	-.191
					.316	.001349	.001169	.180
average difference = $\frac{\sum \Delta C_{\ell_B} }{n}$.211

TABLE 26. SUBSONIC WING-BODY-TAIL
ROLLING MOMENT DUE TO SIDESLIP
DATA SUMMARY AND SUBSTANTIATION

REF	$\Lambda_{c/4}$	A	d/b	r	C_L	C_{ℓ_B}		ΔC_{ℓ_B} ($\times 10^3$)
						CALC	TEST	
23	-12	6.0	.108	3	.139	-.001784	-.00141	-0.374
				5		-.002188	-.00191	-0.278
26	-15	7.2	.143	0	-.120	-.0013	-.0023	1.0
					.097	-.0010	-.0018	0.8
					.237	-.0007	-.0013	0.6
					.472	-.0003	-.0011	0.8
					.669	0	-.0004	0.4
	-30	5.4	.160	0	-.076	-.0014	-.0022	0.8
					.088	-.0010	-.0018	0.8
					.241	-.0005	-.0013	0.8
					.392	-.0001	-.0008	0.7
					.561	.0004	-.0007	1.1
					.698	.0008	-.0003	1.1
	-45	3.3	.197	0	-.063	-.0016	-.0024	0.8
					.059	-.0011	-.0021	1.0
					.182	-.0007	-.0017	1.0
					.290	-.0003	-.0011	0.8
					.412	.0002	-.0006	0.8
					.533	.0006	-.0003	0.9
					.650	.0010	-.0003	1.3
29	-30	4.9	.112	8	-.014	-.002486	-.002688	0.202
						-.002458	-.002613	0.155

$$\text{average difference} = \frac{\sum |\Delta C_{\ell_B}|}{n} = 0.750$$

TABLE 27. EFFECT OF CONTROL SURFACE DEFLECTION ON LIFT
DATA SUMMARY AND SUBSTANTIATION

Ref	$h_c/4$	A	Flap Type	n_i	r_o	CALC $C_{L\delta}$	TEST $C_{L\delta}$	$\Delta C_{L\delta}$
9	-35	5.8	Split	.10	.60	.4162	.3667	.0495
					.97	.5918	.5733	.0185
					.37	.2967	.3133	-.0166
					.97	.3514	.4075	-.0561
					.80	.2831	.3110	-.0279
16	-45	3.1		0	.62	.3490	.295	.0540
					.97	.4579	.400	.0579
	-30	4.7			.62	.5489	.467	.0819
					.97	.7202	.665	.0552
21	-36	3.9		0	.50	.3648	.2989	.0659
26	-15	7.2		.14	.56	.5097	.5883	-.0786
	-30	5.4		.16	.58	.3783	.3290	.0493
	-45	3.3		.18	.59	.2594	.2126	.0468
30	-45	4.4	Plain	.53	.90	.0470	.0743	-.0273
9	-35	5.8	Single-slotted	.10	.60	.6253	.6001	.0252
					.97	.8893	.8784	.0109
					.37	.4457	.4615	-.0158
			Double-slotted	.10	.60	.8486	.6976	.1510
					.97	1.2068	1.1362	.0706
					.37	.6049	.5686	.0363
			Leading-edge	0	.97	.7165	.7545	-.0380
					.41	-.0334	-.0224	-.0110
					.58	-.0444	-.0350	-.0094
					.41	-.0446	-.0360	-.0086
10	-45	3.6		0	1.00	-.0383	-.0143	-.0240
						-.0638	-.0371	-.0267
9	-35	5.8	Slat	0	.41	-.0394	-.0054	-.0340
					.58	-.0524	-.0197	-.0327
					.75	-.0658	-.0293	-.0365
			Kreuger	0	.41	-.0421	-.0185	-.0236
					.58	-.0617	-.0517	-.0100
					.75	-.0848	-.0733	-.0115

$$\text{Average Difference} = \frac{\sum |\Delta C_{L\delta}|}{n}$$

Split Flap = .0506
 Single Slotted Flap = .0170
 Double Slotted Flap = .0740
 Plain Flap = .0273
 Leading Edge Flap = .0159
 Slat = .0344
 Kreuger = .0150

*Equation 8 used to obtain split flap results.

TABLE 28. EFFECT OF CONTROL SURFACE DEFLECTION ON LIFT-CURVE SLOPE
DATA SUMMARY AND SUBSTANTIATION

Ref	$\Delta c/4$	A	Flap Type	η_i	η_o	$(C_{L_\alpha})_\delta$		E percent error
						CALC	TEST	
21	-36	3.94	Kreuger	0	.98	.06232	.06615	-5.79
9	-35	5.79	Leading-edge	0	.75	.06557	.06901	-4.98
					.58	.06520	.06284	3.76
					.41	.06482	.06202	4.51
			Slat	0	.75	.07083	.06415	10.41
					.58	.06939	.06372	8.90
					.41	.06791	.06174	9.99
			Single-slotted	.10	.60	.06630	.06532	1.50
					.97	.06743	.06754	-.16
					.37	.06570	.06602	-.48
			Double-slotted	.10	.80	.06639	.06750	-1.64
					.97			
					.37			
					.60	.06886	.06517	5.66
					.97	.07111	.06980	1.88
					.80	.06766	.06849	-1.21
					.97	.06904	.07193	-4.02

$$\text{Average Difference} = \frac{\sum |\%E|}{n} = 4.33$$

TABLE 29. EFFECT OF CONTROL SURFACE DEFLECTION ON MAXIMUM LIFT COEFFICIENT
DATA SUMMARY AND SUBSTANTIATION

Ref	$\Delta c/4$	A	Re ($\times 10^{-6}$)	Flap Type	η_i	η_o	CALC *	$\Delta C_{L_{max}}$ TEST	$\Delta(\Delta C_{L_{max}})$
16	-45	3.12	8.08	Split	0	.62	.23512	.15142	.08370
						.97	.31728	.23243	.08485
	-30	4.69	4.92		0	.62	.40149	.29370	.10779
						.97	.53215	.42176	.11039
21	-36	3.94	6.90		0	.50	.26949	.28656	-.01707
9	-35	5.79	7.00		.10	.60	.24139	.24	.00139
						.97	.35963	.35	.00963
					.37	.80	.16968	.14	.02968
						.97	.21763	.15	.06763
				Single slotted	.10	.60	.37515	.28	.09515
						.97	.55891	.42	.13891
					.37	.80	.26370	.18	.08370
						.97	.33822	.24	.09822
				Double- slotted	.10	.60	.46969	.40	.06969
						.97	.64976	.61	.03976
					.37	.80	.33016	.24	.09016
						.97	.42345	.36	.06345
				Slats	0	.41	.1123	.1064	.0059
						.58	.2209	.1796	.0413
						.75	.3758	.1880	.1878

$$\text{Average Difference} = \frac{\sum |\Delta(\Delta C_{L_{max}})|}{n}$$

Split Flap = .05690
 Single-Slotted Flap = .10400
 Double-Slotted Flap = .06577
 Slats = .07833

*Trailing edge flap values obtained by using Figure 17 in place of Datcom Figure 6.1.4.3-10

TABLE 30. EFFECT OF CONTROL SURFACE DEFLECTION ON PITCHING MOMENT
DATA SUMMARY AND SUBSTANTIATION

Ref	$\Delta c/4$	A	Flap Type	η_i	η_o	CALC	ΔC_m TEST	$\Delta(\Delta C_m)$
16	-45	3.12	Split	0	.62	-.31723	-.13250	-18473
					.97	-.26135	-.12347	-.13788
	-30	4.69		0	.62	-.30393	-.17542	-.12851
21	-36	3.94		0	.98	-.27518	-.178	-.09718
					.14	-.16651	-.08424	-.08227
	-15	7.15		.14	.56	-.16289	-.09012	-.07277
26	-30	5.36		.16	.58	-.15321	-.05926	-.09395
					.18	-.25204	-.20329	-.04875
	-45	3.28		.18	.59	-.17162	-.15829	-.01333
9	-35	5.79		.10	.60	-.00487	-.03514	.03027
					.97	.03891	-.00357	.04248
				.37	.80			
30	-30	6.80	Plain	.55	.91	.01147	.01066	.00081
					.53	.01549	.01655	-.00106
	-45	4.40		.53	.90			
9	-35	5.79	Single-slotted	.10	.60	-.36121	-.20543	-.15578
					.97	-.30565	-.19257	-.11308
				.37	.80	-.08068	-.05229	-.02839
			Double-slotted	.10	.60	-.03244	.06000	-.09244
					.97	-.47582	-.36486	-.11096
				.37	.80	-.46036	-.26221	-.19815
10	-45	3.55	Leading-edge Flap	0	.50	-.15520	-.06514	-.09006
					.75	-.12138	.00500	-.12638
				1.00				
9	-35	5.79		0	.41	-.01427	-.01847	.00420
					.58	-.03029	-.02275	-.00754
						-.04363	-.12504	.08141
			Slats	0	.41	-.01757	-.00975	-.00782
					.58	-.03258	-.01718	-.01540
						-.02037	-.01857	-.00180
			Kreuger	0	.41	-.03820	-.02257	-.01563
					.58	-.06118	-.03186	-.02932
						-.02600	-.01714	-.00886
					.41	-.04878	-.02657	-.02221
					.58	-.08083	-.04529	-.03554
					.75			

$$\text{Average Difference} = \frac{\sum |\Delta(\Delta C_m)|}{n}$$

Trailing Edge Devices = .08905

Leading Edge Devices = .02088

TABLE 31. EFFECT OF ANGLE OF ATTACK ON CONTROL SURFACE HINGE MOMENT
DATA SUMMARY AND SUBSTANTIATION

<u>Ref</u>	<u>$\Lambda c/4$</u>	<u>A</u>	<u>Flap Type</u>	<u>η_i</u>	<u>η_o</u>	<u>CALC</u>	<u>C_{h_α} TEST</u>	<u>ΔC_{h_α}</u>
30	-30	6.80	Plain	.55	.91	-.15601	-.13188	-.02413
25	-45	4.40		.53	.90	-.11899	-.25956	.14057
	-35	5.79		.59	.98	-.08466	-.26356	.17890

$$\text{Average Difference} = \frac{\sum |\Delta C_{h_\alpha}|}{n} = .11453/\text{rad}$$

TABLE 32. EFFECT OF CONTROL SURFACE DEFLECTION ON ROLLING MOMENT
DATA SUMMARY AND SUBSTANTIATION

<u>Ref</u>	<u>$\Lambda c/4$</u>	<u>A</u>	<u>Flap Type</u>	<u>η_i</u>	<u>η_o</u>	<u>CALC</u>	<u>C_{ℓ_δ} TEST</u>	<u>ΔC_{ℓ_δ}</u>
30	-30	6.86	Plain	.55	.91	.14576	.09090	.05489
	-45	4.40		.53	.90	.12506	.04562	.07944
25	-35	5.79		.59	.98	.12570	.06574	.05996
			Spoiler	0	.40	.00122	.00327	-.00205
					.63	.00204	.00538	-.00334
					.98	.02067	.01985	.00082
				0	.40	.00896	.01387	-.00491
					.63	.01501	.01848	-.00347
					.98	.02067	.01985	.00082

$$\text{Average Difference} = \frac{\sum |\Delta C_{\ell_\delta}|}{n}$$

$$\text{Plain} = .06475$$

$$\text{Spoiler} = .00257$$

TABLE 33. EFFECT OF CONTROL SURFACE DEFLECTION
ON YAWING MOMENT
DATA SUMMARY AND SUBSTANTIATION

REF	$\Lambda_{c/4}$	A	FLAP TYPE	η_i	η_o	C_L	CALC	C_n	TEST	ΔC_n
25	-35	5.8	PLAIN	.59	.98	.089	-.00018	-.00092		.00074
						.334	-.00065	-.00168		.00103
						.641	-.00116	-.00272		.00156
			SPOILER	0		h_s				
						.40	.04	.00118	.00344	-.00226
						.63		.00222	.00478	-.00256
						.98		.00464	.00478	-.00014
				0		.40	.10	.00296	.00993	-.00697
						.63		.00554	.01356	-.00802
						.98		.01160	.01356	-.00196

$$\text{average difference} = \frac{\sum |\Delta C_n|}{n}$$

PLAIN = .00111

SPOILER = .00365

TABLE 34. SUBSONIC WING-ALONE C_{Lq}
DATA SUMMARY AND SUBSTANTIATION

<u>REF</u>	<u>$\Lambda_{c/4}$</u>	<u>A</u>	<u>CALC</u>	C_{Lq} <u>TEST</u>	<u>E percent error</u>
31	45	2.6	0.9079	0.9200	-1.32
	-45	2.6	1.3915	1.4667	-5.13

TABLE 35. SUBSONIC WING-ALONE C_{Mq}
DATA SUMMARY AND SUBSTANTIATION

<u>REF</u>	<u>$\Lambda_{c/4}$</u>	<u>A</u>	<u>CALC.</u>	C_{Mq} <u>TEST</u>	<u>E percent error</u>
31	45	2.6	-.5869	-.5655	3.78
	-45	2.6	-.7000	-.8345	-16.12

TABLE 36. SUBSONIC WING-ALONE C_{Y_P}
DATA SUMMARY AND SUBSTANTIATION

REF	$\Lambda_{c/4}$	A	C_L	CALC C_{Y_P}	TEST	ΔC_{Y_P}
12	45	2.6	.038	.0384	.0311	.0073
			.050	.0498	.0494	.0004
			.100	.0997	.0962	.0035
	-45	2.6	.050	-.0133	-.0424	.0291
			.100	-.0267	-.0589	.0322

$$\text{average difference} = \frac{\sum |\Delta C_{Y_P}|}{n} = .0145$$

TABLE 37. SUBSONIC WING-ALONE C_{ℓ_P}
DATA SUMMARY AND SUBSTANTIATION

REF	$\Lambda_{c/4}$	A	C_L	CALC C_{ℓ_P}	TEST	E percent error
12	45	2.6	0	-.1984	-.2249	-11.78
	-45	2.6	0	-.1984	-.2158	-8.06
32	42	5.9	.060	-.3164	-.3097	2.16
			.269	-.3179	-.2951	7.73
		3.0	.311	-.2213	-.2600	-14.88
			.669	-.2360	-.2310	2.16
	-38	5.9	.335	-.3193	-.3504	-8.88
			.800	-.3292	-.3613	-8.88
		3.0	.310	-.2198	-.2351	-6.51
			.689	-.2330	-.2903	-19.74

$$\text{average error} = \frac{\sum \%E}{n} = 9.08$$